CALIFORNIA STATE UNIVERSITY, NORTHRIDGE

STRUCTURAL ANALYSIS OF MESOZOIC DEFORMATIONS IN THE CENTRAL SLATE RANGE, EASTERN CALIFORNIA

A thesis submitted in partial satisfaction of the requirements for the degree of Master of Science in

Geology

by

Julie Ann Fowler

August, 1982

The Thesis of Julie Ann Fowler is approved:

Dr. Gregory A. Davis (USC)

Dr. Terry E. Davis (CSULA)

Dr. George C. Dunne (CSUN), Chair

California State University, Northridge

ACKNOWLEDGMENTS

The suggestion of the topic, the support and discussions during the study by my chairman, Dr. George C. Dunne, are gratefully appreciated. I would like to thank the members of my committee, Dr. Gregory A. Davis and Dr. Terry E. Davis, for their helpful discussions and comments during the preparation of this thesis. I also gratefully acknowledge the loan of the aerial photographs of my study area by Dr. George I. Smith of the U.S. Geological Survey, Menlo Park, California. My special thanks to my husband, Richard, who was never-ending in his support and encouragement.

Financial support was provided by a research grant from Sigma XI and the Department of Geological Sciences, California State University, Northridge.

TABLE OF CONTENTS

LIST OF ILLUSTRATIONS

ABSTRACT

STRUCTURAL ANALYSIS OF MESOZOIC DEFORMATIONS

IN THE CENTRAL SLATE RANGE, EASTERN CALIFORNIA

by

Julie Ann Fowler

Master of Science in Geology

Eastern Sierran wall rocks in the central portion of the Slate Range have undergone several phases of Mesozoic deformation resulting in the folding and faulting of Permian (?) - Triassic (?) metasedimentary and metavolcanic rocks. Additionally, five phases of pre-, syn- and(or) post-tectonic intrusion occurred in the study area. Five generations of folding are recognized, several of which are correlative with regionally recognized structures. Early-formed fold generations, F_1, F_2 and F_3, are oriented in a northeasterly direction. Axial plane cleavage is developed only in the F_1 generation. Fold trends changed to a northwesterly direction during the F_4 generation which also has a poorly developed axial plane cleavage. The F_5 generation is pervasive and is represented by kink folds, warps and minor folds.

F_1 folds are cut by west-trending strike- and oblique-slip faults,

and both folds and faults are truncated by the northwest-striking Ophir thrust fault, which has been refolded about a N.50°W. orientation by the F_4 fold generation. Three other minor thrust faults associated with this compressional phase also developed. Minor folds and mineral lineations present in Triassic (?) metavolcanic rocks indicate a northeastward direction of tectonic transport of the thrust plates.

Plutonic rocks representative of the three main phases of igneous intrusion in the region, the alkalic suite, calc-alkalic suite and peraluminous suite are present in the study area. This conclusion is supported by petrography and major element chemistry. Most of the plutonic rocks present seem to post-date penetrative structures. Mostly northwest-trending mafic dikes provisionally correlative with the Independence dike swarm are also exposed.

Major structural features, F_1 and F_4 folds, and their age relationships correlate well with features exposed to the north and south along the eastern side of the Sierran batholith. The orientation and deformational style of the Ophir and related thrust faults correlate well with the Middle or Late Jurassic Argus-Sterling thrust system exposed to the north.

INTRODUCTION

Purpose

The Slate Range extends approximately 45 km northwest from the Garlock fault, bordering Panamint Valley on the west. Although the range is composed predominantly of Mesozoic intrusive rocks of probable Sierran affinity, small areas of metasedimentary rocks occur as roof pendants (Fig. 1). Located on the east side of Searles Lake (Fig. 1), the area of interest is composed of a strongly deformed sequence of interbedded metasedimentary and metaigneous rocks.

Reconnaissance studies showed that the Ophir complex, named by Moore (1976) for the intensely deformed rocks in the roof pendant in the central Slate Range, has a complex yet decipherable history. The Ophir complex is probably the southernmost roof pendant in the Slate Range to consist of potentially recognizable strata and datable rocks; rocks in pendants further south are highly deformed and thoroughly metamorphosed. These more southerly pendants are logistically difficult to study because they are in a restricted part of the U.S. Naval Ordnance Test Station, China Lake.

The purpose of this investigation was to decipher the structural history of the area and relate it to areas along strike to the north. The Ophir complex would thus provide a link between the Mojave Desert south of the Garlock fault and Sierran wallrocks to the north. This was accomplished by detailed mapping, and attempting to correlate strata exposed in the study area with regionally recognized units. Additionally, this study examined the petrology, chemistry and in-

Figure 1. Index map to eastern California with the location of the study area.

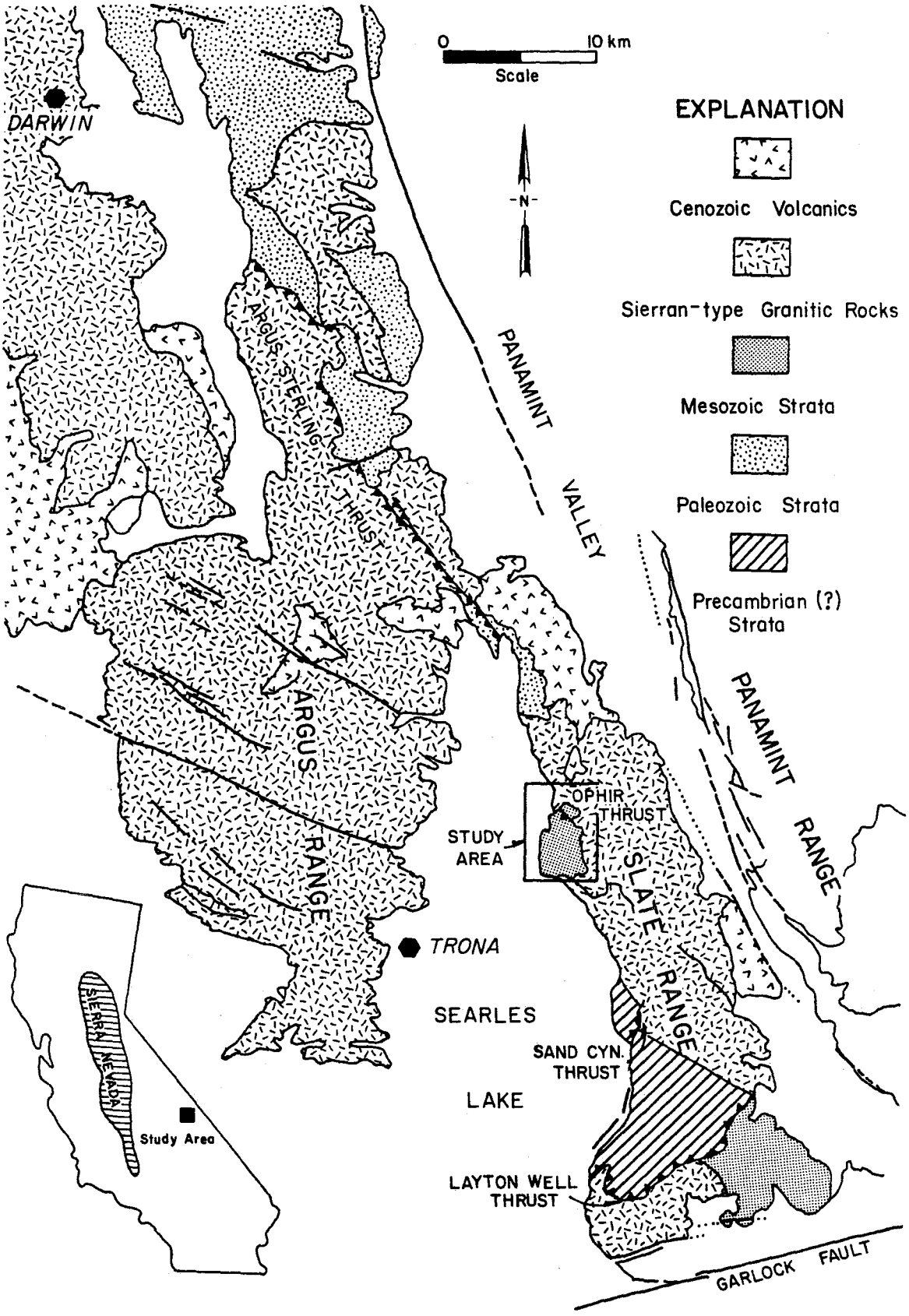
0
10 km
Scale
EXPLANATION
Cenozoic Volcanics
Sierran-type Granitic Rocks
Mesozoic Strata
Paleozoic Strata
Precambrian (?) Strata
N
DARWIN
ARGUS-STERLING THRUST
PANAMINT VALLEY
ARGUS RANGE
PANAMINT RANGE
OPHIR THRUST
STUDY AREA
SLATE RANGE
TRONA
SEARLES LAKE
SAND CYN. THRUST
LAYTON WELL THRUST
GARLOCK FAULT
SIERRA NEVADA
Study Area

trusive history of the plutonic bodies present in the study area to establish their relationship to the alkalic, calc-alkaline and peraluminous rocks known to occur along the eastern margin of the Sierra Nevada batholith. Mafic dikes exposed in the area were studied to see if they are related to the Independence dike swarm.

Regional Geologic Setting

The study area lies within the Cordilleran miogeosyncline on the eastern margin of the Sierra Nevada batholith and just west of major exposures of Precambrian rocks in the Panamint Range. Well-studied areas to the north have revealed a complex structural history that can be tied in part to the development of the batholith and in part to regional deformation recognized in the batholith and its western wall rocks.

Mesozoic plutonic activity within the region is exhibited by three intrusive suites, an alkalic suite that is widely exposed in the Hunter Mountain batholith to the north (Dunne, 1979), a calc-alkaline suite of which most of the batholith is comprised, and an areally restricted peraluminous suite (Miller and Bradfish, 1980). Batholithic intrusion and related temperature rise resulted in a stress-transmitting rigid crust underlain by a ductile crust (Armstrong and Dick, 1974; Moore, 1976). Tectonic compression folded and faulted the upper, more brittle layer, as exhibited by the Argus-Sterling thrust. Also during this period of deformation, a phase of crustal extension of short duration resulted in the emplacement of the Independence dike swarm.

Late Cenozoic time is represented by widespread Tertiary vol-

canism and extensive normal faulting reflected in the present basin and range topography.

Previous Works

Initial reconnaissance mapping by Smith and others (1968) revealed the Slate Range to be composed of a sequence of metasedimentary and metaigneous rocks thought to be of Precambrian age. Moore (1976), as part of a Ph.D. study, remapped the northern Slate Range, including the present study area, at a scale of 1:24,000. He showed the Ophir complex to be a complexly folded and faulted sequence of metasedimentary and metaigneous rocks of probable Permian-Triassic age. He further related the structure of the rocks, on the basis of their deformational style and position, to the Argus-Sterling thrust system of Late Jurassic age exposed in the northern Slate Range and Argus Range.

Additional studies which are pertinent to the understanding of the study area include Johnson (1957) and Labotka and others (1980) concerning the Panamint Range, and Hall and MacKevett (1962), Hall and Stephens (1962), and Hall (1971), concerning the northern Argus Range and the Darwin quadrangle.

Methods

Field work was conducted intermittently during the fall and spring from January, 1978 to April, 1980. A total of 45 days was spent in the field. All mapping was done directly onto an enlarged copy of a portion of the Manly Peak and Trona 15' topographic quadrangles at a scale of 1:9862. Aerial photographs, loaned by G.I. Smith

of the U.S. Geological Survey, were also used during field mapping.

Twenty thin-sections were examined to describe the petrography of the intrusive and extrusive rocks of the area. In addition, 15 whole rock chemical analyses were run to provide a further basis for correlation of these rocks with magmatic suites of the region. Thin-sections of the metamorphic rocks were analyzed to give an indication of their possible origin.

ROCK UNITS

A wide variety of rock types occurs within the area studied. All of them are discontinuously exposed, thoroughly metamorphosed and locally intensely deformed. Therefore, correlations of study area units with known stratigraphic units in the northern Slate Range and central Argus Range, as well as some correlations between isolated exposures within the study area, are speculative.

The complete sequence of rocks present is represented in the stratigraphic column in Figure 2. The following discussion will be concerned first with the stratified units present within the area and then with the intrusive rocks. Stratified rock units have been placed in three groups to facilitate description:

1) relatively autochthonous rocks;

2) relatively allochthonous rocks; and

3) Quaternary (?) sedimentary and volcanic rocks.

Autochthonous and allochthonous headings are assigned only to help designate rocks in upper and lower plates of thrust faults present within the area, and the related rock sequence is by no means assumed to be in original stratigraphic order.

In this section, each of the separate rock types will be examined, and for each a brief description, mode of origin and, where possible, a tentative correlation will be made. All thicknesses mentioned are considered structural, for no stratigraphic thicknesses have been preserved.

Igneous rocks described in this section are named following the

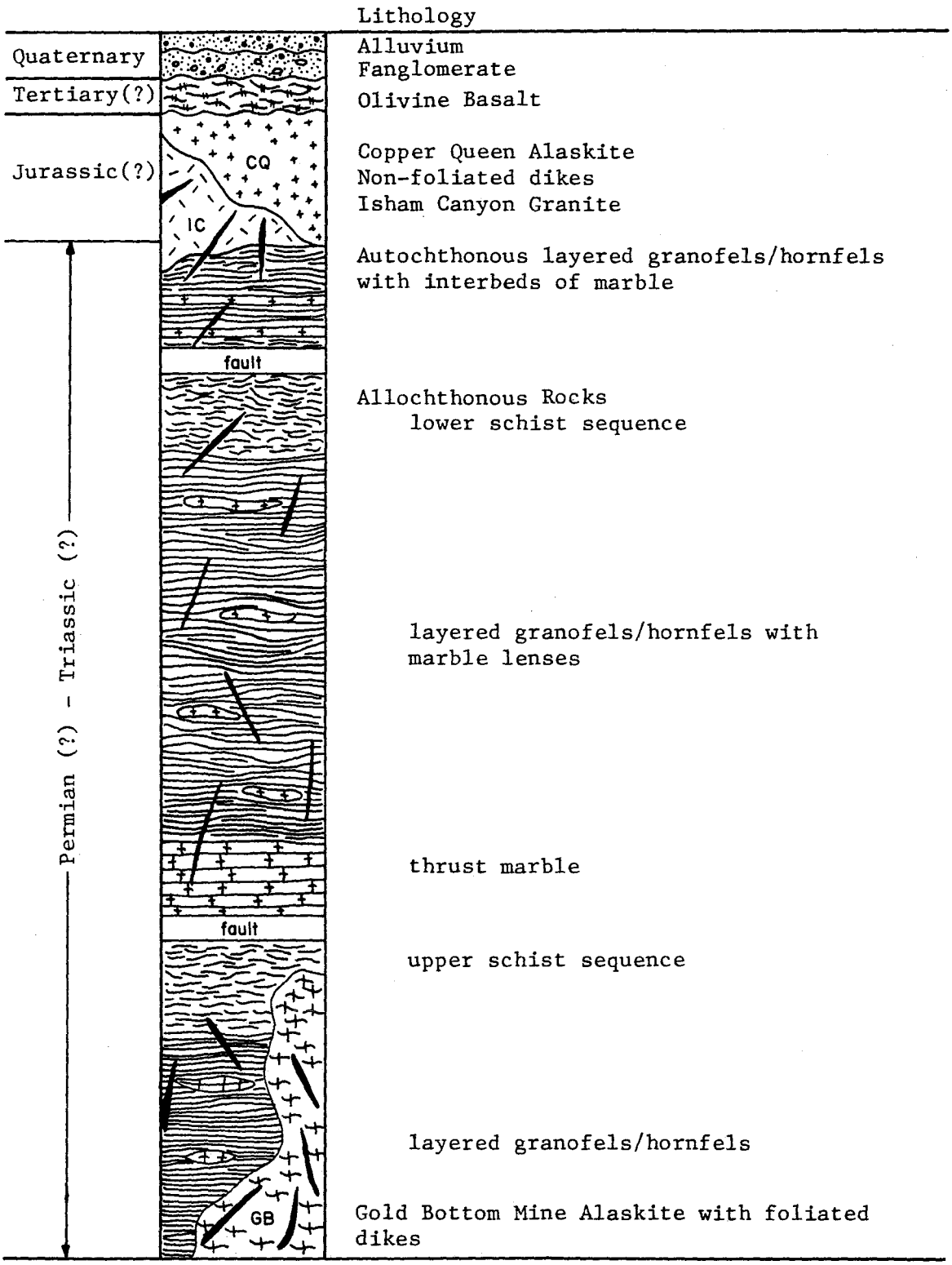

Figure 2. Schematic column of rock units exposed in the central Slate Range.

IUGS Subcommission Classification of Igneous Rocks by Streickheisen (1976).

Autochthonous Rocks

Autochthonous rocks are exposed in two localities within the map area, at the Ophir and Gold Bottom Mine areas (Fig. 3). The rocks consist of layered granofelses and a thin sequence of schists. The exposed layered granofelses are similar at the two localities and have been combined together for discussion; however, a positive correlation is not possible due to distances between exposures and the monotonous nature of the lithology.

Layered Granofels

Autochthonous layered granofelses exposed in the Bundy Canyon area near Ophir Mine consist of a sequence of layered granofelses and inter-bedded siliceous marble layers. The granofelses are approximately 290 m thick and show alternating light-orange and grey-green, fine-grained laminations ranging from 0.3 to 1.5 cm in thickness. Eastward they grade into massive hornfels as the contact with the Isham Canyon pluton is approached. Local areas of hornfelses occur elsewhere within the area due to the close proximity of the pluton. The hornfelses are dark forest green in color with numerous fractures, veinlets of quartz, and porphyroblasts of epidote and garnet.

The interbeds consist of an alternating sequence of light-grey marble and light-brown to olive-green siliceous layers. Some of the siliceous layers are chert-like, while others resemble the granofels sequence. The marble interbeds have a maximum thickness of 10 m with siliceous layers ranging in thickness from 1 to 15 cm.

Figure 3. Map showing the location of the autochthonous rocks. The dashed line on the base map indicates the edge of exposed bedrock.

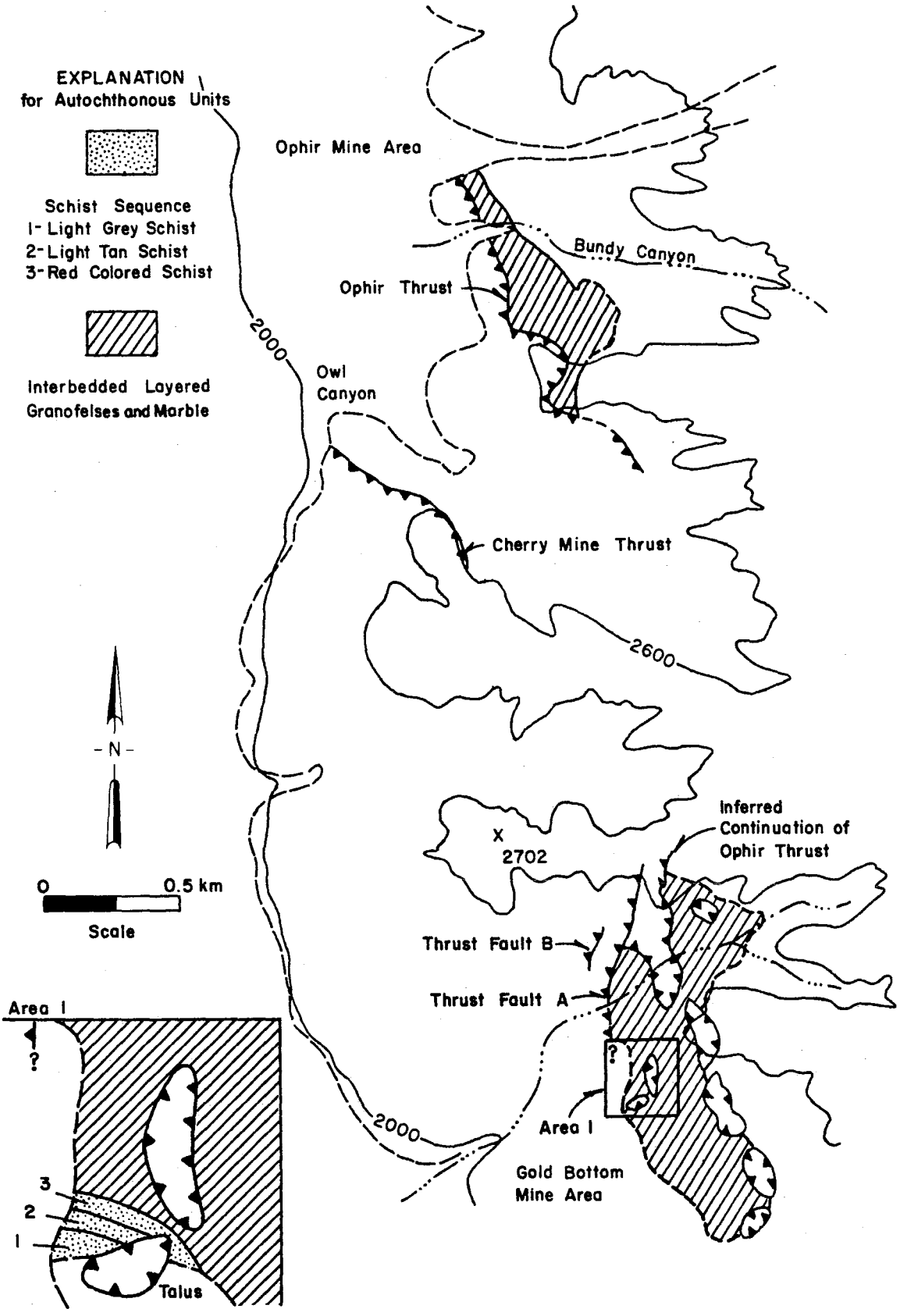
EXPLANATION
for Autochthonous Units
Schist Sequence
1- Light Grey Schist
2- Light Tan Schist
3- Red Colored Schist
Interbedded Layered
Granofelses and Marble
Ophir Mine Area
Bundy Canyon
Ophir Thrust
2000
Owl
Canyon
Cherry Mine Thrust
2600
- N -
0
0.5 km
Scale
X
2702
Inferred
Continuation of
Ophir Thrust
Thrust Fault B
Thrust Fault A
Area I
?
Y
2000
Area I
Gold Bottom
Mine Area
3
2
1
Talus

In the Gold Bottom Mine area, no interbeds of siliceous marble are present within the autochthonous granofelses. Instead, the granofelses consist of finely laminated pale-orange to dark-green compositional layers ranging in thickness from 6 to 8 cm.

Variations in rock types are also present in the autochthonous rocks of the Gold Bottom Mine area. Adjacent to the Ophir thrust the large amount of mineralization and flowage resulted from shear heating during thrusting. In the central portion of the exposure, the granofelses appear to retain primary (?) bedding, apparently not suffering the transposition that affected most of the other areas. Farther east, hornfels with a pervasive foliation becomes the dominant rock type.

Schists

A small exposure of schist (Fig. 3) occurs just south of the Gold Bottom Mine area. A traverse through this schist down the structural sequence from south to north reveals:

1) light silvery-grey schist, very finely foliated, with reddish resistant interbeds;
2) light-tan schist, poorly foliated; and
3) red-stained schist which is strongly foliated.

Allochthonous Rocks

Allochthonous rocks are discontinuously exposed across the field area (Fig. 4) due to intrusion and alluvial cover. Rock types grouped under the heading "allochthonous" include a thrust marble, a layered granofels and a lower and upper schist sequence. The thrust

Figure 4. Map showing the location of the allochthonous rocks.

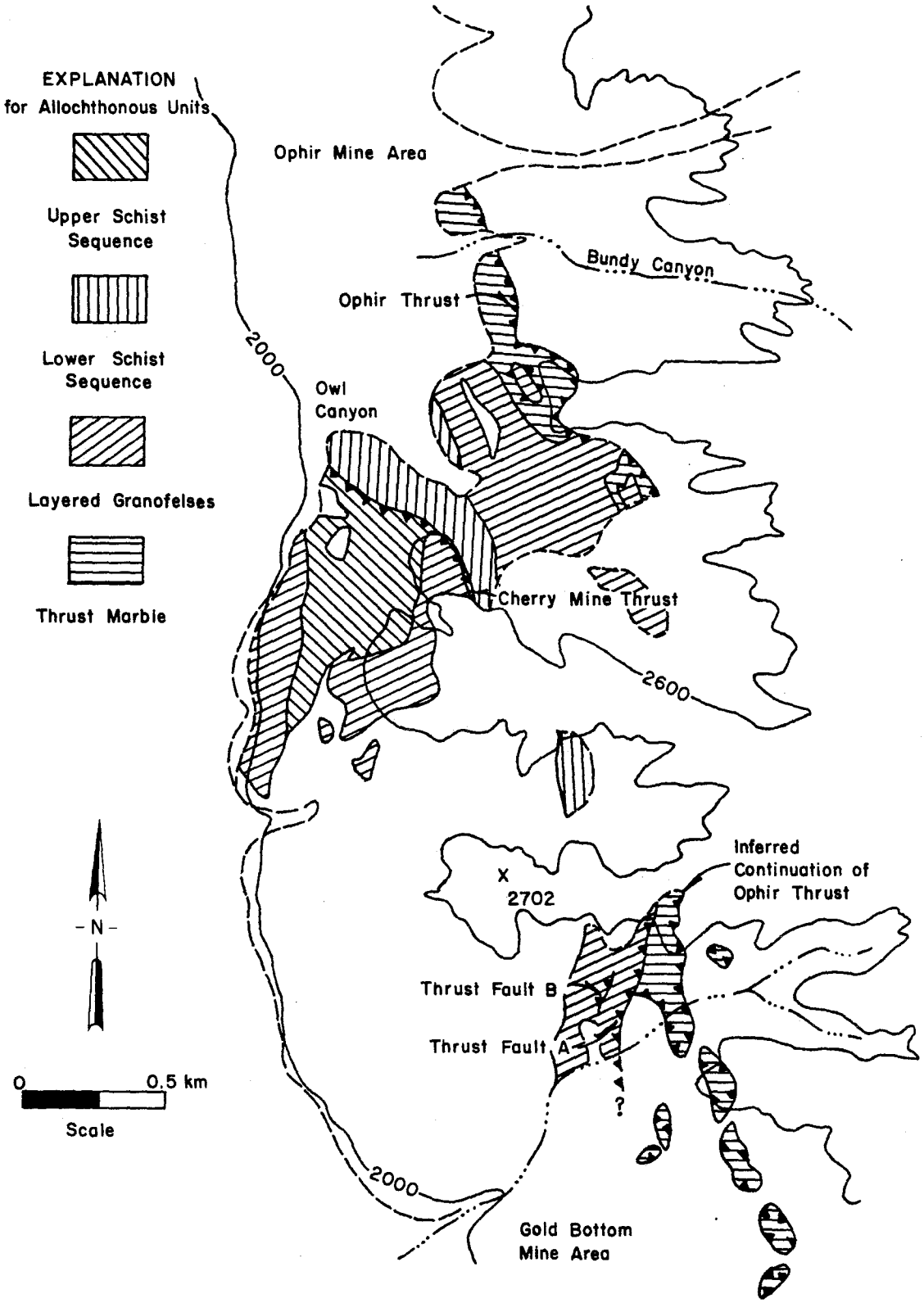
EXPLANATION
for Allochthonous Units
Upper Schist Sequence
Lower Schist Sequence
Layered Granofelses
Thrust Marble
Ophir Mine Area
Bundy Canyon
Ophir Thrust
2000
Owl Canyon
Cherry Mine Thrust
2600
X
2702
Inferred Continuation of Ophir Thrust
Thrust Fault B
Thrust Fault A
?
2000
Gold Bottom Mine Area
N
0
0.5 km
Scale

marble is the basal lithologic unit and movement surface for the main thrust fault, the Ophir thrust. These rock types differ from the autochthonous rocks in that they are thoroughly deformed and metamorphosed, contain a major carbonate unit, and contain a large amount of volcanic material.

Provisional correlations of isolated exposures of allochthonous rocks have been made based on similarity of rock sequences and lithology. Again, the layered granofels/hornfels units have been combined for discussion due to similarities in lithology.

Thrust Marble

The trace of the Ophir thrust fault is delineated by a marble layer that forms the base of the allochthonous plate. This thick carbonate is well foliated and ranges from a light brownish-grey to a dark grey in color. Interlayers of tan to dark-brown siliceous material occur within the marble. These siliceous layers change laterally and vertically from a very sandy marble to discontinuous cherty layers, lenses and pods. Thicknesses of the interbeds range from 0.5 cm to > 3 cm, and they are more abundant near the thrust contact.

Pentagonal pelmatozoan columnals, probably Permian in age, were found by C.H. Stevens in the thrust marble near Ophir Mine (C.H. Stevens, pers. comm., 1980). Rocks sampled from the thrust marble were dissolved for conodonts; however, none were found.

In the Ophir Mine area the contact between the thrust marble and the autochthonous hornfels is sharp. The carbonate shows at its base a 0.6- to 1.2-m-thick zone of poorly developed pink mylonite. The contact between the marble and the overlying metasedimentary rock

and schist sequence appears gradational. It is not known whether or not this contact is depositional or structural.

The thrust marble exposed in the Gold Bottom Mine area also has a thick mylonite zone at its base, similar to that seen in the north. Immediately below the carbonate, the metasedimentary rocks have been strongly metamorphosed and mineralized, forming a zone approximately 1.2 m thick. The upper contact is a fault contact, and the granofels/hornfels unit has overridden the carbonate as another imbricate slice.

Layered Granofels/Hornfels

Allochthonous layered granofels/hornfels rocks crop out extensively in the northern half of the study area (Fig. 4). Lateral changes in lithology and structural fabric are common. Lithologies vary locally from what appears to be primary (?) bedding in a layered granofels to a granular schist. The granofels is characterized by alternating light and dark layers approximately 2.5 cm in thickness, buff-orange to pale green in color, of fine-grained material. Small discontinuous beds commonly about 0.6 m thick, composed of buff to grey siliceous marble, are present within the layered granofels. In addition to interbeds of marble, one strongly sheared pebble conglomerate layer is present. The few clasts that could be identified were composed of quartz.

Locally, a granular schist is the dominant rock type, characteristically having a dark-green color, abundant chlorite and an irregular foliation. Foliation planes range from 0.5 cm to 0.8 cm in thickness and pinch and swell when traced laterally. Small mineral blebs contribute to the irregularities of the surface, giving it a "granular" appearance.

In exposures adjacent to the alaskite of Gold Bottom Mine, the layered granofelses are variably recrystallized to hornfelses. Immediately adjacent to the alaskite, the hornfelses have a well-developed baked zone ranging from 0.6 to 1.5 m in thickness. Away from the baked zone, the hornfelses range in color from a pale green to yellow-green to dark orangish-brown. A sugary texture, a high degree of fracturing and jointing, and a very crude but pervasive foliation are the characteristic features of the hornfelses. Numerous quartz veins and veinlets cut through the rock.

Schists

A sequence of schists is exposed within the allochthonous rocks south of Owl Canyon (Fig. 4). Four pseudo-sections were identified, consisting of a variety of schistose rocks which were too small to be mapped as individual units (Fig. 5). Items recorded were the rock sequence, color, composition and texture. Two further subdivisions, lower and upper schist sequence, were made based on their relationship to the Cherry Mine thrust.

The lower schist sequence consists of eight varieties of greenschist facies rocks exposed at three separate localities (Fig. 5). The sequence has a thickness of 185 m. A summary of rock types, their description, and possible original rock type are shown in Table 1.

The upper schist sequence is exposed in the hanging wall of the Cherry Mine thrust (Fig. 5), is 150 m thick, and is composed of lower greenschist facies rocks (Table 2).

The contacts between the lower and upper schist sequence and the underlying layered granofelses are sharp. It is questionable as to whether or not they are depositional; however, no indications of

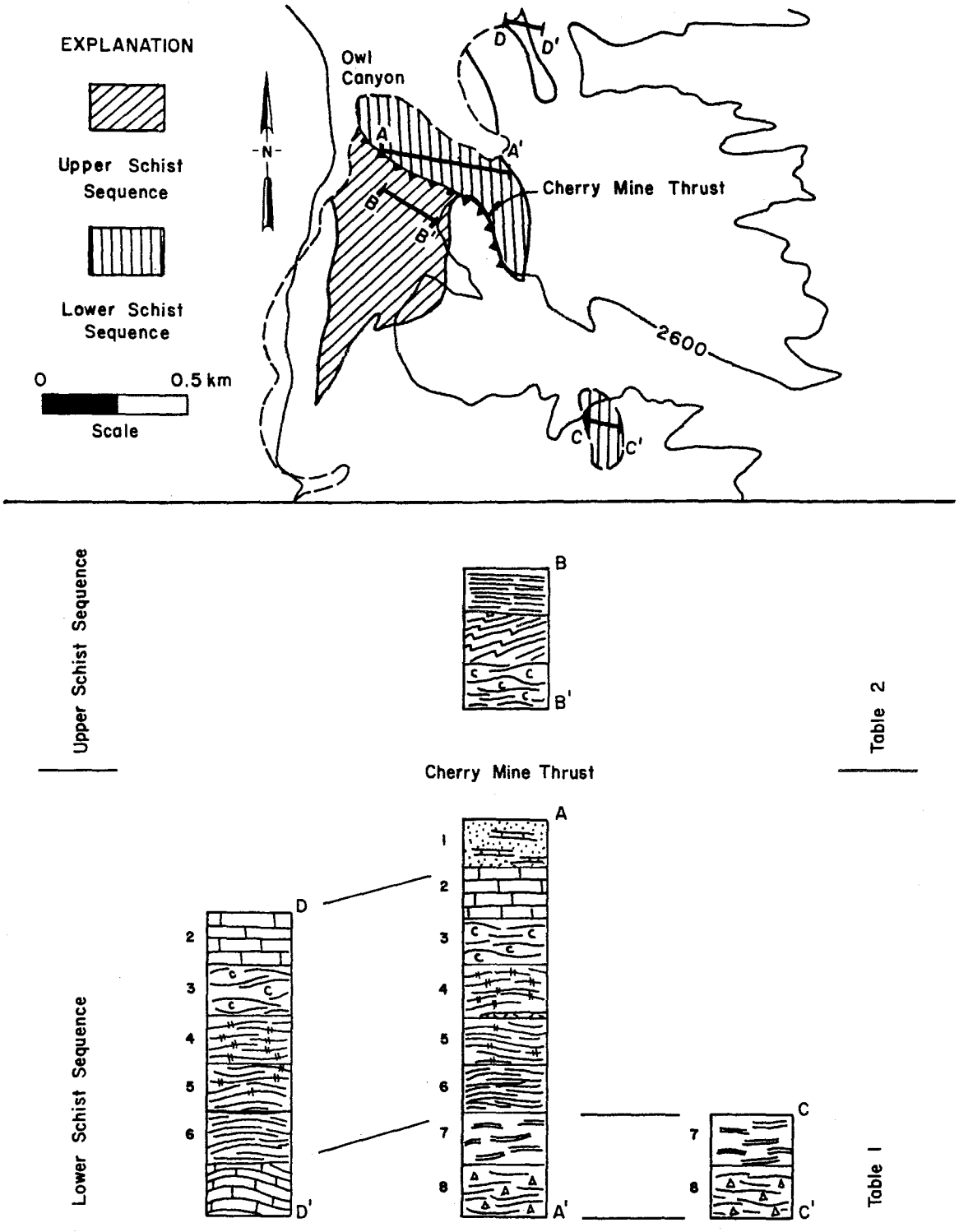

Figure 5. Diagram showing the location, lithologies and correlation of the allochthonous schists.

Table 1. Lower Schist Sequence

No.	Rock Name	Overall Rock Description	Assumed Parent Rock
1	Mica Schist and Calc-silicate	Medium bluish-grey to greenish-grey mica schist with interlayers of orange red calc-silicate. Mica schist contains numerous lenses of fine- to medium-grained quartz. The calc-silicate is thoroughly brecciated with a prominent stretching lineation.	Pelitic rocks and a highly siliceous marble?
2	Marble	Medium grey well laminated siliceous marble. Laminations range in thickness up to 2 mm.	Siliceous limestone
3	Quartz Schist	Varies from a light greenish-grey quartz schist to a pale-green mica quartz schist. Quartz schist consists of alternating sequence of fine-grained quartz and muscovite. Feldspar becomes abundant in the mica quartz schist.	Sandstone
4	Albite Quartz Schist	Moderate-red to pale purple albite quartz schist. Color change is progressive depending on the amount of shearing. Porphyroclasts are predominantly feldspar and quartz, the majority of which show deformation. The rock has a relict trachytic texture.	Flow rock?
5	Mica Quartz Schist	Alternating sequence of dark reddish-brown quartz- and hematite-rich layers with greenish-grey mica/ chlorite layers.	Fine-grained sandstone

Table 1. con't

No.	Rock Name	Overall Rock Description	Assumed Parent Rock
6	Mica Schist	Dark greenish-grey mica schist with a few carbonate interbeds. Porphyroclasts are generally plagioclase and quartz. Siliceous marble interbeds are greyish orange-pink in color.	Fine-grained sandstone
7	Mica Schist	Very light-grey mica schist which is possibly a further deformed version of number 8.	(?)
8	Albite Quartz Schist	Well foliated, medium dark-grey albite quartz schist. Porphyroclasts of tabular feldspar grains and quartz show some preferred orientation. Plagioclase laths and quartz compose the groundmass. The rock has a relict intersertal texture.	Tuff or flow rock?

Table 2. Upper Schist Sequence

No.	Rock Name	Overall Rock Description	Assumed Parent Rock
1	Quartz Mica Schist	Strongly foliated medium light grey schist. Quartz and feldspar are generally present as porphyroclasts and show intense deformation. Groundmass is made up of quartz with some muscovite.	Tuff or flow rock?
2	Mica Schist	Dark-grey, finely laminated mica schist with porphyroclasts of feldspar. Muscovite is the principle mineral of the rock.	(?)

faulting were found.

Age and Correlation

The autochthonous and allochthonous rock sequences consist of layered granofelses interbedded with siliceous carbonates and overlain by a sequence of multicolored schists of probable volcanic origin.

Smith and others (1968) assigned a Precambrian age to the sequence of rocks exposed at the Ophir complex. Their age assignment was based on the dissimilarity of the metasedimentary rocks exposed to any of the sedimentary sections in the surrounding ranges. However, it was noted that they could be an unrecognized facies of Mesozoic or Paleozoic rocks.

Moore (1976) suggested a Permian (?) and Triassic age for rocks exposed at the Ophir and Gold Bottom Mine areas. This age assignment was based on the presence of pentagonal pelmatozoan columnals, previously mentioned, the abundance of volcanic material and general lithologic similarities to Triassic rocks exposed in the Argus Range and regionally.

A detailed study of the sedimentary and volcanic rock sequence in the central Slate Range suggests that Moore's age assignment is basically correct. Autochthonous rocks exposed consist of a sequence of layered granofelses with interbedded siliceous marble layers that are in turn overlain conformably (?) by a small sequence of tuffaceous (?) schists; this suggests a tentative correlation with Triassic marine rocks exposed in the southern Inyo and Panamint Mountains (Johnson, 1957; Merriam, 1963; Oborne and Dunne, 1982).

The allochthonous rocks have been grouped into two sequences for correlations: 1) the sequence of rocks overlying the Ophir thrust

fault; and 2) the sequence of rocks overlying the Cherry Mine thrust fault. In the first sequence, the basal unit, a thrust marble, possibly correlates with the Permian Owens Valley Formation, based on the presence of pentagonal pelmatozoan columnals (C.H. Stevens, pers. comm., 1980). Overlying the marble unit is a thick sequence of layered granofelses with discontinuous interbeds of siliceous marble. These rocks may be in part correlative with the upper portion of the Owens Valley Formation and a portion of the Triassic marine sequence. They are in turn overlain by a sequence of multi-colored schists which thin-section analyses have shown to be originally composed of volcanogenic sediments interbedded with volcanic flow rocks, fine-grained sandstones and an occasional carbonate layer. Lithologies similar to this upper unit are present regionally in exposed Triassic sections in the southern Panamint and Inyo Mountains, Argus Range, western Nevada and possibly in sections exposed in the Mojave Desert (Johnson, 1957; Merriam, 1963; Abbott, 1972; Moore, 1976; Speed, 1977, 1978; Oldow, 1978; Oborne and Dunne, 1982). A tentative correlation with regional Triassic volcanic rocks thus seems likely.

A sequence of layered granofelses overlain by another multi-colored schist sequence comprises the second group of allochthonous rocks. One area within the layered granofelses above the Cherry Mine thrust strongly resembles the calcareous shales of the Permian Owens Valley Formation or the Triassic marine rocks. In many localities, metamorphism is so complete that tentative correlation is not possible. The multi-colored schist sequence is similar to the upper unit of rocks in the first group. Thin-section analysis also suggests that these are volcanogenic sediments and are probably correlative with

the same regional Triassic volcanic rocks. In summary, stratified bedrock units exposed in the Ophir complex of the central Slate Range are probably Permian and Triassic in age.

Tertiary (?)

Olivine Basalt

Scattered remnants of widespread basalt flows occur at various localities within the study area (Fig. 6). The basalt weathers medium brown, is vesicular, with phenocrysts of olivine, augite and plagioclase, and has a trachytic texture. Flattened vesicles are common.

Olivine basalt is exposed in the northern Slate and the Argus, Panamint and Coso Ranges to the north and northwest. Correlation based on lithologic similarities of the study area basalts with these basalts suggests an age of about 4 m.y.B.P. (Hall and MacKevett, 1962; Hall, 1971; Moore, 1976; Duffield and others, 1980).

Quaternary

Fanglomerate

The eastern portion of the field area consists of an older fanglomerate which is being dissected by the present drainage (Fig. 6). The fanglomerate consists of pebbles, cobbles and boulders in a sandy matrix. The clasts are locally derived, with minor amounts of carbonate and basalt and a large proportion of the plutonic rocks of the area (predominantly Copper Queen Alaskite).

Moore (1976) suggested a Pliocene or Pleistocene age be assigned to the fanglomerate, as basalt is interbedded with the basal gravels. This age assignment is reasonable.

Figure 6. Map showing the location of Tertiary and Quaternary rocks exposed within the study area.

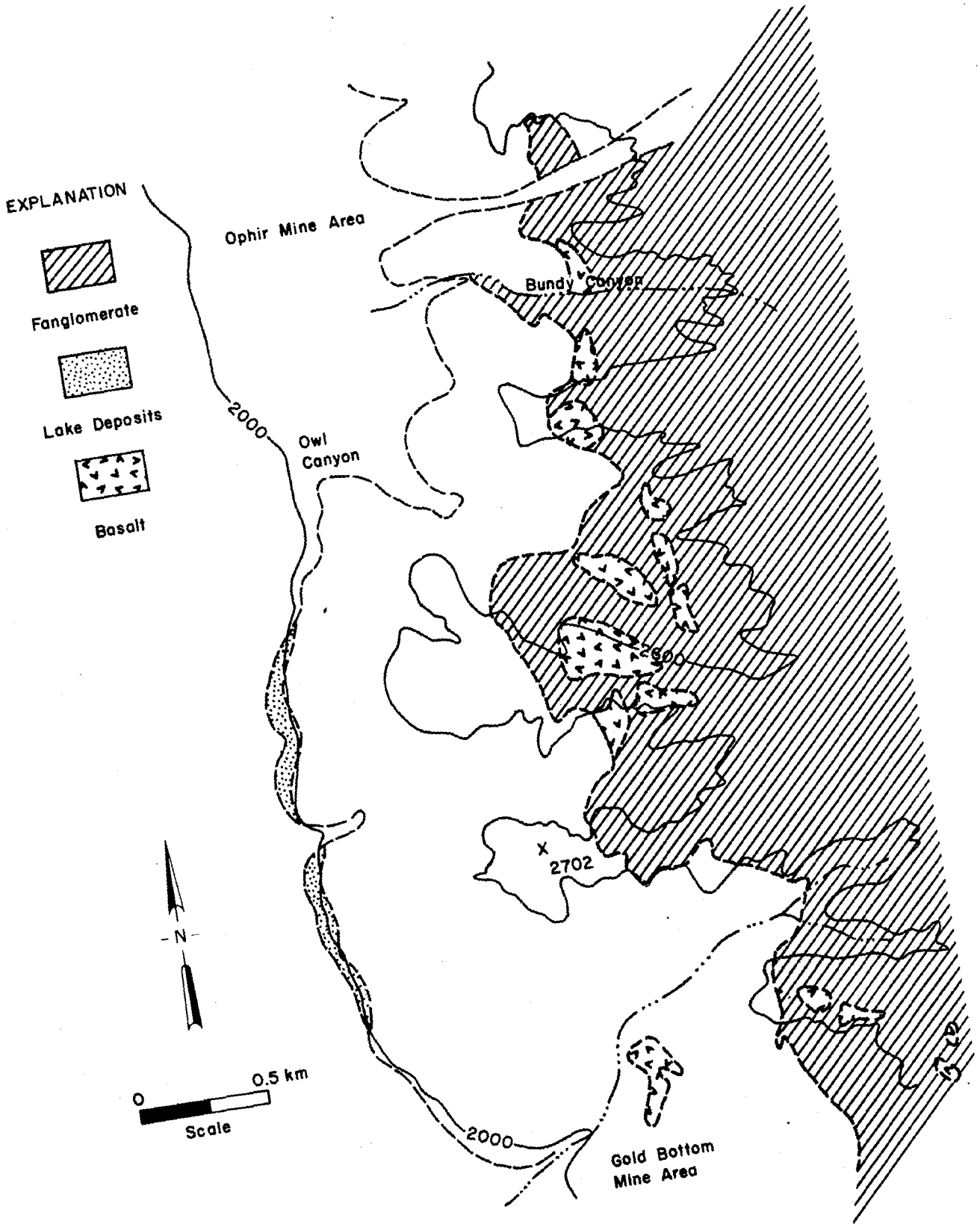
EXPLANATION
Fanglomerate
Lake Deposits
Basalt
Ophir Mine Area
Bundy Cooper
2000
Owl
Canyon
2600
X
2702
N
0
0.5 km
Scale
2000
Gold Bottom
Mine Area

Quaternary Lake Deposits

Pleistocene lake deposits consisting of moderately rounded gravels with a few scattered cobbles occur along the western front of the range in scattered localities (Fig. 6). The gravels are mainly granitic in composition. Toward the playa, silts and sands become the major constituents.

These deposits show the characteristics of beach deposits. Clast sizes coarsen upsection, away from the playa, changing from a silt and sand mixture to moderately rounded gravels. Old shorelines of Lake Searles, represented by strandlines, are present along the western front of the range. Pleistocene deposits of Lake Searles are considered to be mostly Wisconsinan in age (Smith and others, 1968).

Mesozoic Plutonic Rocks

Four plutons with compositions ranging from diorite to alaskite are exposed in the study area. These include the Stockwell Mine diorite, alaskite of Gold Bottom Mine, Isham Canyon granite, and the Copper Queen alaskite (Fig. 7). Twelve representative samples were collected from these plutons and chemically analyzed by methods described in Appendix I. These analyses were not intended for a detailed study of the various igneous bodies; rather, the purpose was to assign the rocks within the study area to the appropriate regional intrusive suite based on modal, chemical and normative compositions. The results of these analyses are presented in Table 3.

These plutons represent the three main phases of igneous intrusion in the region, an alkalic suite, a calc-alkalic suite, and a peraluminous suite (Bateman and others, 1963; Dunne and others, 1978;

Figure 7. Map showing the location of Mesozoic intrusives exposed within the study area.

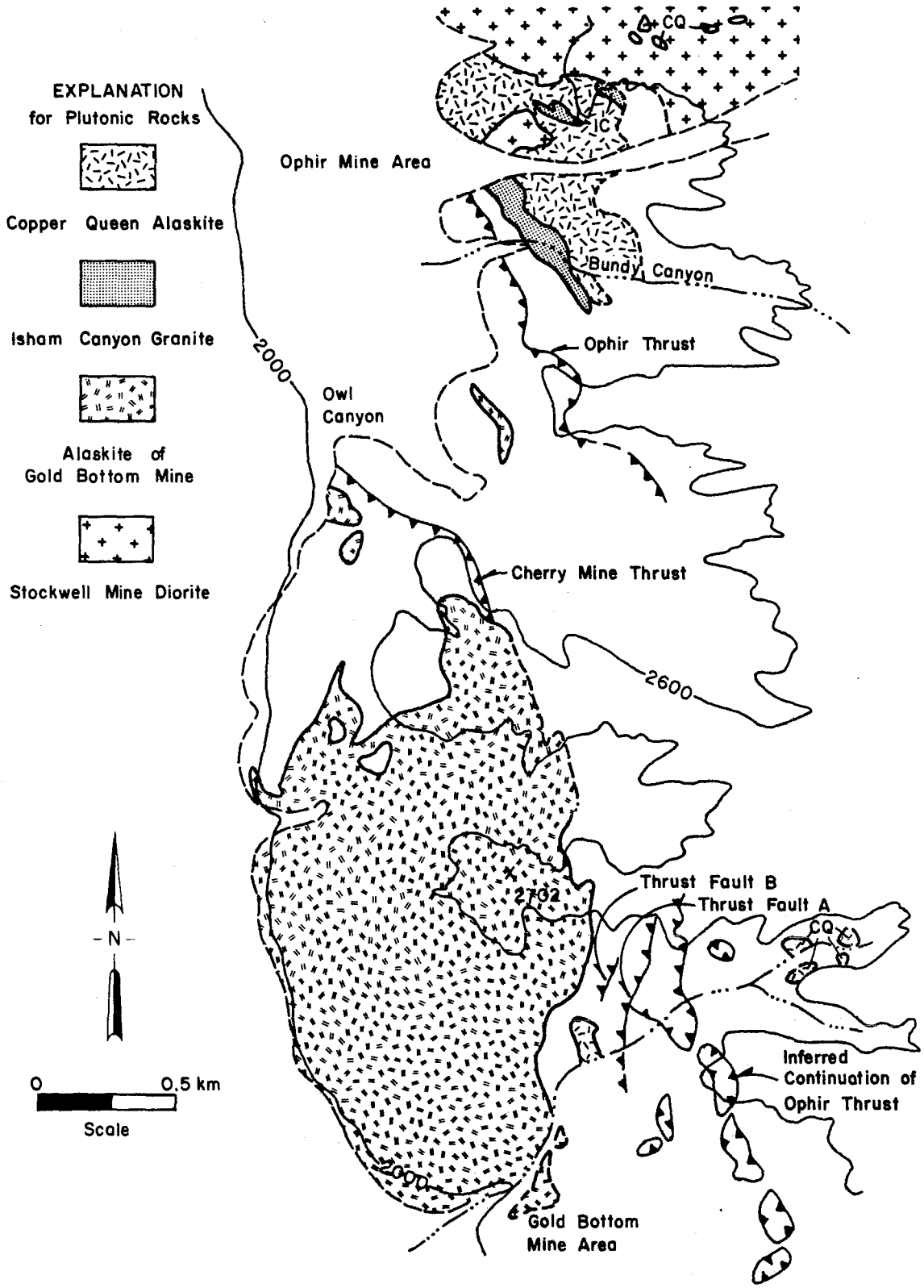
EXPLANATION
for Plutonic Rocks
Copper Queen Alaskite
Isham Canyon Granite
Alaskite of
Gold Bottom Mine
Stockwell Mine Diorite
Ophir Mine Area
CQ
IC
Bundy Canyon
Ophir Thrust
2000
Owl
Canyon
Cherry Mine Thrust
2600
2702
Thrust Fault B
Thrust Fault A
CQ
Inferred
Continuation of
Ophir Thrust
2000
Gold Bottom
Mine Area
N
0
0.5 km
Scale

Table 3. Chemical Composition and Normative Mineralogy - Slate Range Samples of Plutonic Rocks

Plutonic Rocks	Stockwell Mine Diorite		Gold Bottom Mine Alaskite		
Sample No.	SR-84	SR-89	SR-68	SR-273	SR-282
SiO_2	46.64	50.27	74.44	65.34	74.78
Al_2O_3	15.91	19.98	12.40	14.80	13.45
FeO_T	9.40	8.11	-----	1.09	0.85
MgO	5.07	3.77	0.44	1.18	0.23
CaO	10.76	7.89	1.93	4.05	1.01
Na_2O	2.53	4.25	1.83	2.52	2.82
K_2O	0.87	1.60	5.85	8.09	4.70
TiO_2	1.29	1.21	0.26	0.47	0.07
P_2O_5	0.28	0.29	0.16	0.17	0.05
MnO	0.20	0.17	0.03	0.06	0.07
Total	92.95	97.54	97.34	97.77	98.03
CIPW*					
Q	-----	-----	38.11	12.40	38.05
c	-----	-----	-----	-----	2.05
or	5.53	9.70	35.52	48.91	28.34
ab	23.03	32.89	15.91	21.81	24.34
an	31.72	31.49	8.57	5.29	4.78
ne	-----	2.16	-----	-----	-----
wo	-----	-----	-----	1.21	-----
di	19.78	5.61	-----	9.06	-----
hy	5.79	-----	1.13	-----	2.19
ol	10.81	15.12	-----	-----	-----
il	2.64	2.36	0.07	0.91	0.14
ap	0.71	0.70	0.39	0.41	0.12
ru	-----	-----	0.18	-----	-----
sp	-----	-----	0.14	-----	-----

Notes: -- Below detectable limits.
* Constituents normalized to 100%.

Table 3. con't

Plutonic Rocks

	Isham Canyon Granite			Copper Queen Alaskite	
Sample No.	SR-83	SR-85	SR-97	SR-64	SR-65
SiO_2	70.49	76.04	68.65	78.02	78.30
Al_2O_3	14.94	13.45	14.09	11.75	11.71
FeO_T	2.52	0.79	3.50	-----	0.21
MgO	1.11	-----	1.03	0.37	0.37
CaO	3.00	0.36	3.07	0.79	0.55
Na_2O	3.26	4.44	2.70	3.10	3.01
K_2O	4.70	4.82	4.57	4.50	4.66
TiO_2	0.34	-----	0.45	0.03	0.04
P_2O_5	0.16	0.03	0.14	0.08	0.08
MnO	0.05	0.03	0.07	0.01	0.01
Total	100.57	99.96	98.27	98.65	98.94
CIPW*					
Q	24.21	30.40	25.85	41.30	41.73
c	-----	0.35	-----	0.54	0.91
or	27.62	28.50	27.49	26.96	27.84
ab	27.43	37.58	23.25	26.59	25.74
an	12.18	1.59	13.05	3.44	2.23
ne	-----	-----	-----	-----	-----
wo	-----	-----	-----	-----	-----
di	1.33	-----	1.29	-----	-----
hy	6.22	1.51	7.87	0.93	1.27
ol	-----	-----	-----	-----	-----
il	0.64	-----	0.87	0.02	0.08
ap	0.38	0.07	0.34	0.19	0.19
ru	-----	-----	-----	0.02	-----
sp	-----	-----	-----	-----	-----

Note: -- Below detectable limits.
* Constituents normalized to 100%.

Table 3. con't

Plutonic Rocks

Sample No.	Copper Queen Alaskite SR-71	SR-96
SiO_2	76.76	78.82
Al_2O_3	12.54	13.33
FeO_T	0.06	0.36
MgO	0.37	-----
CaO	0.25	0.25
Na_2O	3.75	4.08
K_2O	4.39	4.38
TiO_2	-----	-----
P_2O_5	0.12	0.04
MnO	0.02	0.08
Total	98.26	101.29
CIPW*		
Q	37.98	37.09
c	1.48	1.50
or	26.41	25.56
ab	32.29	34.08
an	0.47	0.97
ne	-----	-----
wo	-----	-----
di	-----	-----
hy	1.09	0.71
ol	-----	-----
il	-----	-----
ap	0.29	0.09
ru	-----	-----
sp	-----	-----

Notes: -- Below detectable limits.
* Constituents normalized to 100%.

Sylvester and others, 1978; Miller and Bradfish, 1980).

McAllister (1956) described and named a series of heterogeneous quartz monzonitic rocks exposed in the north end of Panamint Valley as the Hunter Mountain Quartz Monzonite. Correlative alkalic rocks also crop out in the Darwin quadrangle, the Argus Range and the White-Inyo Mountains (Fig. 8; Hall and MacKevett, 1962; Moore, 1976; Dunne and others, 1978; Sylvester and others, 1978).

Principal petrologic features of the closest well-studied alkalic intrusion, the Hunter Mountain batholith, are as follows. Three main facies are present, ranging in composition from quartz monzonite to monzogabbro (Dunne and others, 1978). These rocks were emplaced during the period from 185 to 156 m.y.B.P. (Early to Middle Jurassic; Dunne, 1979). Typically, they are quartz-poor and alkali-feldspar rich. They have a low to moderate SiO_2 content (52 to 62 wt %), are enriched in $K_2O + Na_2O$ (8 wt %) and have high Sr abundances (Miller, 1977; Dunne and others, 1978; Sylvester and others, 1978). Common to these rocks is normative nepheline (Dunne and others, 1978).

The calc-alkalic suite is the next prominent regional rock type and comprises the Sierra Nevada batholith and compositionally similar "Sierran-type" rocks. Sierran-type rocks are found as far east as the Panamint Range, and they are chemically and modally similar to and are considered to be satellites of the main batholith (Fig. 8; Hall and MacKevett, 1962; Ross, 1965, 1969; Dunne and others, 1978).

A synopsis of the main characteristics is presented below. Sierran rocks range in composition from granite to granodiorite and were emplaced intermittently from 215 to 75 m.y.B.P. (Bateman and others, 1963; Dunne and others, 1978). Characteristically, Sierran

Figure 8. Generalized geologic map showing the distribution of granitic rock types after Dunne and others (1978), Miller and Bradfish (1980) and Dunne (pers. comm., 1982).

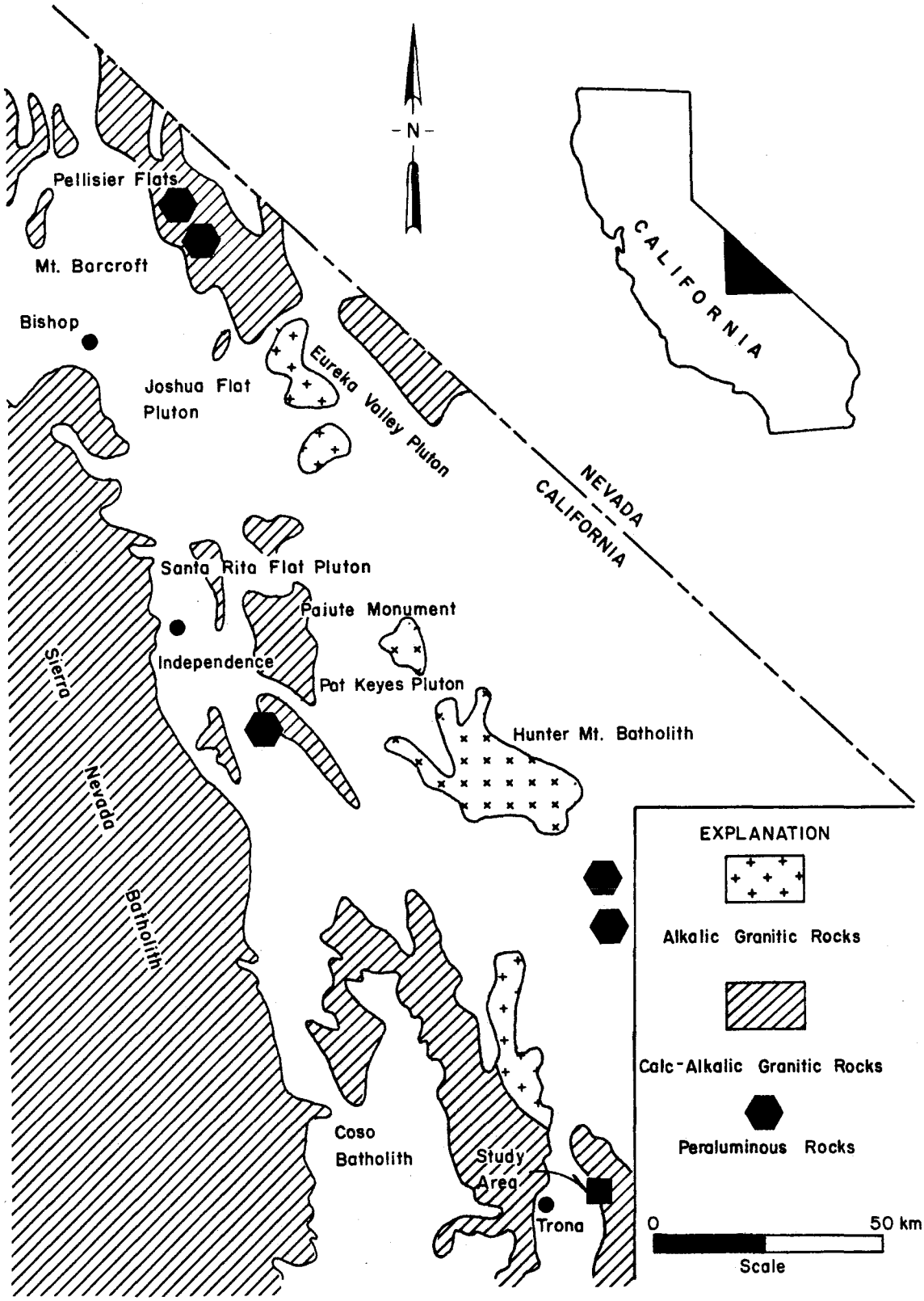
N
CALIFORNIA
Pellisier Flats
Mt. Barcroft
Bishop
Joshua Flat
Pluton
Eureka Valley Pluton
NEVADA
CALIFORNIA
Santa Rita Flat Pluton
Paiute Monument
Independence
Pat Keyes Pluton
Hunter Mt. Batholith
Sierra
Nevada
Batholith
Coso
Batholith
Study
Area
Trona
EXPLANATION
Alkalic Granitic Rocks
Calc-Alkalic Granitic Rocks
Peraluminous Rocks
0
50 km
Scale

rocks show a lower K-feldspar/quartz ration than the alkalic rocks discussed earlier (Dunne and others, 1978). They also show an enrichment in SiO_2 and normative quartz (Dunne and others, 1978).

The third suite of plutonic rocks occurs in a belt extending from northern Sonora into British Columbia. These rocks are peraluminous and range in age from Jurassic to mid-Tertiary (120 to 50 m.y.B.P.). Compositions vary from granite to granodiorite, with primary muscovite, Al-rich biotite and garnet being common. These rocks show a high SiO_2 content (> 70 wt %), $Al_2O_3/(CaO + Na_2O + K_2O)$ ratio > 1, high K_2O and Na_2O, high initial Sr ratios and normative corundum (> 1 wt %; Miller and Bradfish, 1980; Clarke, 1981).

Stockwell Mine Diorite

The northern portion of the field area consists predominantly of the Stockwell Mine diorite (Fig. 7). This medium-grey, hornblende-rich diorite is highly variable in both composition and texture. Table 4 presents the modal data for the Stockwell Mine diorite, based on a point count analysis (1200 points) of both stained slabs and thin sections. Plagioclase and hornblende comprise the majority of the rock. Biotite is present in variable but commonly minor amounts. The most notable characteristic of the rock is the paucity of potassium feldspar. Accessories include opaques and zircon. Intense alteration has occurred locally, as manifested by the presence of abundant chlorite and epidote. Texturally, the pluton ranges from a fine-grained rock with a "salt and pepper"-like appearance to a coarse crystalline variety with prominent hornblende phenocrysts.

Intrusion of the Stockwell diorite by the Isham Canyon granite and the Copper Queen alaskite has resulted in irregular contacts in

Table 4. Summary of major petrologic properties for the plutonic rocks of the central Slate Range.

	Stockwell Mine Diorite		Gold Bottom Mine Alaskite	Isham Canyon Granite		Copper Queen Alaskite	
Sample No.	SR-84	SR-89	SR-68	SR-83	SR-64	SR-65	SR-71
% Plag	39	66	22	36	21	36	30
(An)	36	33	10	30	30	30	16
% K-spar	--	--	57	--	46	27	36
% Qtz	3	5	21	27	33	37	34
% Bio	--	9	--	4	--	--	--
% Hbl	58	20	--	3	--	--	--
% Cpx	--	--	--	--	--	--	--

the diorite. The diorite was also intruded by a series of small dark green mafic dikes. In contrast to the other intrusive bodies, the Stockwell Mine diorite has a low relief. The Stockwell Mine diorite has not been dated. Moore (1976) correlated it with a 145 m.y. old biotite-bearing diorite exposed in Coyote Canyon in the Panamint Range.

Two samples from the Stockwell Mine diorite were chemically analyzed; the results are presented in Table 3. Characteristically, the diorite has a low SiO_2 content (46 and 50 wt %), high CaO concentrations (7.9 and 10.0 wt %) and low concentrations of the alkalis. Normative mineralogy includes nepheline, olivine, hypersthene and diopside. Correlation based on chemistry and normative and modal mineralogy suggests that the Stockwell Mine diorite may be tentatively assigned to the Hunter Mountain batholith (see Discussion).

Alaskite of Gold Bottom Mine

The central portion of the study area (Fig. 7) is occupied by the strongly deformed alaskite of Gold Bottom Mine. This alaskite intrudes metasedimentary and metavolcanic rocks of the allochthonous plate.

Typically a greenish-grey to greyish-pink alaskite, it is composed predominantly of potassium feldspar with minor amounts of quartz and plagioclase (Table 4). Accessories include zircon and apatite; no mafics are present in the rocks. Texturally, the alaskite is medium-grained, hypidiomorphic granular. Numerous quartz veinlets and stringers cut the alaskite, which contains a pervasive, locally well-developed cataclastic planar foliation. It is exhibited in thin section by the alignment of complete, crushed, broken and sheared grains, forming a "mortar-like" texture. Foliation planes

are approximately 0.1 to 0.2 cm in spacing.

The contacts between the alaskite and the overlying country rocks are sharp. The country rocks show prominent contact metamorphism. Where the alaskite has been intruded by the younger Copper Queen alaskite, no contact metamorphism is evident.

Chemically, the alaskite is relatively high in SiO_2 (65 to 75 wt %; Table 3). Values of K_2O for the samples analyzed averaged 5.2 wt %. Concentrations of total FeO are low, generally < 1 %. The alaskite has approximately equal amounts of normative quartz, potassium feldspar and plagioclase, and contains no normative nepheline (Table 3).

Moore (1976) assigned an age of pre-Late Jurassic to the alaskite. His age assignment is based on two points: 1) the alaskite intrudes rocks of inferred Triassic age; and 2) structures in the alaskite are inferred to be related to the emplacement of the Ophir thrust, which he considered to be the same age (Late Jurassic) as the Argus-Sterling thrust. Based on field relationships this age is reasonable.

Isham Canyon Granite

The Isham Canyon pluton is composed of a pale pink granite which crops out in Bundy Canyon east of the Ophir thrust (Fig. 7). The granite is composed predominantly of quartz and potassium and plagioclase feldspar, with a minor amount (< 10 %) of small anhedral to subhedral grains of biotite and hornblende (Table 4). Accessories include apatite, zircon and opaques. The medium- to coarse-grained granite has an overall hypidiomorphic granular texture.

Evidence of some tectonic deformation is exhibited by irregular twinning and kinking of plagioclase grains, and bent and broken potas-

sium feldspar and biotite grains. Early-formed minerals show some subsequent reaction with the melt. Chlorite alteration of the biotite and hornblende is fairly complete.

Characteristically, the Isham Canyon pluton forms resistant knobs, in contrast to the surrounding layered granofelses/hornfelses and igneous rocks. The contact between the pluton and the country rock is characterized by an intrusion breccia (Fig. 9) and a contact aureole. A sharp contact exists between the younger Copper Queen alaskite and the Isham Canyon granite. A large amount of fracturing and shearing has occurred along the contact, with the Isham Canyon granite having a baked zone of greyish-green to dark-green rocks. The contact zone in the Isham Canyon rock shows an enrichment of quartz and epidote. It is also cut by numerous small aplite dikes. Outcrops of the Isham Canyon granite are discontinuous, and are usually truncated by the younger alaskite.

Small pods of Isham Canyon granite are also present to the north of Bundy Canyon. These pods intrude the older Stockwell Mine diorite.

The Isham Canyon granite has a moderately high concentration of SiO_2 (68 to 76 wt %; Table 3). The alkalis and CaO are approximately equal in concentrations between samples, except for one sample which is low in CaO. Normative plagioclase, quartz and potassium feldspar are present in approximately equivalent amounts. Again, no normative nepheline is present.

Moore (1976) relates the Isham Canyon "quartz monzonite" to the Hunter Mountain quartz monzonite or the Argus Sterling Mine quartz monzonite based on mineralogic similarities. Based on compositional

Figure 9. Intrusion breccia along the contact between the Isham Canyon granite and the country rock.

similarities to a hornblende-biotite quartz monzonite present at Manly Peak, a minimum age of 137 m.y. was tentatively suggested for this pluton (Moore, 1976).

Copper Queen Alaskite

The Copper Queen alaskite is the youngest intrusive within the area studied. Its main exposure is in Copper Queen Canyon southeast of the study area (Fig. 7). Characteristically moderate pink in color, it is composed of nearly equal amounts of plagioclase, potassium feldspar and quartz (Table 4). Accessories include zircon and a few mafics. The alaskite is coarse-grained with an hypidiomorphic

granular texture. Bending and fracturing of some of the grains was observed in thin section. This probably occurred during emplacement when the intrusion was a crystal mush.

Numerous aplitic veins and veinlets occur throughout the surrounding country rocks, suggesting that a substantial amount of late-stage fluid was probably present during the emplacement of the alaskite. The contact between the alaskite and the layered granofels/hornfels is generally sharp, with a well-developed baked zone. However, where the Copper Queen alaskite has intruded the alaskite of Gold Bottom Mine, a sharp contact exists, but no baked zone is present.

Chemically, the Copper Queen alaskite has the highest SiO_2 content of the intrusives exposed (78 wt %; Table 3). The alkalis have nearly equivalent concentrations (Na_2O = 3%; K_2O = 4%) and the remainder of the elements are < 1% in concentration. Normative mineralogy shows the alaskite enriched in quartz with approximately equal amounts of plagioclase and potassium feldspar. No normative nepheline is present.

Moore (1976) postulates a latest Jurassic to Early Cretaceous age for the Copper Queen pluton on the basis of mineralogic similarities to the Bendire Canyon pluton, in the Argus Range, and other leucocratic bodies in the Inyo Mountains. This age is in agreement with field relationships.

Discussion

Slate Range intrusives are exposed near the eastern limit of the Sierran intrusive rocks and on trend with the Hunter Mountain batholith or "alkalic" rocks (Fig. 8). Rocks exposed range in composition

from diorite to granite and are thought to be latest Jurassic in age. Based on mineral composition and chemistry, the intrusives of the Slate Range can be divided into three groups.

The first group contains only one pluton, the Stockwell Mine diorite. Mineralogically, the Stockwell Mine diorite is composed predominantly of plagioclase and hornblende with minor amounts of biotite. The most notable characteristic is the paucity of potassium feldspar. Chemically, it has a low SiO_2 content and moderate concentrations of CaO and the alkalis. The normative mineralogy includes nepheline.

The second group includes two plutons, the alaskite of Gold Bottom Mine and the Isham Canyon granite. These rocks are generally enriched in quartz, plagioclase and potassium feldspar. Mafics, such as biotite and hornblende, are a minor constituent if present. Chemically, they have a high SiO_2 content and approximately equal concentrations of CaO and the alkalis. These rocks are generally enriched in normative quartz, plagioclase and potassium feldspar, with no normative nepheline present.

Only one pluton, the Copper Queen alaskite, belongs to the last group. Analyses of the alaskite suggest that it possibly correlates with the suite of peraluminous plutonic rocks. Copper Queen rocks are enriched in SiO_2, have an $Al_2O_3/(CaO + Na_2O + K_2O)$ ratio > 1, and contain normative corundum.

Figure 10 is a ternary diagram comparing essential modal mineralogy of the central Slate Range to alkalic and Sierran/Sierran-type intrusives. Modal data of the Stockwell Mine diorite plot outside both of the regional fields due to the lack of potassium feldspar.

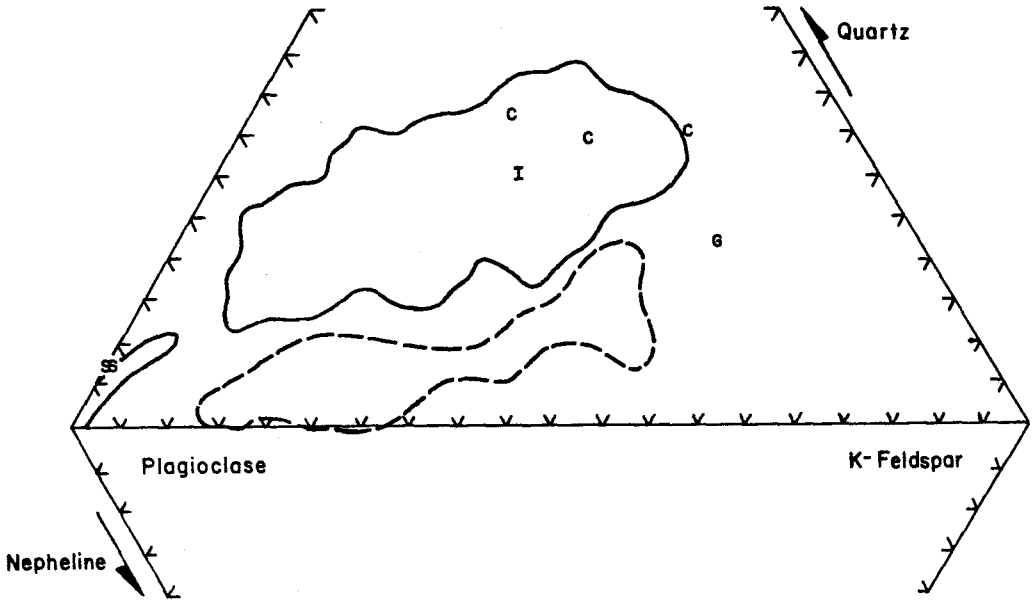

Figure 10. Comparison of essential modal mineralogy of the central Slate Range (points: S-Stockwell diorite, G-alaskite of Gold Bottom Mine, I-Isham Canyon granite, C-Copper Queen alaskite), Sierran/Sierran-like (solid line) and alkalic (dashed line) plutons. Data is from Moore (1963), Bateman (1965) and Dunne and others (1978).

One sample, the Isham Canyon granite, correlates well with the Sierra Nevada. However, the sample from the alaskite of Gold Bottom Mine does not, plotting outside of the Sierran field. This is due to an enrichment in potassium feldspar, possibly resulting from the introduction of K_2O-rich fluids during intrusion or movement of K_2O-rich fluids during deformation. Samples of the Copper Queen alaskite plot well within the modal field defined by the Sierran/Sierran-like rocks. This is not surprising, because the essential mineralogy of the calc-alkalic Sierran rocks and the peraluminous suite should be essentially the same.

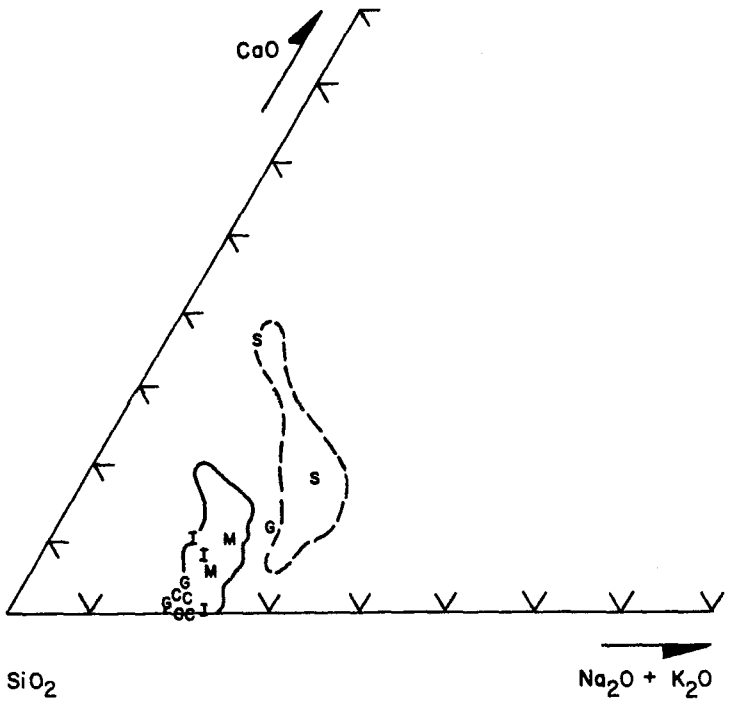

Figure 11. Comparison of CaO, $Na_2O + K_2O$ and SiO_2 content of the central Slate Range (points: S-Stockwell diorite, G-alaskite of Gold Bottom Mine, I-Isham Canyon granite, C-Copper Queen alaskite, M-data from Mueller), with Sierran/Sierran-like (solid line) and alkalic (dashed line) plutons. Data is from Moore (1963), Bateman (1965), Dunne and others (1978) and Mueller (pers. comm., 1975).

Two samples chemically analyzed from the Stockwell Mine diorite plot well within the alkalic field on a plot of CaO, $Na_2O + K_2O$ and SiO_2 concentrations (Fig. 11). Both samples show a low concentration of SiO_2 (46 and 50 wt %) and moderate concentrations of CaO and the alkalis.

Analyses from the alaskite of Gold Bottom Mine and the Isham Canyon granite fall well within the Sierran field (Fig. 11). The

concentrations of SiO_2 average about 72 wt %. The values for K_2O are at least 4 wt %, which is in agreement with those determined by Bateman and Dodge (1970). Only one exception occurs in this data set; this is one of the analyses of the alaskite of Gold Bottom Mine. Chemically this analysis (SR-273) plots closer to the alkalic field having a lower concentration of SiO_2 (65 wt %). This discrepancy in chemistry is probably due to the introduction of late stage K_2O-rich fluids to the rock. Because it is located in close proximity to the Cherry Mine thrust (Plate 1), a strong shearing and alteration of this sample has occurred that has resulted in the secondary growth of potassium feldspar porphyroblasts.

Comparison of the Copper Queen pluton to alkalic and Sierran suites (Fig. 11) shows that CaO, $Na_2O + K_2O$ and SiO_2 values correspond to values determined for Sierran/Sierran-like rocks. This is to be expected if the compositions are similar between Sierran/Sierran-like rocks and peraluminous rocks. Other factors which further suggest a probable peraluminous association are high concentrations of SiO_2 (> 76 wt %), moderate amounts of K_2O and Na_2O (> 3 wt %), and $Al_2O_3/(CaO + Na_2O + K_2O)$ ratios > 1.4.

Mueller (pers. comm., 1975) determined major and trace element chemistry on three samples from what he thought was a composite pluton near Ophir Mine. Field relationships indicate that his "Ophir Mine pluton" is not a composite body, but consists of both the Isham Canyon granite and Copper Queen alaskite. Evaluation of the chemical data presented by Mueller suggests that two of the analyses (SiO_2 = 68%) are probably samples from the Isham Canyon pluton

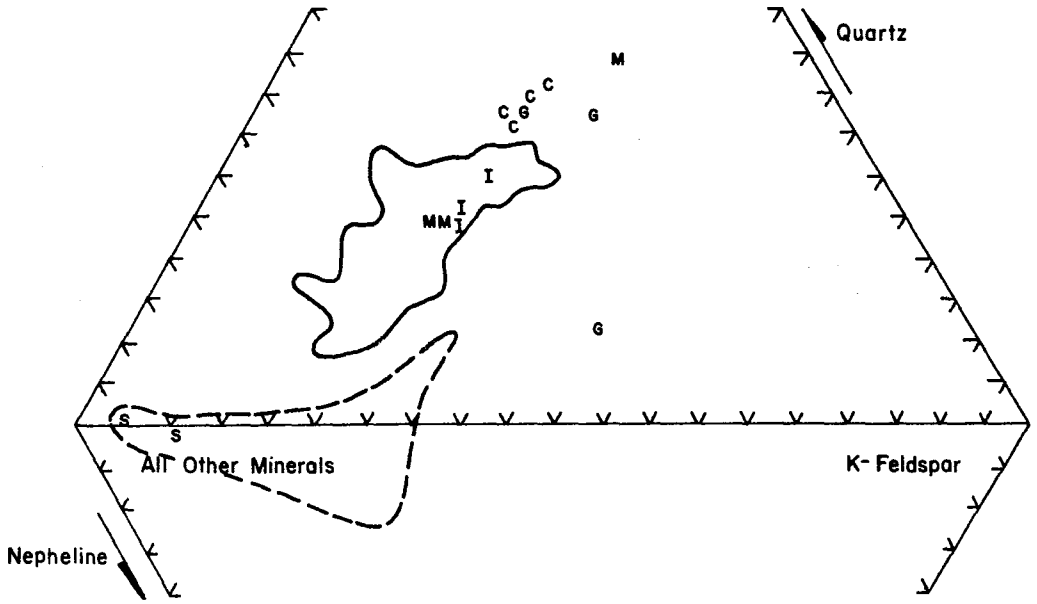

Figure 12. Comparison of normative mineralogy of the central Slate Range (points: S-Stockwell diorite, G-alaskite of Gold Bottom Mine, I-Isham Canyon granite, C-Copper Queen alaskite, M-data from Mueller), Sierran/Sierran-like (solid line) and alkalic (dashed line) plutons. Data is from Moore (1963), Bateman (1965), Dunne and others (1978) and Mueller (pers. comm., 1975).

and the third analysis (SiO_2 = 80%) is from the Copper Queen alaskite. Discrepancies between other elements also agree with this interpretation. The three analyses are plotted on Figure 11. All three analyses plot within the Sierran/Sierran-like field grouped with their respective rock types determined from this study.

Normative mineralogy from this study for the Stockwell diorite includes nepheline, olivine, hypersthene and diopside, again placing the rocks well within the alkalic field (Fig. 12). Normative mineralogy for the Isham Canyon granite also suggests a Sierran affinity (Fig. 12). These rocks are generally rich in normative quartz (values of about

25 wt %), have similar amounts of potassium feldspar and other minerals, and contain no normative nepheline. The analyses for the alaskite of Gold Bottom Mine plot outside of the Sierran/Sierran-like field (Fig. 12), having a higher abundance of normative quartz and potassium feldspar, reflecting the change in the chemistry of the rocks noted earlier. Normative minerals for the Copper Queen alaskite plot well above the Sierran field (Fig. 12), showing a strong enrichment in normative quartz, reflecting the high SiO_2 content of these rocks. Normative corundum is also present in the Copper Queen alaskite.

Normative mineralogy determined for the rocks analyzed by Mueller (pers. comm., 1975) again suggest derivation from two plutons, the Isham Canyon granite and the Copper Queen alaskite. When plotted (Fig. 12), the analyses again group by their respective pluton.

In summary, mineralogical and chemical properties of these rocks make plausible the correlation of the Stockwell Mine diorite with the alkalic suite, the alaskite of Gold Bottom Mine and Isham Canyon granite with the Sierran suite and the Copper Queen alaskite with the peraluminous suite. The presence of all three suites of plutonic rock indicate changes in the source magmas within the region through time, from alkalic to calc-alkalic to peraluminous.

Mesozoic Dike Rocks

Two types of mafic dikes have been recognized within the central Slate Range (Fig. 13). One set of mafic dikes is strongly foliated and oriented in a northeasterly direction. The other set is non-foliated and oriented in a northwesterly direction.

Figure 13. Map showing the location of all of the mafic dikes exposed in the study area. Rose diagrams illustrate the difference in orientation between the foliated and non-foliated dikes.

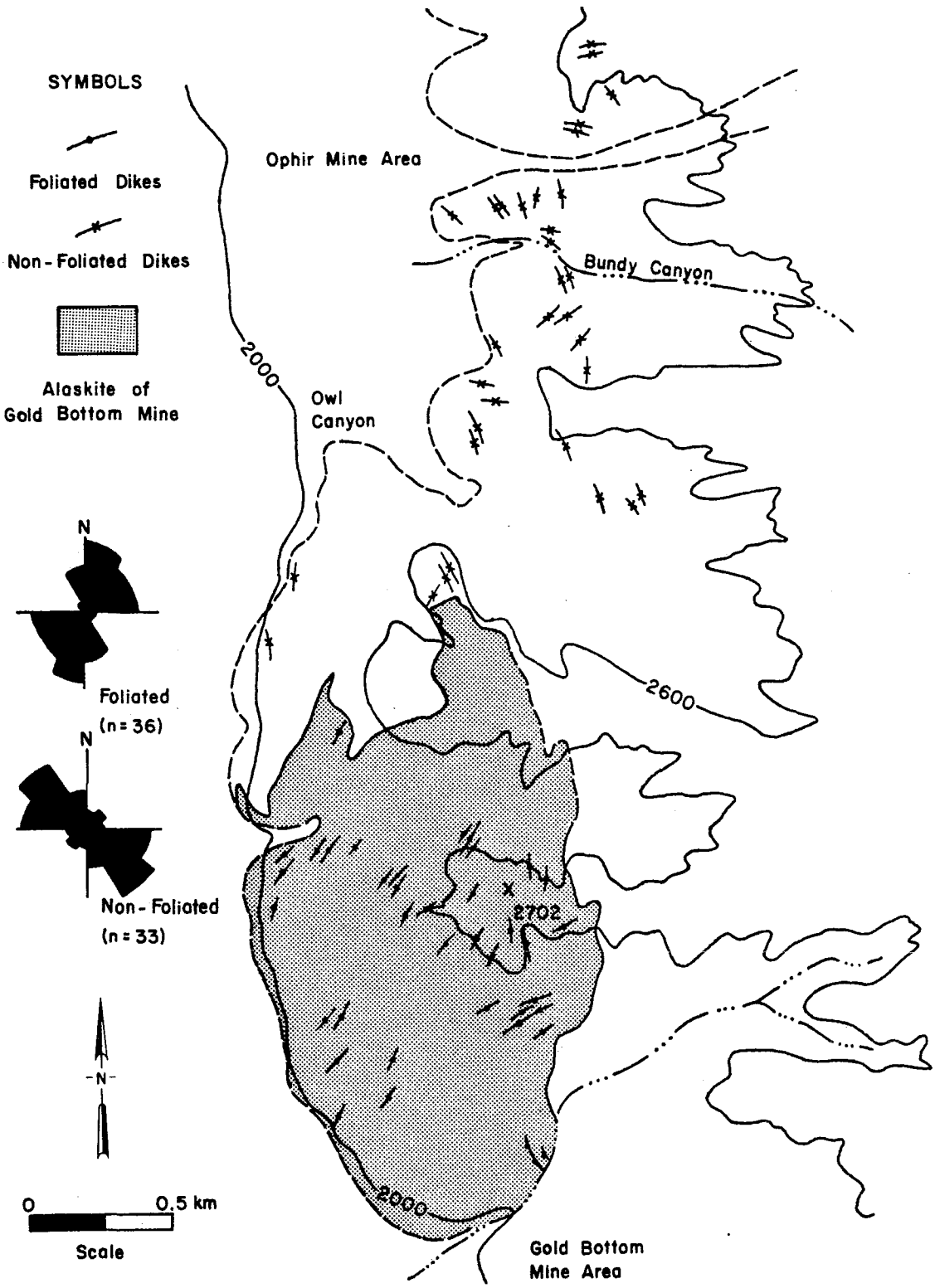
SYMBOLS
Foliated Dikes
Non-Foliated Dikes
Alaskite of Gold Bottom Mine
Ophir Mine Area
Bundy Canyon
2000
Owl Canyon
2600
2702
2000
Gold Bottom Mine Area
N
Foliated (n = 36)
N
Non-Foliated (n = 33)
N
0
0.5 km
Scale

Three representative samples of the non-foliated dikes were collected and chemically analyzed by the method described in Appendix 1. The results are presented in Table 5.

A major regional dike swarm extends for at least 250 km from the central Sierra Nevada to south of the Garlock fault (Fig. 14). A synopsis of its characteristics is presented here. Originally described and named by Moore and Hopson (1961), the Independence dike swarm is an en echelon series of northwest-striking dikes, ranging in composition from a fine-grained microcrystalline diorite or diorite porphyry to a microcrystalline granite or granite porphyry (Moore and Hopson, 1961; Chen and Moore, 1979). Rocks sampled along the trace of the swarm give a concordant U/Pb age of 148 m.y.B.P. (Chen, 1977; Chen and Moore, 1979).

The mafic variety of dikes has a primary mineralogy of green hornblende or augite, plagioclase, biotite and a subordinate amount of quartz (Moore and Hopson, 1961). As the rocks become more felsic, plagioclase, potassium feldspar and quartz become the primary minerals. The dikes are classified as calc-alkaline to weakly basaltic, with SiO_2 concentrations ranging from 45 to 71 wt % (Chen and Moore, 1979). An enrichment of CaO relative to the alkalis is common.

Foliated Dikes

The foliated dikes are oriented predominantly in a northeasterly direction (Fig. 13) and occur mainly within the alaskite of Gold Bottom Mine in the southern half of the study area. The dike rocks are generally dark green in color and are aphanitic. The degree of foliation varies from faint to intense, parallels the dike walls, and the strike and dip of the whole dike almost always follows that

Table 5. Chemical Composition and Normative Mineralogy - Slate Range Samples of Non-Foliated Mafic Dikes

Mafic Dikes

Sample No.	Non-Foliated SR-93	SR-95	SR-236
SiO_2	54.77	48.42	49.17
Al_2O_3	14.70	17.43	15.36
FeO_T	7.35	8.72	6.54
MgO	4.63	4.61	3.72
CaO	6.40	7.96	7.41
Na_2O	2.98	4.04	3.77
K_2O	3.38	2.39	4.27
TiO_2	0.88	1.64	1.03
P_2O_5	0.36	0.71	0.42
MnO	0.28	0.19	0.14
Total	95.73	96.11	91.83
CIPW*			
Q	1.99	-----	-----
c	-----	-----	-----
or	20.87	14.70	27.48
ab	26.34	25.39	18.96
an	17.50	23.27	13.48
ne	-----	5.51	8.55
wo	-----	-----	-----
di	10.97	10.82	19.59
hy	19.72	-----	-----
ol	-----	15.36	8.76
il	1.75	3.24	2.13
ap	0.89	1.75	1.08
ru	-----	-----	-----
sp	-----	-----	-----

Notes: -- Below detectable limits.
* Constituents normalized to 100%.

Figure 14. Generalized geologic map (after Jennings, 1977; Chen and Moore, 1979) showing the distribution of the Independence dike swarm.

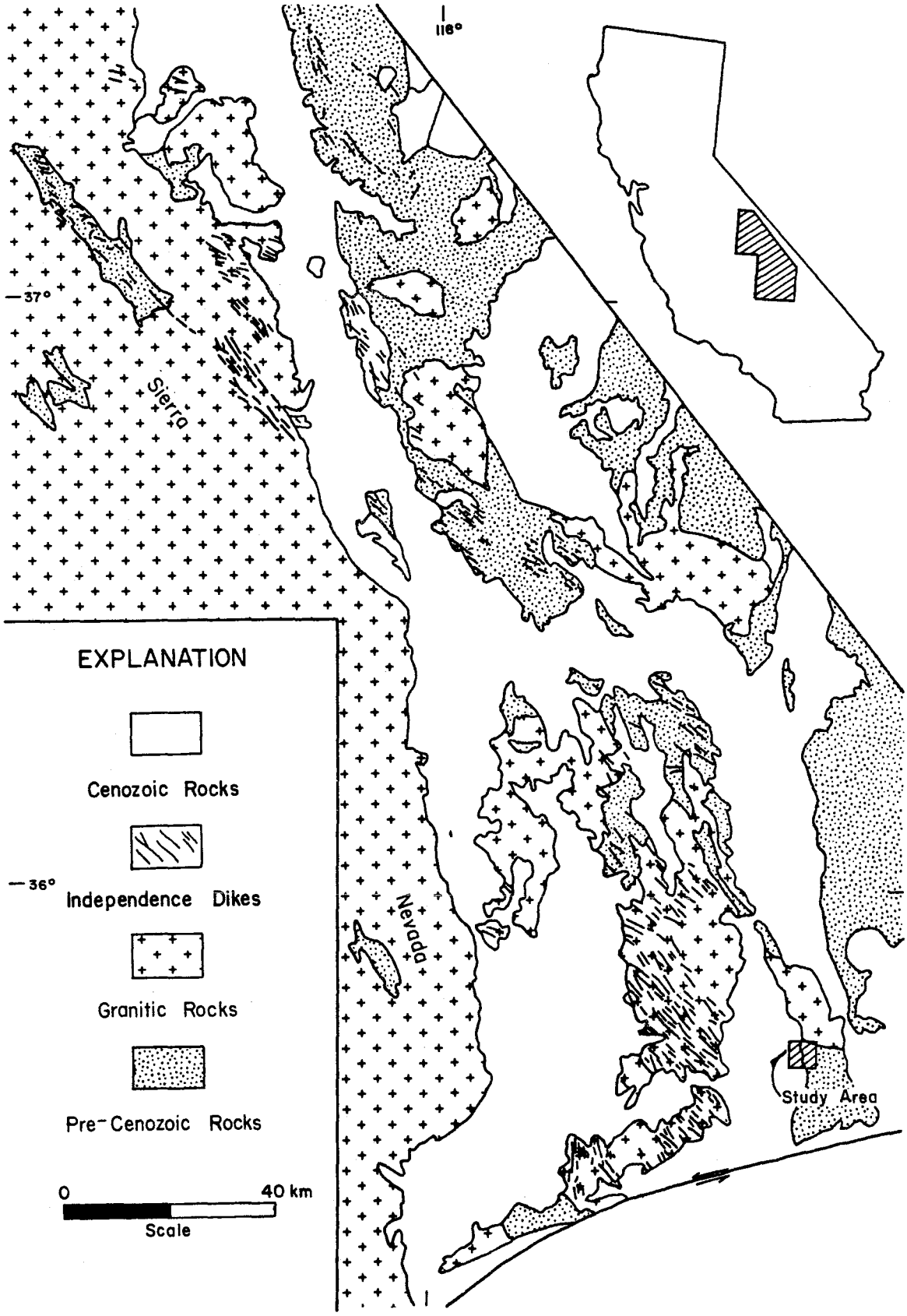
118°
37°
36°
Sierra
Nevada
Study Area
EXPLANATION
Cenozoic Rocks
Independence Dikes
Granitic Rocks
Pre-Cenozoic Rocks
0
40 km
Scale

of the enclosing granitic body. The dikes do not appear to have metamorphosed the surrounding country rocks.

The dikes were emplaced prior to or at the same time as the deformation of the enclosing alaskite of Gold Bottom Mine and are older than the non-foliated set.

Non-Foliated Dikes

The non-foliated dikes are oriented in a northwesterly direction (Fig. 13). The dikes are pervasive, intruding all of the rock units present except the Copper Queen alaskite. Occasionally, the dikes follow the foliation of the surrounding country rocks. They exhibit chilled margins.

The dikes range in color from greenish-black on a fresh surface to a dark greenish-grey to a moderate brown on a weathered surface. Both porphyritic and aphanitic varieties occur. The porphyritic variety generally has phenocrysts of hornblende ranging in size up to 4 mm (1 mm is the average). Occasionally plagioclase and quartz occur as phenocrysts. Alteration of the dikes to chlorite and epidote is fairly complete.

Table 6 presents the modal data for three mafic dikes based on point count analysis (1200 points) of thin sections.

Discussion

Non-foliated dikes in the central Slate Range trend in the same direction as the Independence dike swarm. However, the swarm was not considered to continue into the central Slate Range.

Mineralogically, the dikes examined from the study area are similar in composition to those of the Independence dike swarm. Pheno-

Table 6. Summary of major petrologic properties of the mafic dikes exposed in the central Slate Range.

Sample No.	Mafic Dikes SR-80	SR-93	SR-95
% Plag	40*	30	35*
(An)	--	24	27
% K-spar	--	--	--
% Qtz	5	10	8
% Bio	4	15	10
% Hbl	45	44	45
% Cpx	--	--	--

Note: * Indicates total feldspar.

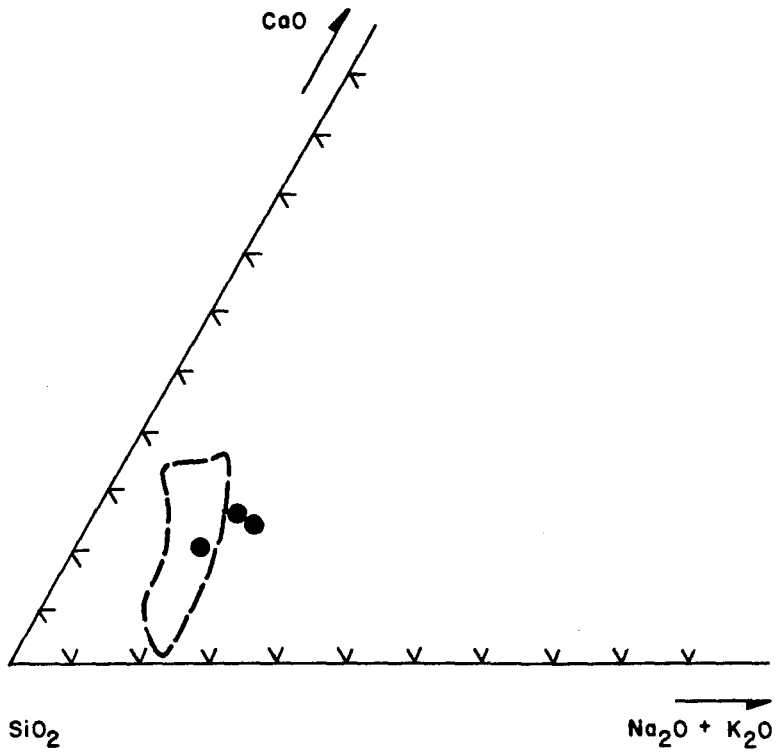

Figure 15. Comparison of CaO, $Na_2O + K_2O$ and SiO_2 content of the Independence dike swarm (dashed line) and related(?) dikes (• symbol) in the central Slate Range. Data from Chen and Moore (1979) is dashed.

crysts of hornblende and plagioclase give a porphyritic appearance to the dikes. Quartz and biotite also compose the primary mineralogy. Accessory minerals include zircon, sphene and opaques. Alteration of the rock to epidote is common. Thus, the Slate Range dikes are modally similar to the Independence dikes (Moore and Hopson, 1961).

Chemical concentrations of CaO, $Na_2O + K_2O$ and SiO_2 for 10 samples of the Independence dikes are compared to those samples analyzed from the Slate Range (Fig. 15). Concentrations determined for the Slate Range samples are similar to those determined for the Independence dikes; only a 2 to 3 wt % variation exists in the amount

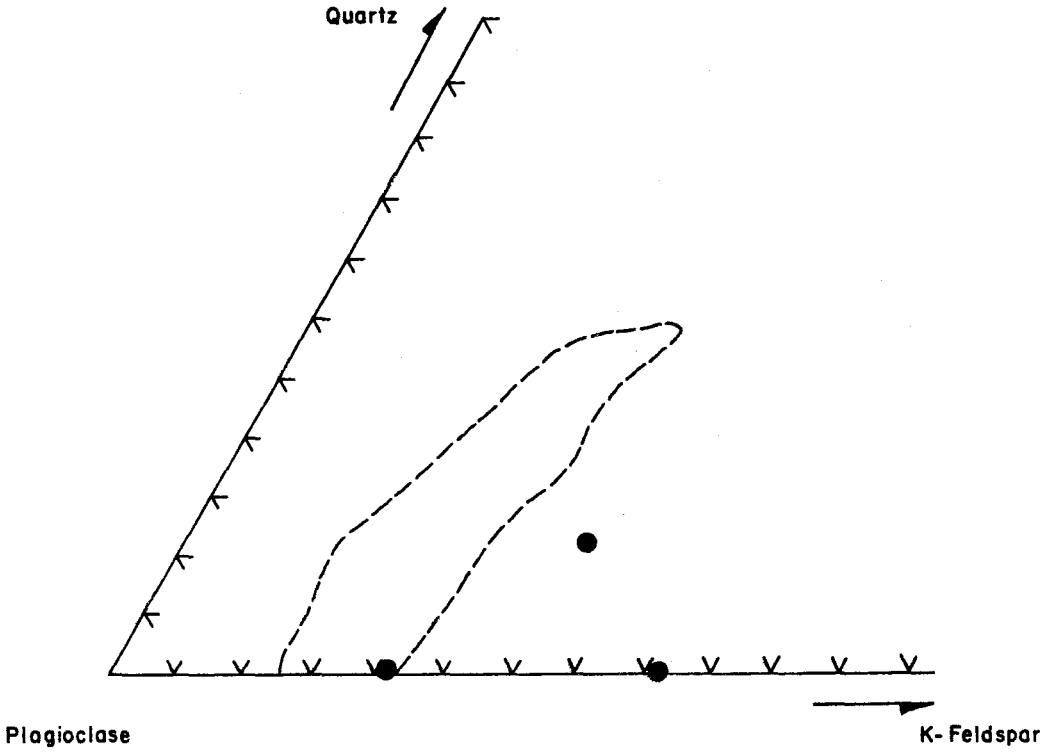

Figure 16. Comparison of normative mineralogy of the Independence dike swarm (dashed line) and related(?) dikes (● symbol) in the central Slate Range. Data from Chen and Moore (1979) is dashed.

of SiO_2.

Normative mineralogies for the dikes also appear to agree with those calculated from the data of Chen and Moore (1979; Fig. 16). Values for normative quartz and feldspar are similar. The one Slate Range sample (SR-95) which contains less than 50 wt % SiO_2 also shows normative olivine.

In summary, modal, chemical and normative data suggest that the Independence dike swarm is also present in the central Slate Range.

STRUCTURE

Five deformational events are inferred or recognized from structures mapped in the central Slate Range. Folds and related axial plane foliations affected all of the rock types present, except for late stage intrusives and Quaternary sedimentary and volcanic rocks. These folds produce a variety of fold geometries with two dominant orientations, one to the northeast and one to the northwest. These orientations can be correlated to regional features.

Faults within the study area are of three types, strike-separation and oblique-slip faults, thrust faults, and normal faults. Strike-separation and oblique-slip faults present in autochthonous layered granofelses near Ophir Mine are considered to be the oldest faults. Four northwest-striking thrust faults, the Ophir, Cherry Mine and two minor ones labelled A and B, are present. The oblique-, strike- and thrust-separation faults are thought to have originated during Mesozoic compressional deformation genetically linked to the emplacement of the Sierra Nevada batholith. The final faulting event is represented by Cenozoic normal faulting related to basin and range formation.

Folds

Folds belonging to five deformational events were recognized within the area mapped. These folds and their associated features were assigned to a specific generation and then grouped into a relative chronological order, although some of the age assignments are fairly

artificial and considerable uncertainity exists in assigning many folds to a specific generation.

The folds mapped were assigned to fold generations based on style and overprinting relationships; style, as used here, is the shape of the fold in profile, whether the fold is cylindrical or not, the presence or absence of axial plane cleavage, and associated lineations and microstructures. Established fold generations were assigned a number designation (F_1 - oldest; F_5 - youngest) and structures related to that fold generation were given a letter designation (Table 7).

Five fold generations are seen involving both autochthonous and allochthonous rocks. Age relationships between structures of the autochthon and the allochthon are unknown (some structures are present in the autochthon, some in the allochthon, and some in both); therefore, separate discussions and symbols for autochthonous and allochthonous rocks have been used (first generation folds are referred to as autochthonous F_1 folds and allochthonous F_1 folds). None of the structures mapped were considered to be of primary sedimentary origin; therefore, there is no F_0 generation.

The fold terminology used in the following text is that of Fleuty (1964). Amplitudes and wavelengths were recorded whenever possible, amplitude as the height of the fold measured along a perpendicular from the point of maximum curvature in the trough to the crest of the fold, and the wavelength as one-half the natural wavelength. The asymmetry of minor folds was recorded during mapping and used in conjunction with the Hansen method (1971) for the determination of slip orientation and direction of the thrust faults present in the study area. The area was divided into several domains for

Table 7. Summary of planar and linear elements created during each folding event.

Fold Generation	Planar Elements
F1	1) Axial Plane Cleavage - S_1
	2) Axial Plane Cleavage - Sa_1*
F4	1) Axial Plane Cleavage - Sa_4
	Linear Elements
F1	1) Minor Folds - L_1
F2	1) Minor Folds to Overturned Synform - La_{2a}
	2) Minor Folds to Carbonate Folds - La_{2b}
F3	1) Minor Folds - La_3
F4	1) Minor Folds - La_{4a}
	2) Mineral Lineations - La_{4b}
F5	1) Crenulations - La_{5a}
	2) Minor Folds - La_{5b}
	3) Warps - La_{5c}
	4) Kinks - La_{5d}
Unaffiliated	1) Crenulations

Note: *Lower case letter a in the symbol notation refers to structures in allochthonous units.
There is a direct correspondence with the number designation and the fold generation.

data analysis (Fig. 17). Table 8 is a summary of fold characteristics, foliations and lineations for the various generations of folds.

F_1 Folds

In the following discussion, F_1 folds in the autochthon and allochthon are discussed separately. This is done because the folds discussed are present in blocks separated by thrust faults and also because within a given block they occur in separate areas, and the relationship between the two areas is unknown.

Folds were assigned to the F_1 generation primarily on the basis of cross-cutting relationships, orientation and the presence of axial plane cleavage. Autochthonous F_1 folds are cut by left-normal oblique-slip faults; both folds and faults are cut by the Ophir thrust, and the folds are intruded by the Isham Canyon and Copper Queen plutons. Less deformed metasedimentary rock, possibly having primary (?) bedding, are folded by the allochthonous F_1 fold. Recognition of allochthonous F_1 folds is provisional; this feature may represent only an early phase of F_2 folding.

Autochthonous F_1 Folds

Autochthonous F_1 Folds are present only at Ophir Mine (Fig. 18). There, two folds, a synform and an antiform, are immediately adjacent to the Ophir thrust fault (Fig. 18). They can be traced from Bundy Canyon to the next canyon immediately south, where they are truncated by the overlying Ophir thrust fault.

The fold axes are oriented 30^{o}, N.48^{o}E. with the average axial plane striking N.51^{o}E. and dipping 86^{o}NW. (Fig. 19a and b); they are cylindrical, asymmetrical, and southeast vergent. The northernmost portion of the synform is overturned, and as it is traced to the

Table 8. Summary of the fold generations and their associated features.

Fold Generation	Scale	Rock Units Involved	Location	Orientation-Hinge Line/ Hinge Surface	Shape, Asymmetry, Vergence	Associated Foliations*	Associated Lineations*	Other Notable Characteristics
F_1	macro	Autochthonous layered granofels	South of Ophir Complex	20° N.40°E./ N.43°E. 82°N.W.	Isoclinal, overturned, asymmetrical with southeast vergence	Primary (?) bedding and bedding-parallel mimetic cleavage[1] Axial plane cleavage (S_1)[2]	Minor folds (L_1)	
	macro	Allochthonous layered granofels	South of Owl Canyon	32° N.48°W.	Open (?)	Primary (?) bedding and bedding-parallel mimetic cleavage[1] Axial plane cleavage (Sa_1)[2]		
F_2	macro	Allochthonous layered granofels	South of Owl Canyon	8° N.4°E.	Close, overturned to the west	Axial plane cleavage (Sa_1)[1]	Minor folds (La_{2a})	
	macro	Allochthonous schists and marbles	Owl Canyon	10° S.54°E.	Isoclinal, overturned to the east	Transposed foliation[1]	Minor folds (La_{2b})	
F_3	meso	Alaskite of Gold Bottom Mine and allochthonous schists	South of Owl Canyon	7° N.33°E.	Chevron	Axial plane cleavage (Sa_1)[1] Axial plane cleavage (?)[2]	Minor folds (La_3)	Hinge areas to folds are broken and offset with minor gouge zones.
F_4	macro	Basal carbonate of the Ophir thrust and autochthonous layered granofels	Ophir Complex to Gold Bottom Mine	20° N.50°W./ N.45°W. 72°S.W.	Open	Transposed foliation[1] Axial plane cleavage (Sa_4)[2]	Minor folds (La_{4a}) Mineral Lineations (La_{4b})	
F_5	macro and meso	All rock units	Pervasive through entire area	North-south and east-west orientation	Warps, single and conjugate kink bands, and minor folds	N.A.	Crenulations (La_{5a}) Minor folds (La_{5b}) Warps (La_{5c}) Kinks (La_{5d})	

Notes: * - Discussed further in text.
1 - Involved in folding; 2 - Created during folding.

Figure 17. Map showing the location of structural domains.

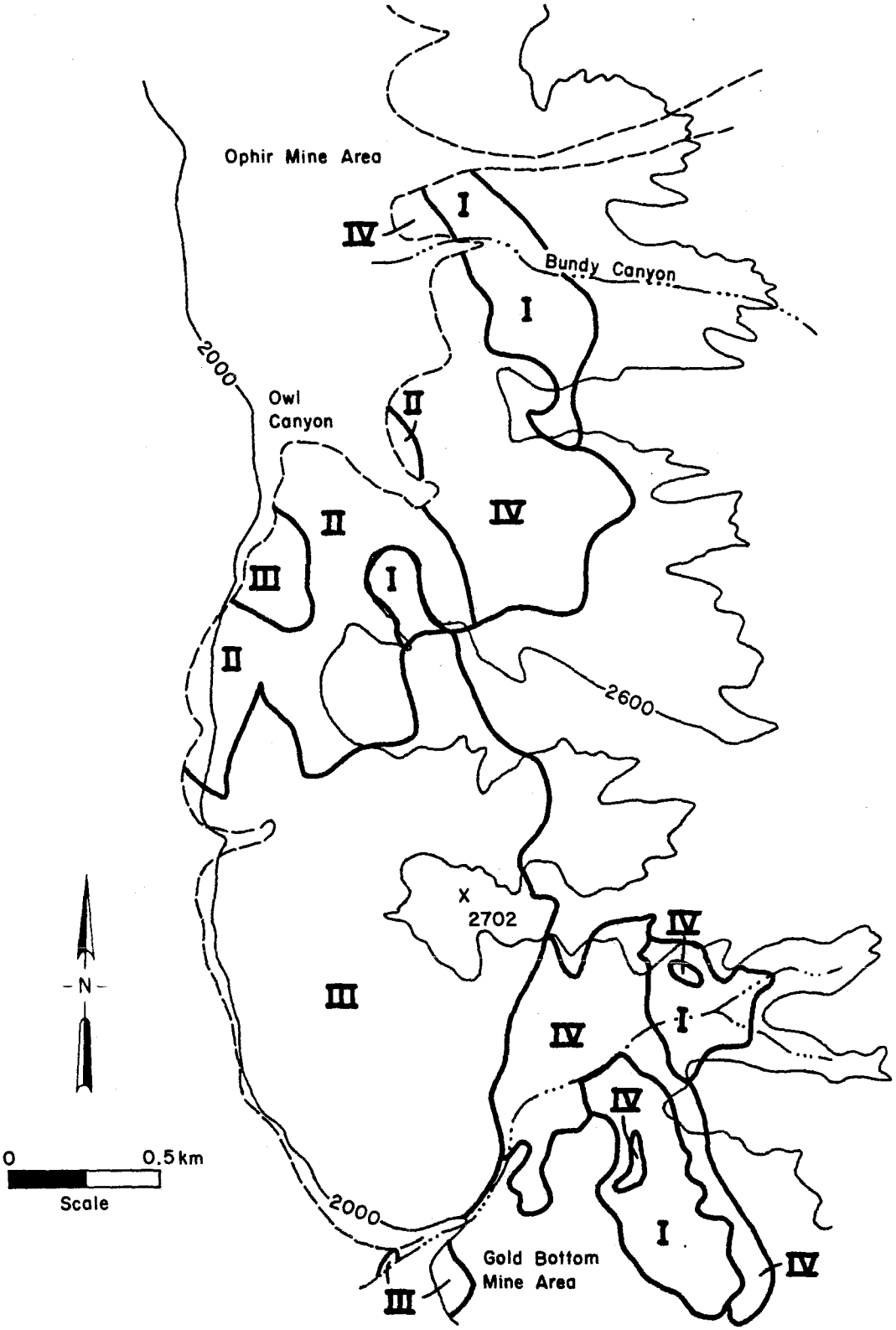
Ophir Mine Area
Bundy Canyon
Owl
Canyon
2000
2600
X
2702
N
0
0.5 km
Scale
2000
Gold Bottom
Mine Area
I
II
III
IV

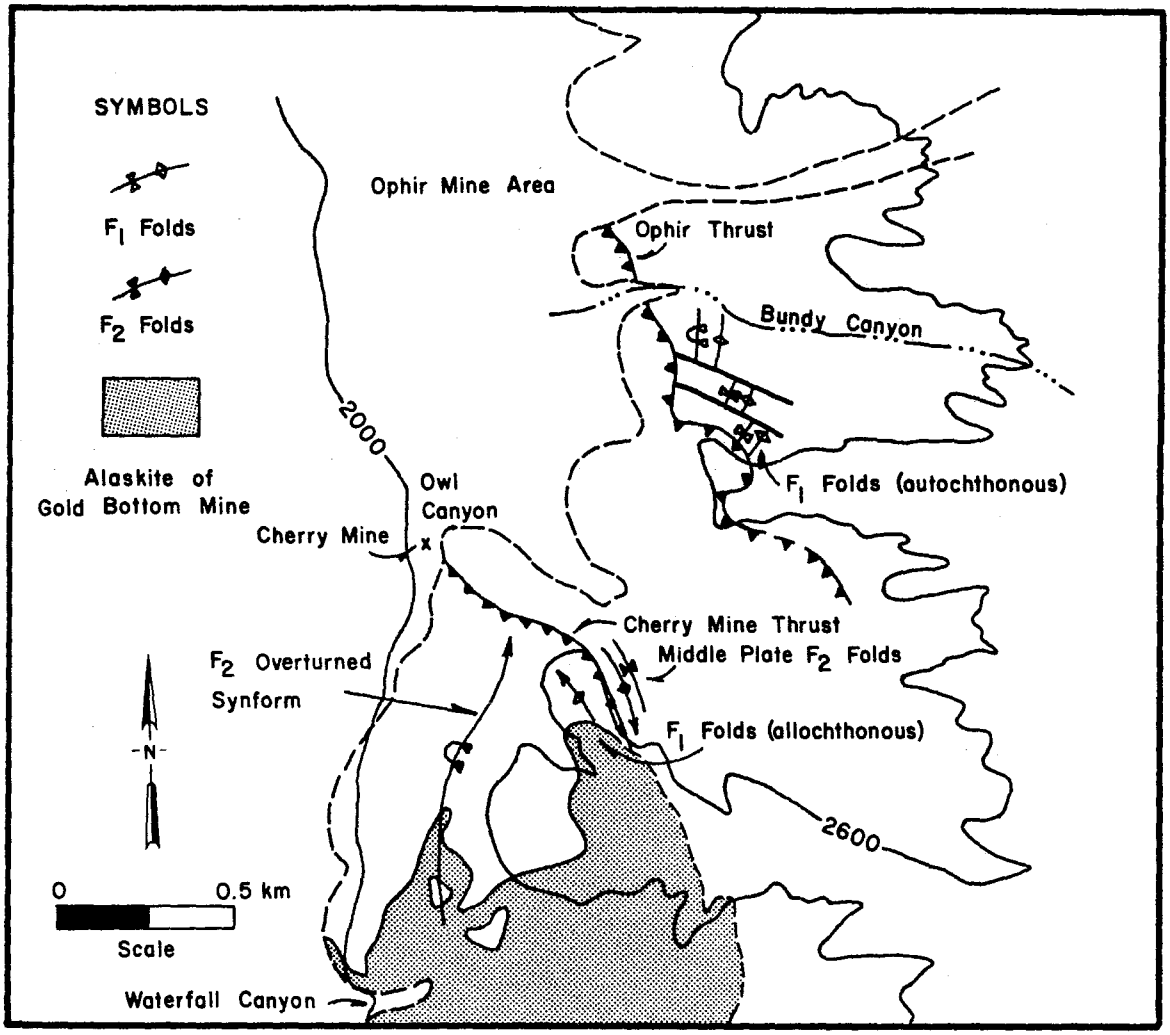

Figure 18. Map showing the location of the F_1 and F_2 generation of folds.

south, becomes upright. The antiform is everywhere upright.

Primary (?) bedding (S_0) and a bedding-parallel mimetic cleavage are locally recognized. Cross-cutting them is a locally well-developed axial plane cleavage, S_1.

Examples of minor folds (L_1) associated with the F_1 folding event are shown in Figure 20. Asymmetrical and usually harmonic, the minor folds range in amplitude from 2.5 to 25 cm (average is 12.7 cm) and in wavelength from 5 to 25 cm (average is 17.5 cm). When plotted (Fig.

Figure 19. Contoured stereonet plots of linear and planar features of autochthonous F_1 folds exposed in domain 1. All data are plotted on lower-hemisphere, equal-area projections. Contours are 3, 5, 7 and 9 % points per 1 % area. Long dashed line represents the best fit great circle. Short dashed line and "x" are axial plane and pi point, respectively.

A) Poles to bedding and bedding-parallel mimetic cleavage; 72 points contoured.
B) Poles to axial plane cleavage.
C) Hinge lines to minor folds; 32 points contoured.

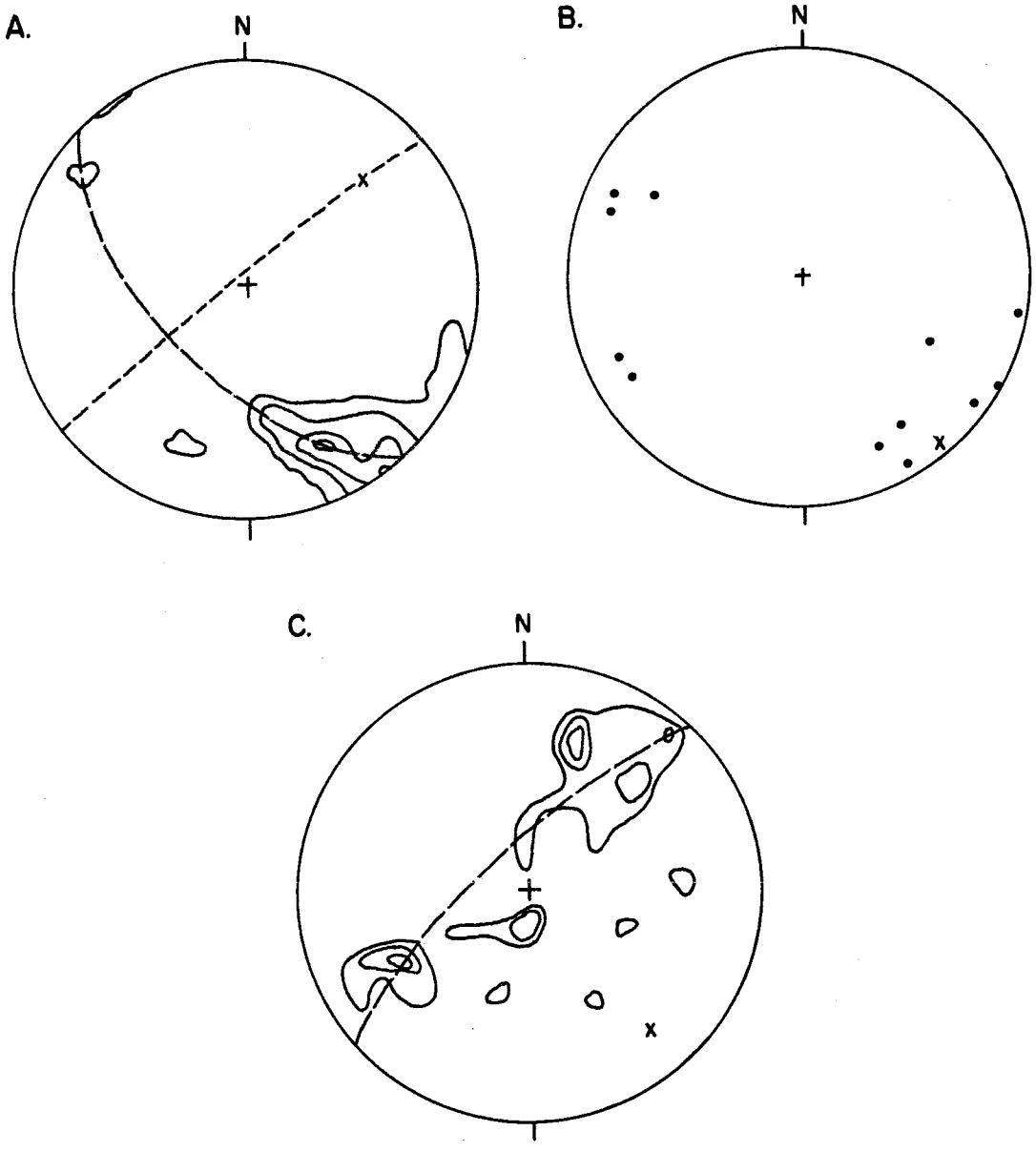
A.
N
B.
N
C.
N

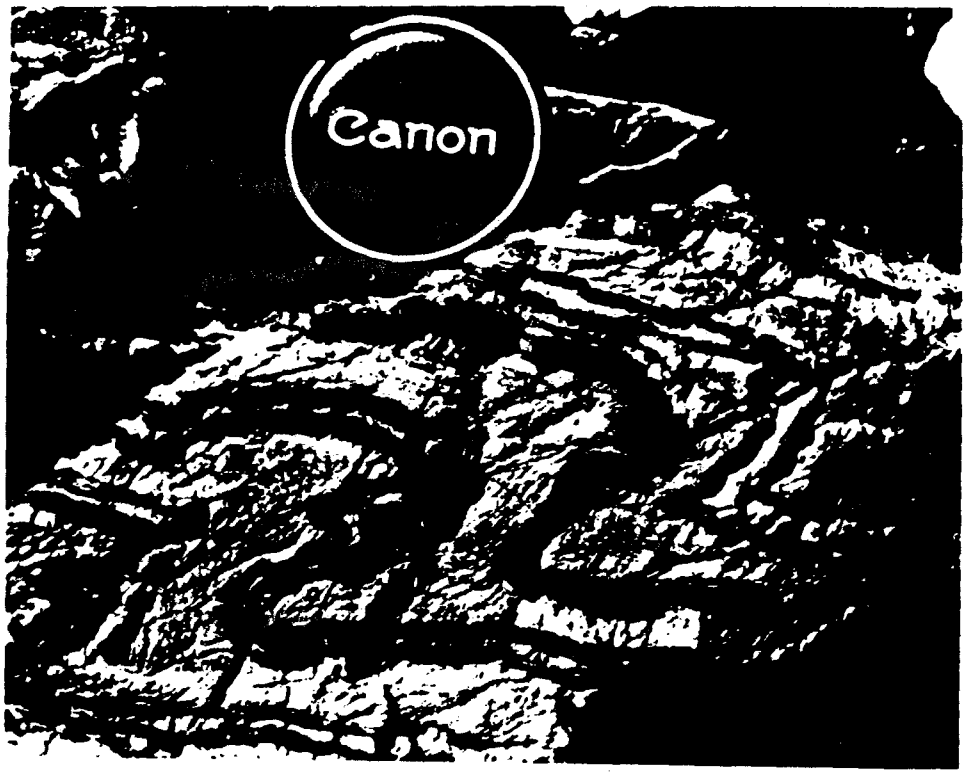

Figure 20. Photograph shows a minor F_1 fold present in the siliceous marble interbeds within the autochthonous rock sequence at Ophir mine.

19c), the hinge lines to the minor folds exhibit a girdle distribution as a result of refolding by later F_5 generation folds.

Autochthonous F_1 folds are essentially parallel folds (Ramsay, 1967) and were produced by a combination of flexural flow and slip (Donath and Parker, 1964). Evidence for this mechanism is the constant thickness of compositional layering and the presence of flow between competent beds, resulting in boudins, local pinching and swelling of foliation and disharmonic folds.

Allochthonous F_1 Folds

An antiform, provisionally assigned to the F_1 generation, is located in the allochthonous layered granofels south of Owl Canyon (Fig.

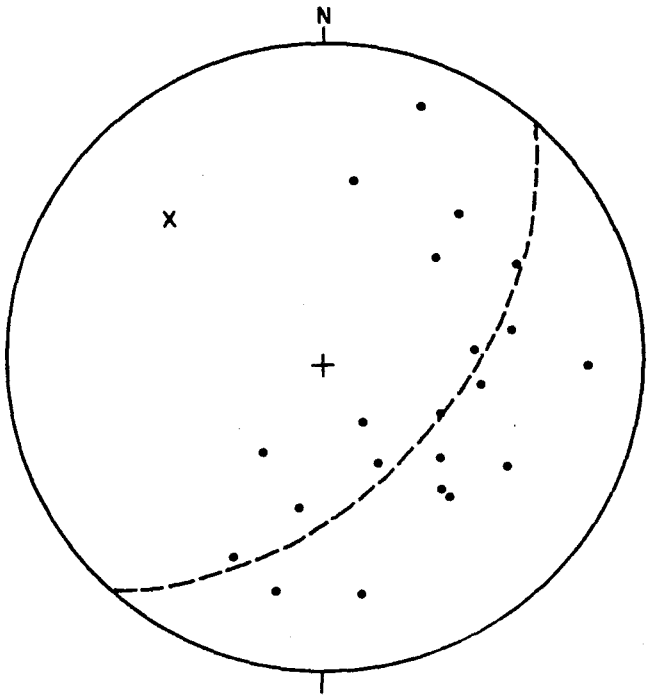

Figure 21. Stereonet plot of poles of bedding and bedding-parallel mimetic cleavage for the allochthonous F_1 fold exposed in domain 1. Data are plotted on a lower-hemisphere, equal-area projection. Dashed line and "x" are best fit great circle and pi point, respectively.

18). This fold can be trace southward until it is truncated by the alaskite of Gold Bottom Mine, and it is terminated to the north by the Cherry Mine thrust fault.

Only the hinge area of the antiform remains, the limbs having been removed during the emplacement of the Cherry Mine thrust. It has an axial orientation of 32°, N.48°W. (Fig. 21). Because only a minor amount of the antiform remains, the shape of the fold in profile is only speculative. From the data available, the fold is considered to be upright and cylindrical (Fig. 21).

Again, primary (?) bedding and bedding-parallel mimetic cleavage

are locally recognized. The other foliation recognized is a cleavage axial planar (Sa_1) to the F_1 allochthonous fold. This cleavage may result from F_1 folding or from the reactivation of the F_1 antiform during the earliest phase of F_2 folding and is itself folded by the F_2 event. There are no lineations associated with this fold. Because the data are limited, the geometry and mechanism of formation are unknown.

F_2 Folds

Two major fold sets were formed during the F_2 folding event, a major overturned synform, previously described by Moore (1976) as an antiform, and folds in a sequence of carbonate/schist layers present adjacent to the overlying Cherry Mine thrust. The sequence of folded carbonate/schist layers is exposed in a thrust slice between the lower Ophir thrust and the upper Cherry Mine thrust, referred to here as the middle plate. Because the relationship between the rocks overlying and underlying the Cherry Mine thrust fault is unknown, the fold sets are discussed separately.

The major overturned synform is assigned to the F_2 fold generation because it folds the axial plane cleavage of the allochthonous F_1 fold and is then truncated by the Cherry Mine thrust fault and the alaskite of Gold Bottom Mine. Uncertainties exist in this age assignment because the middle plate carbonate folds could have formed at the same time as the major overturned synform or later as a result of thrusting.

Major Overturned Synform

The major overturned F_2 synform is exposed south of Owl Canyon along the western side of the main ridge (Fig. 18). The syn-

form folds highly colored allochthonous schists and layered granofelses.

An axial attitude of 8^{o}, N.4^{o}E. was determined for the synform (Fig. 22). Traced laterally from its northernmost exposure for a distance of about 1.2 km, the fold is truncated by Waterfall Canyon and aligns coincidentally with the trend of a smaller upright synform (F_3 fold) within the alaskite of Gold Bottom Mine (Fig. 18).

In shape, the synform is cylindrical, close and overturned to the east (Fig. 22). It folds the axial plane cleavage of the F_1 allochthonous fold. The F_1 axial plane cleavage (Sa_1), where developed in the alaskite, is manifested by a planar orientation of shear minerals, predominantly quartz and feldspar, indicating that the pluton was relatively cool, or crystalline enough to undergo cataclastic deformation. Near the hinge of the allochthonous F_1 antiform the axial plane cleavage (Sa_1) is perpendicular to the alaskite/hornfels contact cutting across the folded mimetic cleavage; elsewhere, the foliation remains parallel to the contact.

Hinge lines to minor folds (La_{2a}) are the lineation associated with the F_2 major overturned synform. However, folds are scarce, and present predominantly in scattered marble interbeds within the layered granofelses. Amplitudes range from 1.2 to 20 cm (average is 8.8 cm) and wavelengths range from 4 to 40 cm and average 11.3 cm. Refolding of these minor folds about a northwesterly trend occurred during the F_5 folding event (Fig. 22).

Middle Plate Carbonate Folds

A series of four F_2 folds are adjacent to the base of the Cherry Mine thrust fault (Fig. 18), and form alternating antiforms and syn-

Figure 22. Contoured stereonet plots of linear and planar features of the F_2 major overturned synform exposed in domain 2. All data are plotted on lower-hemisphere, equal-area projections. Contours are 1 (short dashed lines), 3 and 5 % points per 1 % area. Long dashed lines and "x" are best fit great circle and pi point, respectively.

A) Folding of axial plane cleavage (Sa_1) of allochthonous F_1 fold; 189 points contoured.

B) Hinge lines to minor folds (La_{2a}).

A.

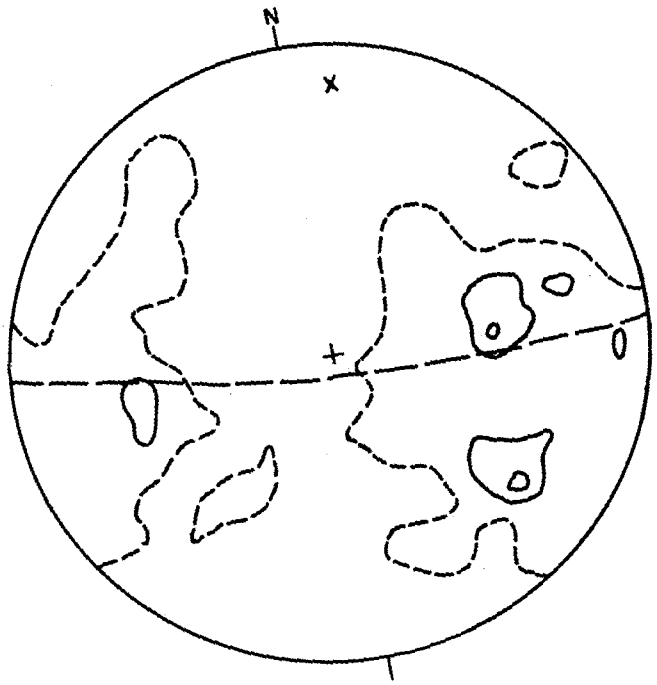

B.

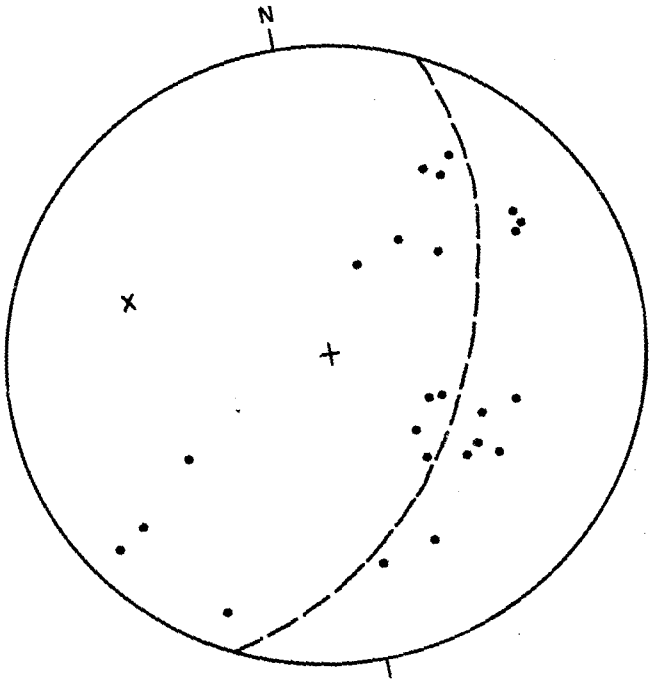

forms which can be traced from the entrance of Cherry Mine southeast along the basal contact of the thrust fault until they are truncated by the alaskite of Gold Bottom Mine. Only the two upper folds can be traced laterally for any distance; the two lower ones are either cut off or covered by talus.

The folds are cylindrical, isoclinal and overturned to the east (Fig. 23). The amplitude is indeterminable; the wavelength is about 25 m. A 12°, S.29°E. trend has been determined (Fig. 23).

Transposed layering created during the emplacement of the Cherry Mine thrust is folded by the middle plate carbonate folds. Rootless intrafolial folds resulting from this transposition are abundant within the marble layers.

Numerous minor folds (La_{2b}) are associated with the middle plate carbonate folds. Sizes differ substantially; amplitudes range from 20 to 30 cm and from 30 to 90 cm, and wavelengths range from 2 cm to 1.5 m. Also, small scale disharmonic folding is present locally.

F_3 Folds

The F_3 generation folds are found in three localities within the allochthonous plate: in the alaskite of Gold Bottom Mine; east of the alaskite; and in schist sequences west of the major F_2 overturned synform (Fig. 24). The F_3 generation of folds has an overall northeasterly trend, folds the major overturned synform (F_2 fold), folds the alaskite of Gold Bottom Mine and is in turn refolded by the F_5 generation of folds.

The average axial orientation of the F_3 fold generation is 7°, N.33°E. (Fig. 25). In profile, F_3 folds have a chevron shape. All

Figure 23. Contoured stereonet plots of linear and planar features of F_2 middle plate carbonate folds in domain 2. All data are plotted on lower-hemisphere, equal-area projections. Contours are 1 (short dashed lines), 3, 5 and 7 % points per 1 % area. Long dashed line and "x" are best fit great circle and pi point, respectively.
A) Poles to transposed foliation; 87 points contoured.
B) Hinge lines to minor folds; 102 points contoured.

A.

B.

Figure 24. Map showing the location of the F_3 and F_4 generation of folds.

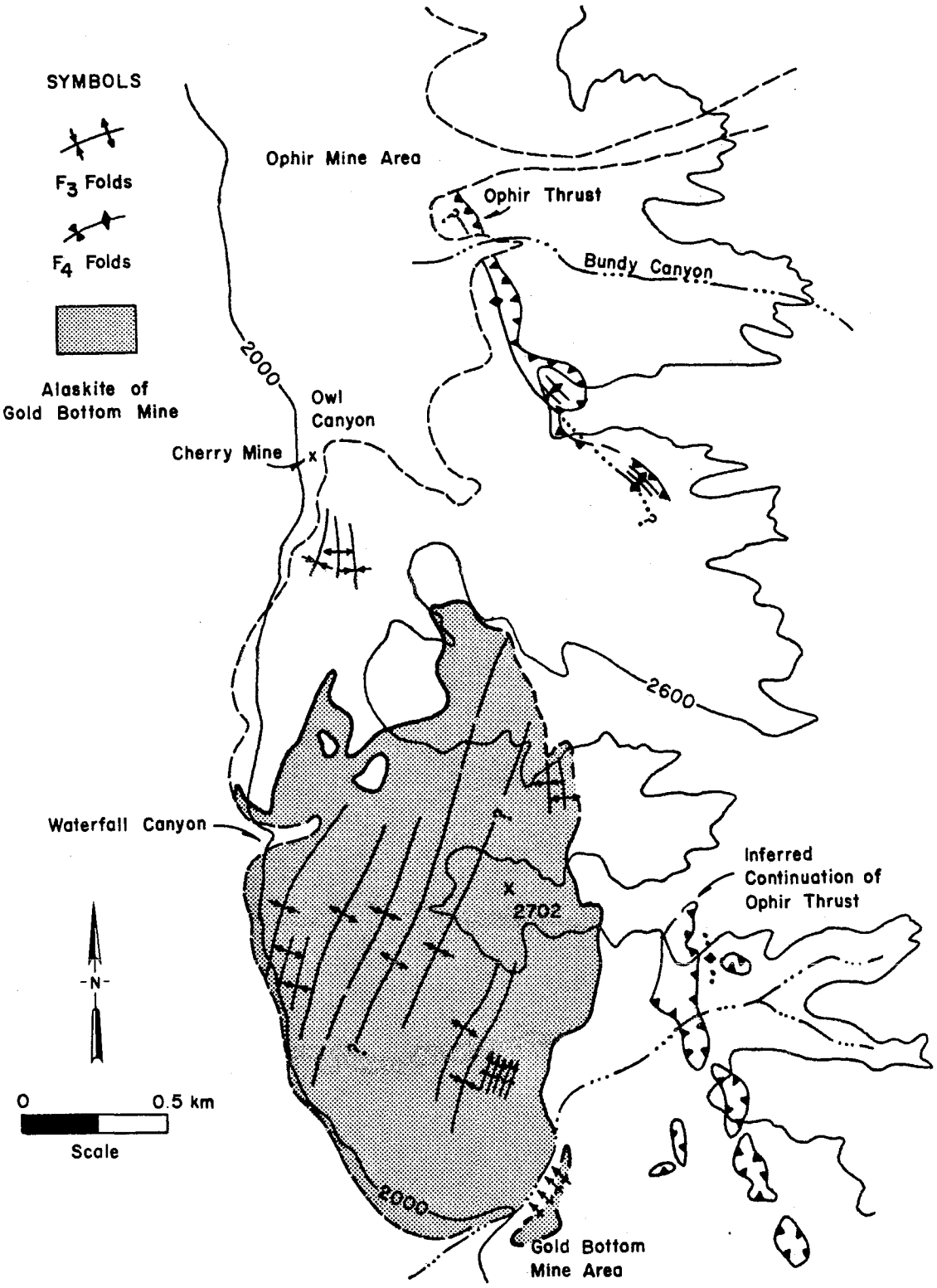
SYMBOLS
F3 Folds
F4 Folds
Alaskite of Gold Bottom Mine
Ophir Mine Area
Ophir Thrust
Bundy Canyon
2000
Owl Canyon
Cherry Mine
2600
Waterfall Canyon
Inferred Continuation of Ophir Thrust
2702
N
0
0.5 km
Scale
2000
Gold Bottom Mine Area

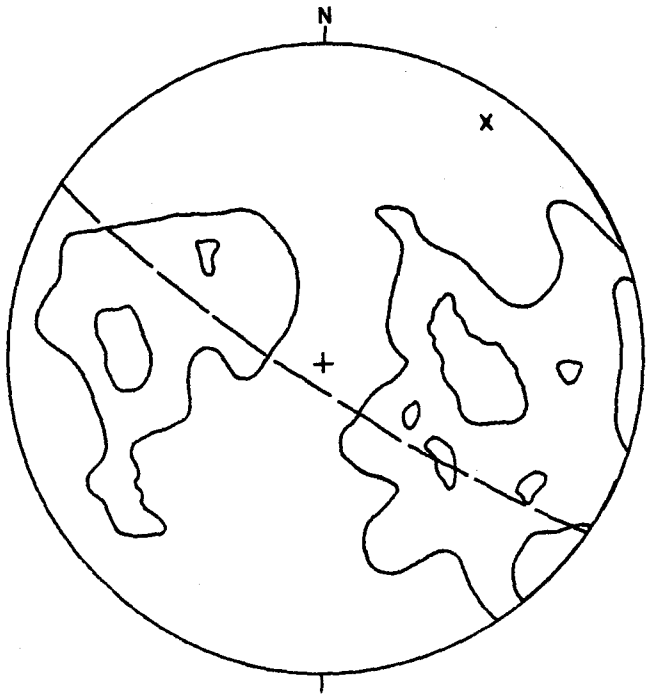

Figure 25. Contoured stereonet plot of poles to folded layering (Sa_1) for F_3 folds exposed in domain 3. Data are plotted on a lower-hemisphere, equal-area projection. Contours are 1 and 3 % points per 1 % area. Dashed line and "x" are best fit great circle and pi point, respectively.

of the F_3 folds encountered in the alaskite of Gold Bottom Mine were fractured or faulted along the hinge surface. This fracturing is interpreted (following Ramsay, 1974) to indicate that shortening continued beyond the critical interlimb angle (about 60^o) until the fold became locked and finally ruptured. Interlimb angles of folds within the area are approximately 40^o, well beneath the critical angle determined by Ramsay. The F_3 folds are upright and cylindrical.

The F_3 generation further folds the axial plane cleavage (Sa_1) developed within the alaskite of Gold Bottom Mine during the F_2 folding event. No pervasive axial plane cleavage was developed during

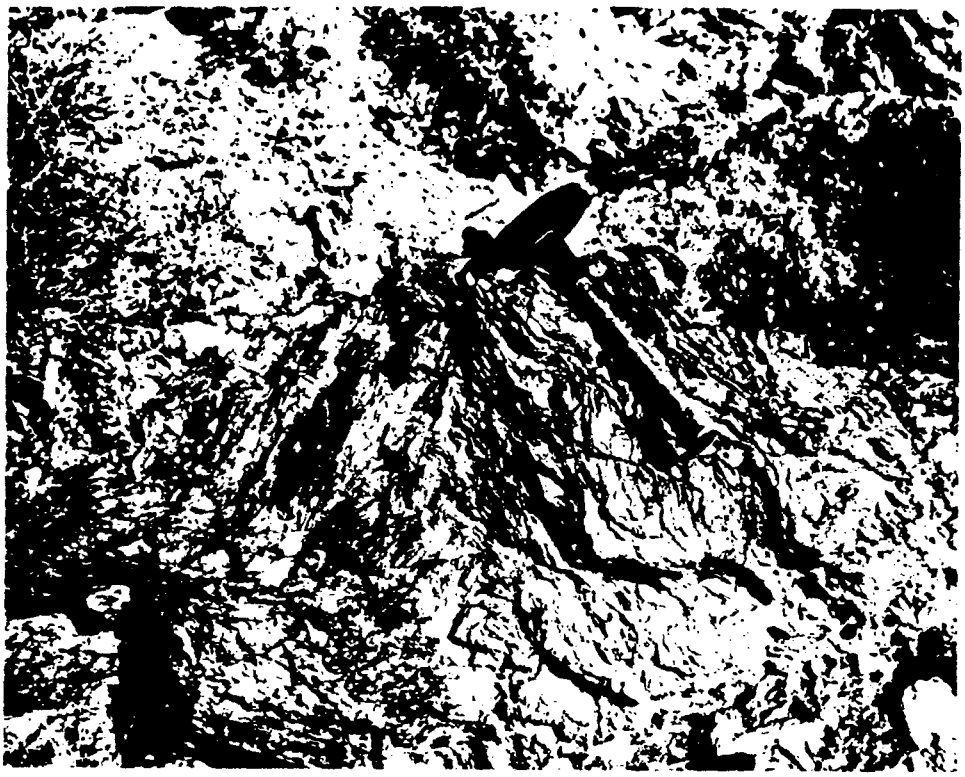

Figure 26. Photograph shows a minor fold of the F_3 generation with the chevron shape characteristic of the alaskite of Gold Bottom Mine.

F_3 folding; however, in one location a poorly-developed foliation, interpreted as axial plane cleavage, was discovered.

Very few minor folds are associated with the F_3 folding event (Fig. 26). The minor folds (La_3) have an open shape and range in amplitude from 10 to 30 cm.

F_4 Folds

The F_4 fold generation is represented by three folds in the study area, an antiform which can be traced discontinuously from the Gold Bottom Mine area to the Ophir Mine in a northwesterly direction, and two smaller folds, a synform and an antiform exposed northwest of

Owl Canyon (Fig. 24). The average axial orientation of the folds is 20°, N.50°W. (Fig. 27a). They are cylindrical, relatively symmetrical and open.

Assignment of the folds to the F_4 generation is based upon cross-cutting relationships; the F_4 antiform folds the Ophir thrust and is in turn folded by the F_5 fold generation. The F_4 fold generation folds a prominent layering within the basal thrust marble that has been transposed due to thrusting. Minor shearing created from the emplacement of the Ophir thrust resulted in this transposed foliation indicated by intrafolial folds. The F_4 folds also generated a poorly developed axial plane cleavage (Sa_4).

Hinge lines to minor folds were developed during F_4 folding. The minor folds (La_{4a}) are symmetrical and range in amplitude from 7.5 to 60 cm. Wavelengths are usually indeterminable. Locally, the minor folds are disharmonic. Minor folds are scattered when plotted on a stereonet (Fig. 27b); the scattered distribution is probably due to refolding by F_5 generation folds.

F_5 Folds

Folds of the F_5 generation are unique because they pervade all rock types, both autochthonous and allochthonous. The abundance of the folds varies from one area to another; however, the rock unit which is affected most by this event appears to be the allochthonous schist.

Crenulations and minor folds will be considered separately from warps and single and conjugate kinks. The reason for this separation is that the warps and kinks are related to the same compressive deformational phases, but the minor folds and crenulations do not show

Figure 27. Contoured stereonet plots of linear and planar features of F_4 folds exposed in domain 4. All data are plotted on lower-hemisphere, equal-area projections. Contours are 1, 3 and 5 % points per 1 % area. Dashed line and "x" are best fit great circle and pi point, respectively.
A) Poles to transposed layering; 162 points contoured.
B) Hinge lines to minor folds.

A.

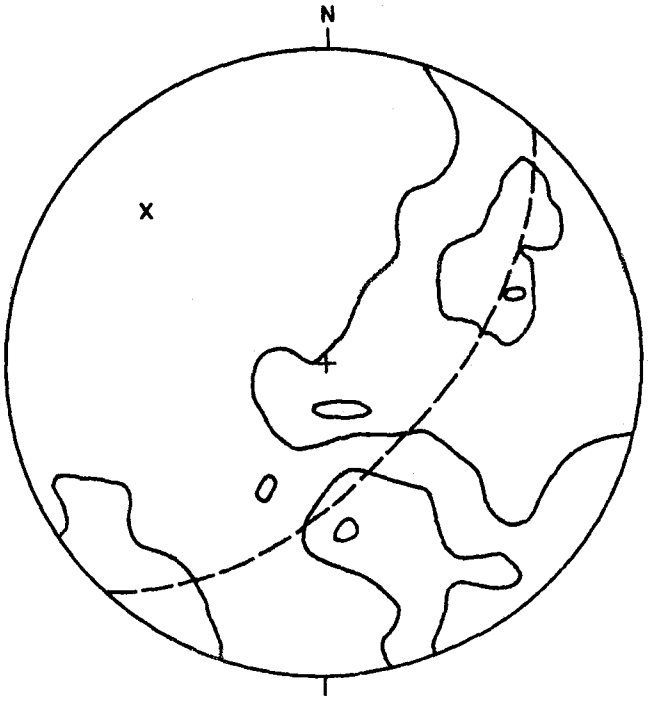

B.

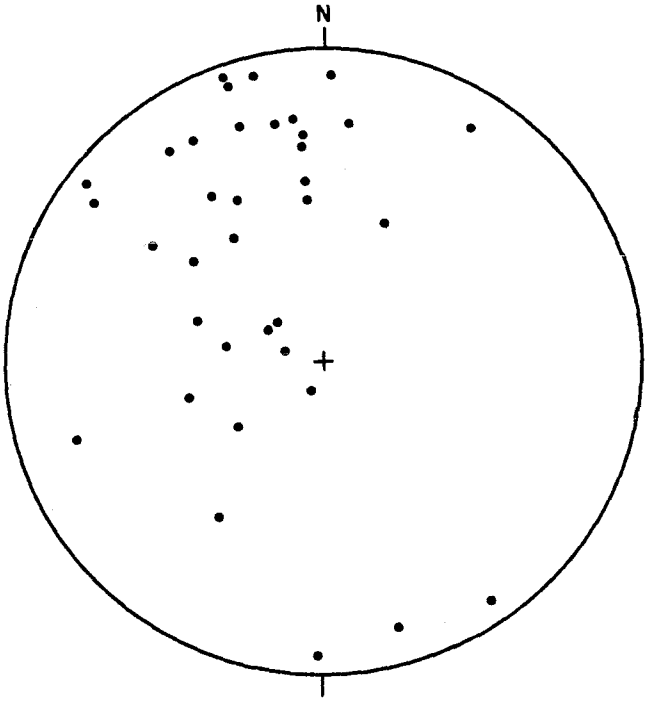

the same clearcut relationship.

The basis for the age assignment of the minor folds, warps and kinks to the F_5 generation is that they are the youngest structure wherever observed, cross-cutting all of the earlier structures. Even though they are grouped into one fold generation for convenience, they may well represent several pulses.

Crenulations and Minor Folds

A strong northwest-trending crenulation (La_{5a}) which strongly overprints an earlier crenulation is present in the allochthonous schist sequence (Fig. 28), with trends ranging from N.5°W. to N.44°W. Amplitudes and wavelengths are on the order of 2.5 cm and 7.5 cm. respectively.

Minor folds (La_{5b}) are present within the alaskite of Gold Bottom Mine and the lower schist sequence (Fig. 28). An average orientation for these folds is 45°, N.55°W. Extending laterally for only a few meters, these folds average 1.2 m in length and refold earlier folds in a northwesterly direction. The folds are cylindrical, and forms change depending on the rock type, from open folds within the carbonate unit to sharper, almost chevron-like folds within the alaskite of Gold Bottom Mine. Amplitudes and wavelengths average 0.9 and 1.8 m, respectively.

Warps and Kinks

Warps are prevalent throughout the area, forming basin and dome patterns where present and affecting all rock types. Warps are most abundant or apparent in the carbonate rocks and allochthonous schist sequences. Two separate sets of orientations are present for these

Figure 28. Map showing the general location of the F_5 generation of folds.

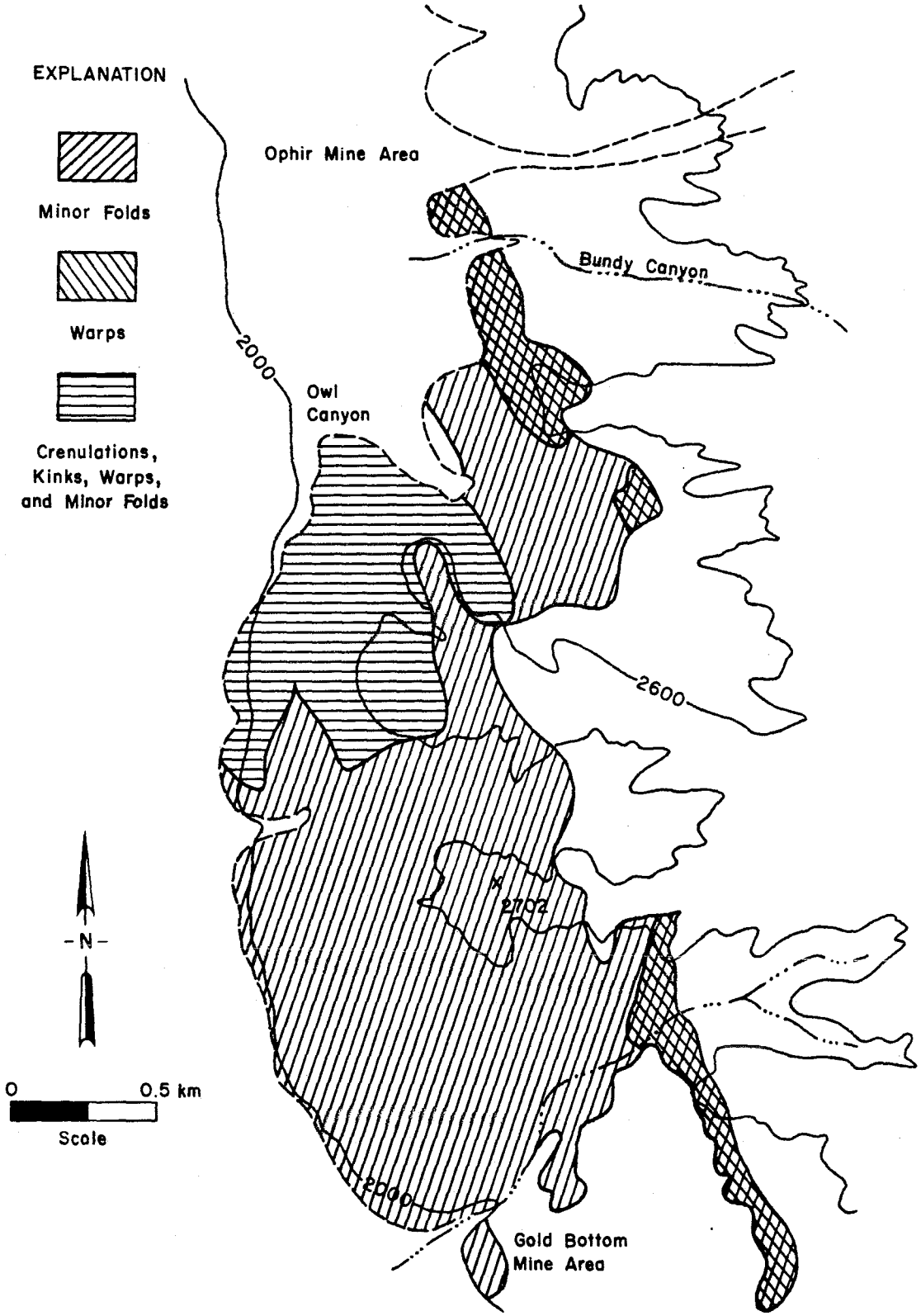
EXPLANATION
Minor Folds
Warps
Crenulations, Kinks, Warps, and Minor Folds
Ophir Mine Area
Bundy Canyon
2000
Owl Canyon
2600
2702
2000
Gold Bottom Mine Area
N
0
0.5 km
Scale

warps (La_{5c}): an east-west orientation (apparently the stronger event); and a north-south orientation created from two separate compressional pulses. The north-south orientation is the youngest event, as indicated by overprinting relationships.

In profile, the warps are generally open. Sizes vary from one locality to another; usually they have amplitudes and wavelengths greater than 0.3 m and 1 m respectively.

Kinks (La_{5d}) are prevalent on the western side of the study area in the upper schist sequence (Fig. 28). Kink types vary from area to area, one area having predominantly single, asymmetrical kinks, another having extensive conjugate kinks, another being covered with small chevron folds, while still other areas are entirely undeformed.

Measurements and plots of two separate sets of conjugate kinks and their dihedral angles also indicate two separate compressional events, one oriented in a north-south direction, and one in an east-west direction. Cross-cutting field relationships between sets of conjugate kinks indicate that the north-south generation is the youngest (the same relative age relationship as established by the warps).

The kinks present are asymmetrical (Fig. 29) and generally discontinuous along the length of the bands (migrating behavior). Hinge surfaces are commonly broken with no apparent offset. The kinks have an average amplitude of 2 cm.

Unaffiliated Structures

Two areas have structures which cannot be assigned to any specific fold generation. These include crenulations present in the schist sequences immediately south of Owl Canyon and structures present in

Figure 29. Single kinks (F_5 generation) present in the upper schist sequence.

the southernmost hornfels unit. Structures present at these localities cannot be related to any other features of the area (Fig. 30). These structures have been assigned separate symbols and have been designated as "unaffiliated" in the explanation of Plate 1.

Crenulation lineations are exposed in the schists comprising the F_2 overturned synform (Fig. 30). These crenulation lineations are scarce because they are obscured by a stronger, later set of crenulations related to the F_5 fold generation. They are generally about 1.3 to 2.5 cm in amplitude with a wavelength of about 2.5 cm. They can also appear locally as faint lines across the rocks.

Structures present in an outcrop of layered granofels/hornfels

Figure 30. Structure index map showing the location of:
A) unaffiliated crenulations; and
B) southernmost granofels unit.

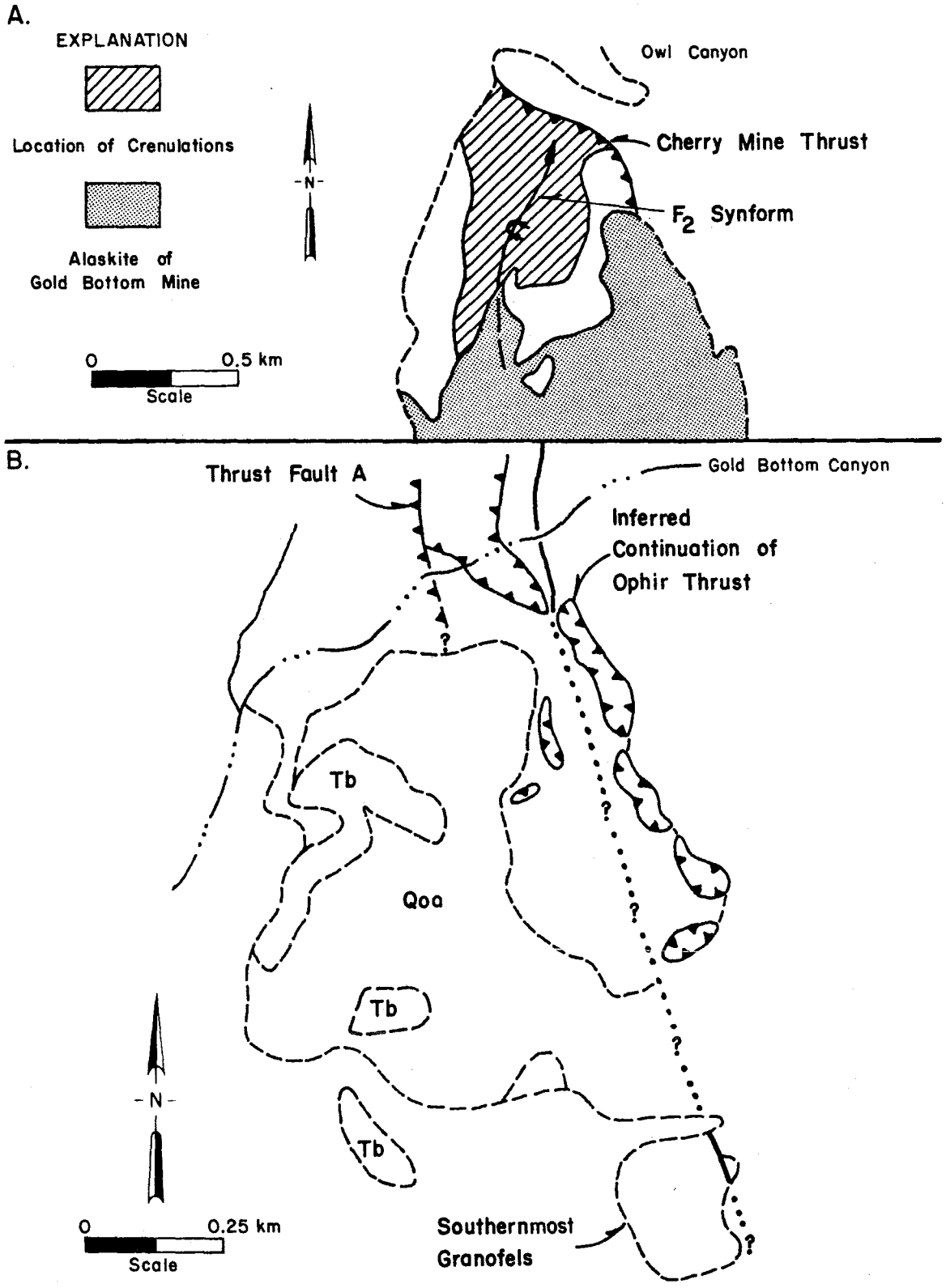
A.
EXPLANATION
Location of Crenulations
Alaskite of
Gold Bottom Mine
0
0.5 km
Scale
N
Owl Canyon
Cherry Mine Thrust
F_2 Synform
B.
Thrust Fault A
Gold Bottom Canyon
Inferred
Continuation of
Ophir Thrust
Tb
Qoa
Tb
Tb
N
0
0.25 km
Scale
Southernmost
Granofels

at the southernmost edge of the map area (Fig. 30), display a complex structural history, having elements which generally cannot be readily correlated with events recognized in the more northerly portions of the study area. The rock unit is exposed to the west of a long north-striking range-front fault in rocks similar to the autochthonous layered granofels/hornfels unit to the north. The layered granofels is a laminated, multi-colored rock predominantly greyish-green with shades of orange and brown. Locally, it appears as a more massive hornfels.

No primary bedding is preserved; instead, alternating thick and thin layers of compositionally different material are present. Close examination of these layers reveals fine laminations with small intrafolial fold noses, suggesting that locally it may represent a transposition foliation. Besides this compositional layering, a second foliation exists in the form of axial plane cleavage. This cleavage is better developed than that present in the autochthonous rocks farther north in the Ophir Mine area and forms a series of northeast-trending, similar-style minor folds. These minor folds may be related to the F_1 folds exposed to the north because they fold transposed layering, have a northeasterly orientation and well-developed axial plane cleavage.

Besides the northeast-trending similar-style folds, two other fold sets are also present in the southernmost hornfels unit. One set is a southeast-plunging set of minor folds which further deform the well-developed axial plane cleavage. This is in turn cross-cut by a series of small conjugate folds. Field relationships suggest

that a large northeast-trending fold is present, but the data are not abundant enough to support the placement of a hinge trace on the map. The relationship between the southeast-plunging minor fold set and other structures present in the area is unknown; the conjugate folds may be related to the F_5 fold generation.

Faults

Faults within this portion of the Slate Range can be placed into three main groups. From oldest to youngest these are:

1) autochthonous strike-separation and oblique-slip faults;
2) thrust faults; and
3) normal faults.

Faults of the first two groups developed during Mesozoic compressive tectonism whereas the normal faults manifest late Cenozoic extensional tectonism. These groups will be discussed in age sequence, with the oldest first.

Strike-Separation and Oblique-Slip Faults

Three minor strike-separation faults and two major oblique-slip faults considered to result from the oldest faulting event are exposed in autochthonous rocks south of Bundy Canyon (Fig. 31). These faults are considered to be the oldest faulting event because they cut the autochthonous F_1 folds and are themselves cut by the Ophir thrust.

The minor strike-separation faults caused left-separation of one limb of the autochthonous F_1 synform (Fig. 31). The faults trend N.75°E. for an exposed distance of 38 to 50 m. The amount of separation of these faults ranges from 8 to 10 m. Slip could not be deter-

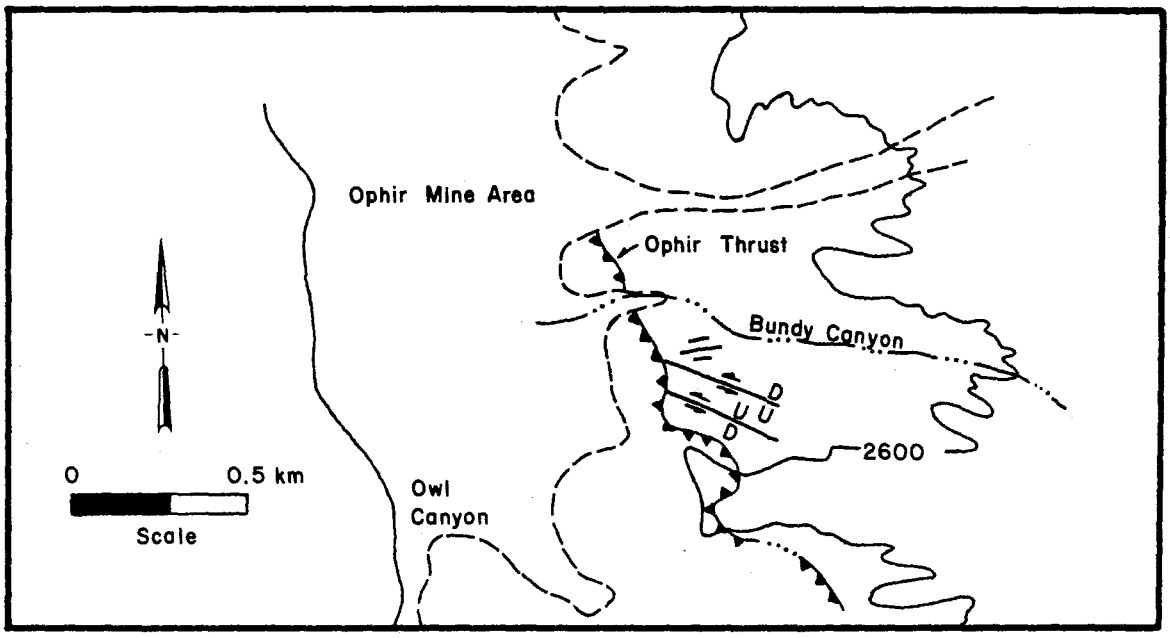

Figure 31. Map showing the location of autochthonous strike-separation and oblique-slip faults. Oblique-slip faults show relative movement.

mined directly, but their sense of separation, broadly similar in trend and proximity to the left-normal slip faults discussed below suggest that these faults may also have left-normal slip.

The two major faults of this group occur south of the minor strike-separation faults (Fig. 31) and offset both autochthonous F_1 folds. These vertical faults strike N.72°W. and extend for a distance of about 300 m. The total amount of slip was determined from offset hinge lines of distinctive beds to be 420 m in a left-normal sense.

Thrust Faults

The four faults of this group (Fig. 32) were mapped as thrust faults, following the usage of previous workers, although the fault surfaces commonly dip at angles greater than 45°. Minor fold axes

Figure 32. Map showing the location of the thrust faults exposed in the central Slate Range.

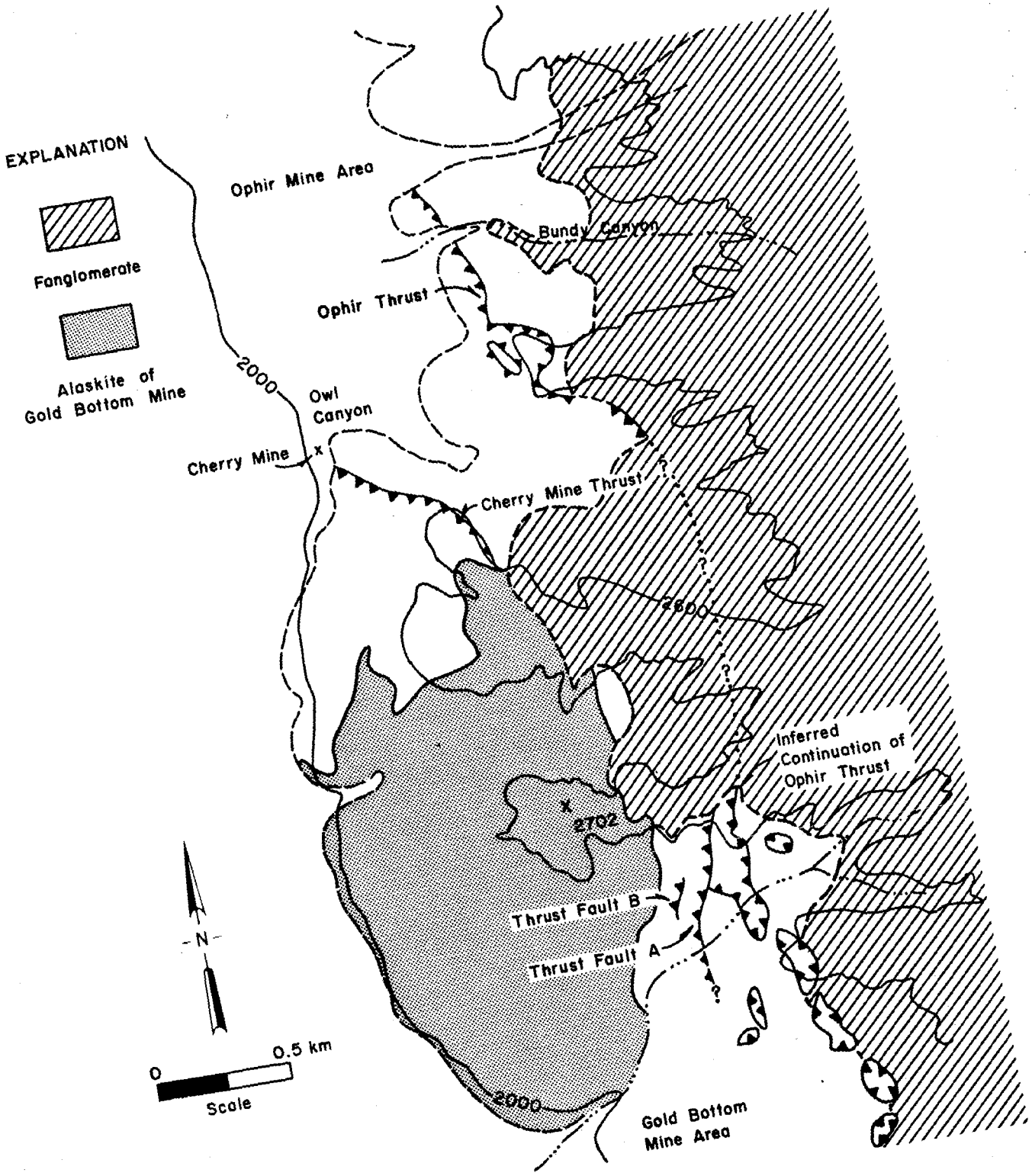
EXPLANATION
Fanglomerate
Alaskite of Gold Bottom Mine
Ophir Mine Area
Bundy Canyon
Ophir Thrust
2000
Owl Canyon
Cherry Mine
Cherry Mine Thrust
2600
Inferred Continuation of Ophir Thrust
2702
Thrust Fault B
Thrust Fault A
N
0
0.5 km
Scale
2000
Gold Bottom Mine Area

and lineations present indicate an eastward movement of the upper plate for one of the faults.

A relationship appears to exist between the Ophir thrust and the Cherry Mine thrust because they appear to have moved at about the same time. The Ophir thrust moved after F_1 folding and prior to F_4 folding, and the Cherry Mine thrust moved after F_2 folding and probably prior to intrusion of the alaskite of Gold Bottom Mine. No clearcut relationships exist between the Ophir thrust and the minor thrust faults, labelled A and B. Thrust faults A and B both predate intrusion of the Copper Queen alaskite. These faults will be discussed in order of their relative importance based on their lateral extent.

Ophir Thrust

The Ophir thrust fault, named by Moore (1976), is discontinuously exposed over a distance of 1.9 km along a northwest trend from the Gold Bottom Mine area to the Ophir Mine (Fig. 32). South of Gold Bottom Mine, the thrust fault occurs as a series of small klippen (Fig. 32).

Two distinct rock types are juxtaposed by the thrust fault along a sharp contact. The basal portion of the thrust plate is everywhere composed of a strongly foliated marble with a well-developed mylonite zone. 0.5 to 1 m thick. This has been thrust over a blackish-brown mineralized hornfels, which changes downward away from the fault into a layered granofels, over an interval typically 5 m thick.

The Ophir thrust fault trends northwest and dips 40° southwest in its southern exposures. Steeper dips occur in the Ophir Mine area due to later folding and warping events. Layering attitudes

between rock of upper and lower plates are discordant, intersecting at angles up to 90°.

Cherry Mine Thrust

The Cherry Mine thrust fault is named here for exposures south of Owl Canyon near the Cherry Mine and forms an irregular trace near the top of the ridge (Fig. 32). The fault contact is sharp, delineated by the presence of a mineralized hornfels zone and the discordant attitudes between the upper and lower plates. Layered granofelses and schists, which are involved in a major F_2 synform, have been thrust over a sequence of schists interlayered with marbles. Thrusting has resulted in the attenuation and removal of a portion of one limb of the synform.

The Cherry Mine thrust fault can be traced for about 830 m northwest from the alaskite of Gold Bottom Mine. The fault surface strikes N.38°W. and dips between 15° and 20° to the southwest.

Thrust Fault A

In Gold Bottom Canyon, two thrust faults striking N.5°E. are present within the upper plate of the Ophir thrust (Fig. 32). Thrust fault A emplaces a strongly foliated hornfels over the Ophir thrust marble. A zone of mineralized rock is present immediately above the thrust surface and extends into the upper plate for approximately 5 m. A well-developed gouge zone is present locally along the fault trace. This may have developed during a normal-slip reactivation of the thrust in late Cenozoic time.

The fault surface has dips ranging from 25° to 50° west, with 30° being typical. Thrust fault A can be traced for 450 m northeastward from Gold Bottom Canyon. The thrust fault cannot be traced

south of Gold Bottom Canyon because erosion has removed the Ophir thrust plate, exposing the underlying autochthonous hornfels/layered granofels. These autochthonous rocks are indistinguishable from rocks which compose the upper plate of thrust fault A.

Thrust Fault B

Thrust fault B is exposed west of thrust fault A and is recognizable over only about 100 m distance (Fig. 32). Thrust fault B occurs within the layered granofels/hornfels unit. The area surrounding the thrust fault is characterized by a well-developed and prominent foliation parallel to the fault.

Thrust fault B strikes N.5°E. and dips approximately 20° west, although local variations exist due to numerous small cross-faults and fractures.

Displacement and Direction of Thrusting

Determination of the amount of slip for the Ophir thrust and other thrust faults is not possible due to the lack of formal stratigraphy and stratigraphic thicknesses; therefore, the only value determinable was minimum breadth measured in the inferred slip direction. This was measured from the klippe to the window, between Bundy and Owl Canyon (Fig. 32). The edge of the window was projected south to where it intersected a line oriented in the direction of slip. The minimum breadth of the thrust fault was thus determined to be 0.9 km.

Direction of tectonic transport was determined by two separate methods: orientation of mineral lineations; and analysis of asymmetry of minor folds found adjacent to the thrust faults using the Hansen

method (Hansen, 1971). Mineral growth lineations (La_{4b}) are well developed in the schists throughout the area. Although orientations of these mineral lineations vary due to late stage warping (F_5), the majority of these lineations plunge west (Fig. 33), indicating an east-west slip line if one assumes growth is parallel to the slip direction. The direction determined from the mineral lineations is consistent with that determined by a plot of the minor folds occurring in the basal thrust carbonate. Using the method described by Hansen (1971) a transport direction of S.76^{o}E. is indicated (Fig. 33).

The eastward direction of upper plate movement determined above is consistent with values determined to the north for the Argus-Sterling thrust system by Moore (1976) and for exposures of thrusts in the Westend Lime Quarry area, northern Slate Range by Scott Magorien (pers. comm., 1979).

Timing of Thrust Movement

Movement of the Ophir thrust fault and other thrust faults probably occurred during Late Jurassic time. As the stratigraphy is unknown, age correlations are based on cross-cutting igneous relationships.

Moore (1976) suggests an age of Late Jurassic based on correlations from the Argus Range and the northern Slate Range. Moore and Harakal (1976) dated the movement of the Argus-Sterling thrust fault as 165 to 140 m.y.B.P. (K-Ar). This age was considered to be valid as far south as the Westend Lime Quarry.

Mueller and others (pers. comm., 1975) report an age of 170 m.y.B.P. for the Copper Queen alaskite, which apparently post-dates

Figure 33. Direction of tectonic transport determined from mineral growth lineations an asymmetry of minor folds. All data are plotted on lower-hemisphere, equal-area projections:

A) mineral growth lineations; and
B) hinge lines to minor folds.

A.

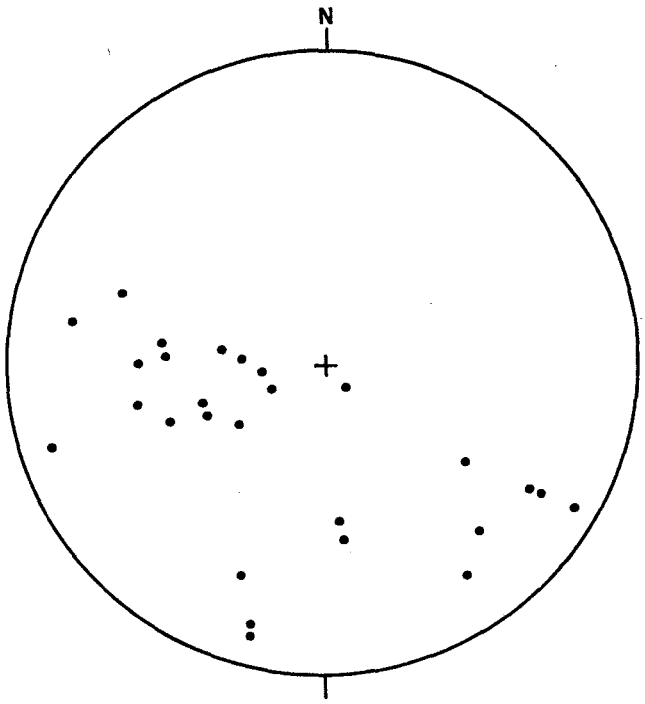
N

B.

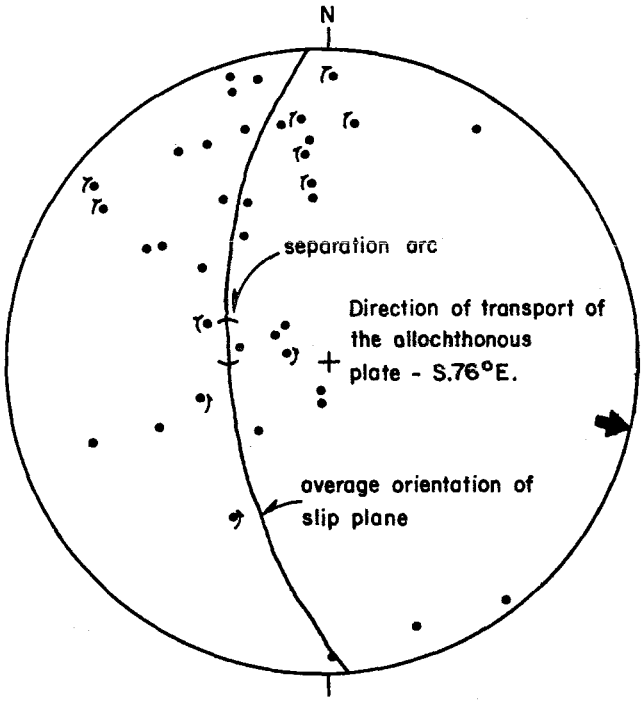
N
separation arc
Direction of transport of the allochthonous plate - S.76°E.
overage orientation of slip plane

all major compressional deformation. Based on chemical and field relationships from this report, the validity of this date is in question. Field relationships show the presence of two plutons at Mueller's sample locality. A comparison of chemical analyses also shows that the isochron was probably derived from samples of both plutons and is thus invalid.

Correlation of the non-foliated dikes present in the study area with the Independence dikes places a minimum age of thrusting at 148 m.y.B.P., as they clearly cut the thrust in the study area.

Normal Faults

The latest generation of faults can be divided into two categories:

1) faults which extend laterally for short distances, generally less than 0.4 km; and
2) normal faults of probable Basin and Range affinity which offset Tertiary (?) volcanics and Quaternary lake deposits.

Faults of the first category (Fig. 34) are delineated by narrow breccia or gouge zones. The faults have no preferred orientation and range in length from 38 to 350 m. Fault planes vary in dip from 50^{o} to 85^{o}, and are oriented in a westerly or southerly direction. The amount and direction of slip was indeterminable.

These faults offset a variety of pre-Cenozoic rock types and structures. Several of the small faults cut relatively younger pre-Cenozoic structures and rock units, and on this basis these small faults are best considered to be of Cenozoic age.

The second set of faults in this group are those that are best

Figure 34. Map showing the location of Cenozoic faults.

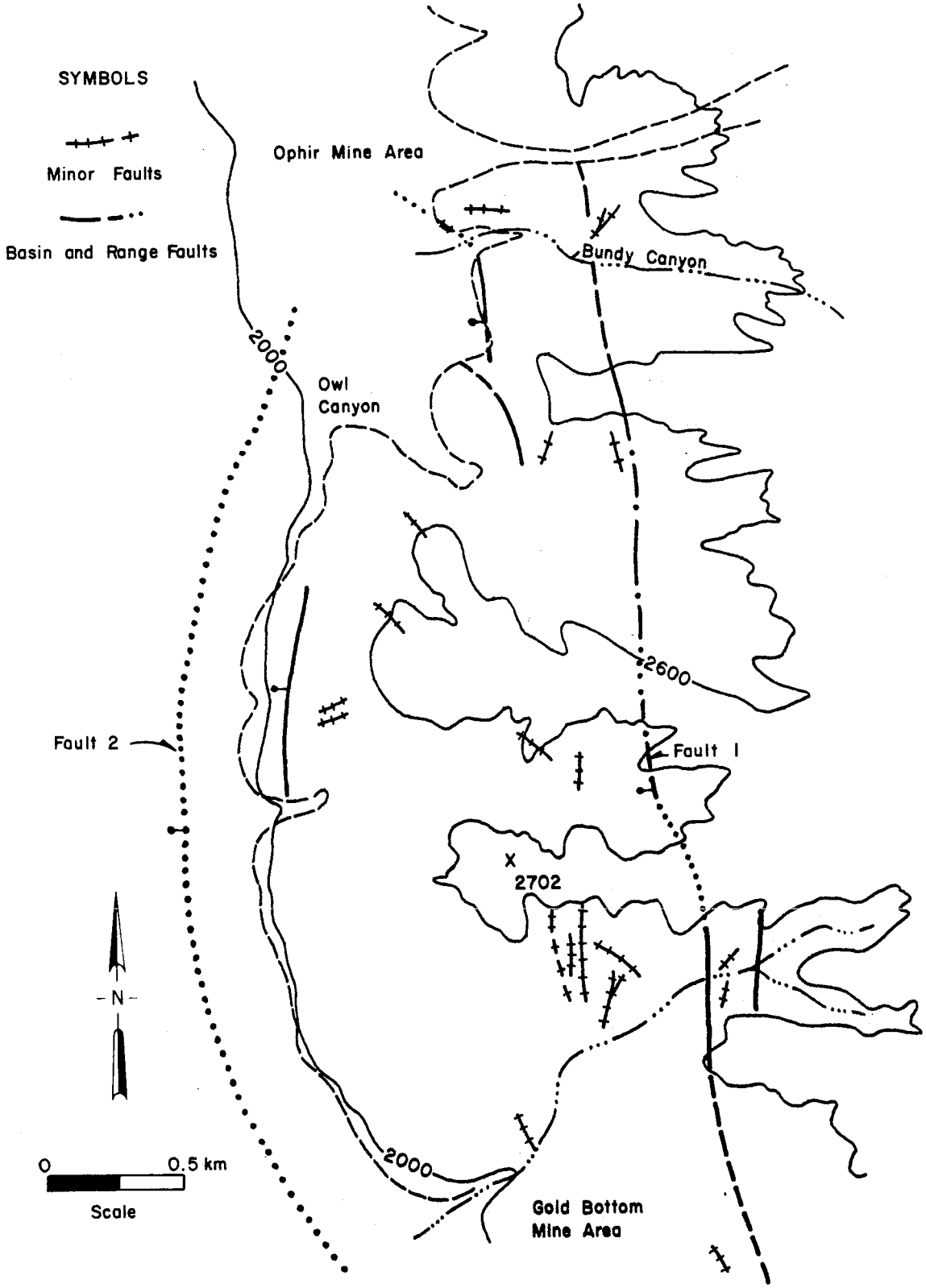
SYMBOLS
Minor Faults
Basin and Range Faults
Ophir Mine Area
Bundy Canyon
2000
Owl
Canyon
2600
Fault 2
Fault 1
X
2702
N
0
0.5 km
Scale
2000
Gold Bottom
Mine Area

related to late Cenozoic basin and range extensional tectonism. This group includes four faults (Fig. 34) oriented in a predominantly north-south direction and varying in length from 225 m to 4.5 km. Dips range from 82° to 88° to the west.

Both Smith and others (1968) and Moore (1976) mapped the longest of these, which extends the length of the area (Fault #1, Fig. 34). Although Moore showed an eastward dip, field observations concur with those of Smith and others in assigning a westward dip to this fault.

Another basin and range fault was mapped by Moore (1976), but not mapped by the author. This inferred fault has a concealed trace within the alluvium in the westernmost portion of the map area (Fault #2, Fig. 34). Three other north-striking, west-dipping faults of probable normal slip are present in the area (Fig. 34). Movement along some of these faults is seen to post-date Cenozoic volcanic rock, inferred by Moore to be correlative with 4 m.y. old basalts in Panamint Butte described by Hall (1971). However, these faults do not cut the more recent fan deposits. Besides probable Quaternary movement, trends and fault characteristics determined are similar to those determined for other basin and range-type faults for the region (Moore, 1976; Wright, 1976; Labotka and others, 1980; Smith and Church, 1980; Duffield and others, 1980; Wright and others, 1981).

DISCUSSION

The following sections will attempt to summarize and relate features seen in the central Slate Range to features exposed to the north and to the south, in the Mojave Desert. Structures present in the central Slate Range have been grouped together in a relative chronologic framework. Structures believed to result from the same deformational phase or pulse are grouped together into generations. Periods of folding, faulting and igneous activity comprise these generations.

Structural History of the central Slate Range

Seven discrete periods or pulses of deformation and(or) intrusion are documented within the study area. The relationships of these deformational pulses to the structural features are summarized in Figure 35. It is arbitrarily assumed that similar structures in the autochthonous and allochthonous plates formed during the same period of time and are thus placed together in the same generation. A synopsis of each pulse from oldest to youngest is presented below.

The first generation of structures include autochthonous and allochthonous F_1 folds and the autochthonous strike-separation and oblique-slip faults. Autochthonous F_1 folds display a northeast trend, southeast vergence and a well-developed axial plane cleavage. The allochthonous F_1 fold has a northwest-trend and a well-developed axial plane cleavage. Both folds involve rocks of probable Permian (?) age. Cross-cutting the autochthonous F_1 folds are the sinistral strike-separation and left-normal oblique-slip faults. Orientations are

Figure 35. Relative chronology of structures and intrusive rocks present in the central Slate Range. Generations of the structures are indicated by the number at the bottom of the chart, these generation brackets are highly speculative. Heavy solid lines indicate age of deformation preferred whereas dashed lines indicate possible age range of deformation from cross-cutting relationships with other structures. Dashed lines with question marks indicate that the relative age is uncertain.

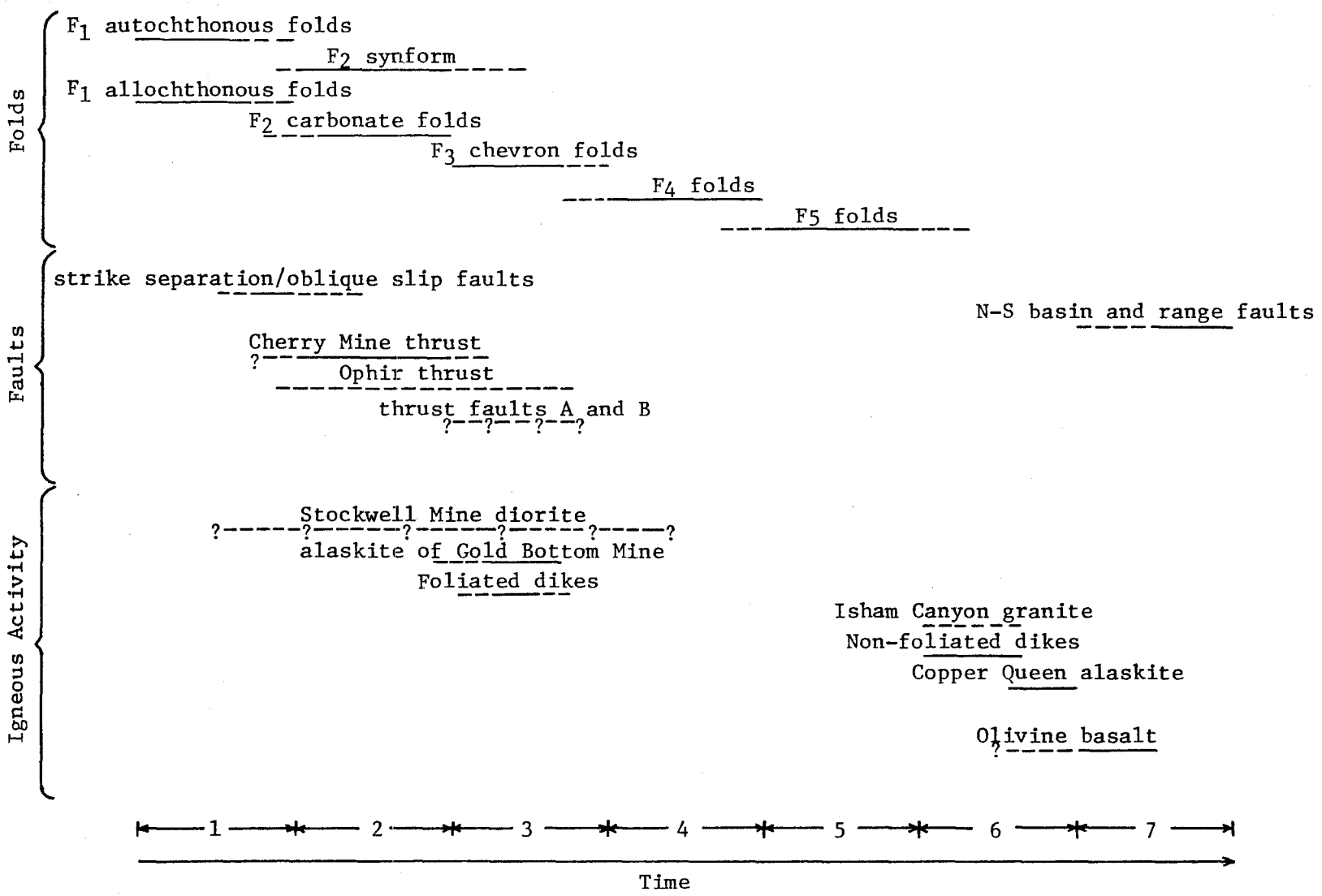
Folds
Faults
Igneous Activity
F1 autochthonous folds
F2 synform
F1 allochthonous folds
F2 carbonate folds
F3 chevron folds
F4 folds
F5 folds
strike separation/oblique slip faults
N-S basin and range faults
Cherry Mine thrust
Ophir thrust
thrust faults A and B
Stockwell Mine diorite
alaskite of Gold Bottom Mine
Foliated dikes
Isham Canyon granite
Non-foliated dikes
Copper Queen alaskite
Olivine basalt
1
2
3
4
5
6
7
Time

N.75°E. and N.72°W. for the strike-separation and oblique-slip faults, respectively. All of the first generation structures are truncated by the later thrust faults, the autochthonous structures by the Ophir thrust and the allochthonous fold by the Cherry Mine thrust.

Two sets of folds, a series of thrust faults and plutonism characterize the second deformational pulse. Emplacement of the Stockwell Mine diorite possibly occurred first with little effect on structures present in the study area. Following the intrusion, folding occurred with the formation of the F_2 fold sets. The F_2 synform folds the axial plane cleavage of the allochthonous F_1 fold about a northeasterly trend. The series of isoclinal middle plate carbonate folds fold a transposed foliation about a southeast trend. Both fold sets are overturned to the east and involve rocks of probable Permian (?) - Triassic (?) age. Emplacement of the Cherry Mine thrust resulted in partial truncation of the F_2 overturned synform. Both the Cherry Mine thrust and middle plate F_2 folds were then truncated by the intrusion of the alaskite of Gold Bottom Mine. This intrusion was followed by the emplacement of the first set of mafic dikes. Folding synchronous with thrusting probably continued; a strong cataclastic foliation was developed within the alaskite of Gold Bottom Mine which was also folded into the F_2 overturned synform. Thrusting also occurred to the east with the emplacement of the Ophir thrust and thrust faults A and B. How the thrusts moved relative to each other is unknown. Again, rocks involved in thrusting are probably Permian (?) - Triassic (?) in age.

Axial plane cleavage to the F_1 allochthonous fold is further folded by the third generation of structures. This folding event

formed a sequence of chevron folds about a northeast trend and possibly developed a new axial plane cleavage (?). Shortening was severe enough that faulting occurred along the hinge planes to the chevron folds.

The fourth generation of deformation formed the folds which affect the Ophir thrust fault, perhaps in response to the final compressive pulse which formed the Ophir thrust. The F_4 generation of folds is characterized by a northwest trend and poorly developed axial plane cleavage.

Crenulations, minor folds, single and conjugate kinks and warps represent the fifth generation of deformation. They are pervasive and fold all pre-existing structures and rock types. It is probably a simplification of the structural history to group them all together because they represent at least two compressive pulses, a north-south event and an east-west event.

Intrusives were the main event of the sixth generation. Emplaced at this time were the Isham Canyon granite, the non-foliated (Independence) dikes and the Copper Queen alaskite.

Generation seven is related to extensional tectonism during Cenozoic time. This period is characterized by the extrusion of an olivine basalt, which is crosscut by long north-south striking basin and range faults.

Regional Framework

Regions surrounding the central Slate Range have undergone several periods of major deformation during Mesozoic time (Fig. 36). A change in plate motion resulted in the formation of an Andean-type arc

Figure 36. Chronology of Mesozoic deformation and intrusion in the White, Inyo, Argus and Slate Ranges and adjacent Mojave Desert. Heavy solid lines indicate age of deformation preferred whereas dashed lines indicate possible age range of deformation from cross-cutting relations with other structures or dated rocks. Diagram modified from Dunne and others (1978). Mojave Desert data is from Burchfiel and Davis (1981).

Sierra Nevada batholith
Hunter Mountain batholith
Peraluminous rocks
left-slip fractures
Swansea-Coso thrust system
NW Folds with APC
Last Chance thrust system
Layton Well thrust
NE trending folds
Sand Canyon thrust
Intrusive Events
Structure
Structure
Mojave Desert
White, Inyo, Argus and Slate Ranges
TRIASSIC
JURASSIC
CRETACEOUS
Early
Middle
Late
Early
Middle
Late
Early
Late
240
220
200
180
160
140
120
100
80
60

along the western Cordillera (Burchfiel and Davis, 1975; 1981). Initial volcanic activity resulting from this arc, beginning in earliest Triassic time in some areas and in late Early Triassic to Middle Triassic time in others, is represented in the stratigraphic section by the presence of volcaniclastic and flow rocks interbedded with marine carbonate rocks throughout the southern Inyo Mountains, Argus and Panamint Ranges, areas in western Nevada, and in the Mojave Desert (Johnson, 1957; Merriam, 1963; Moore, 1976; Dunne and others, 1978; Speed, 1977, 1978; Oldow, 1978; Burchfiel and Davis, 1981; Oborne and Dunne, 1982). Continued subduction produced a large volume of igneous plutonic rock in the region, exemplified by the Sierra Nevada batholith and its satellites (Moore, 1963; Bateman and others, 1965; Dunne and others, 1978). Also, during early Mesozoic time alkalic plutonic rocks were being emplaced (Miller, 1977, 1978; Sylvester and others, 1978). After late Early Jurassic (156 m.y.) time calc-alkaline rocks became the dominant type. Magmatic activity related to the arc to the south, in the Mojave Desert, appears more sporadic than to the north (Burchfiel and Davis, 1981).

The volume of magma emplaced probably resulted in a high heat flow behind the arc. Related to this heat flow and compressional forces present in the region, large-scale crustal shortening in the form of an extensive thrust system, the Swansea-Coso system, developed (Armstrong and Dick, 1974; Moore, 1976; Fig. 37; Table 9).

During a lull in magmatic activity at about 148 m.y.B.P., intrusion of the Independence dike swarm occurred. Oriented in a northwesterly direction and extending from south of the Garlock fault to the central Sierra Nevada, the dike swarm has been related to a change

Figure 37. Geologic map after Jennings (1977) showing the location of the Swansea-Coso thrust system, eastern California. Location of the thrusts from the following reports: Smith and others (1968), Kelley and Stevens (1975), Gulliver (1976) and Moore (1976).

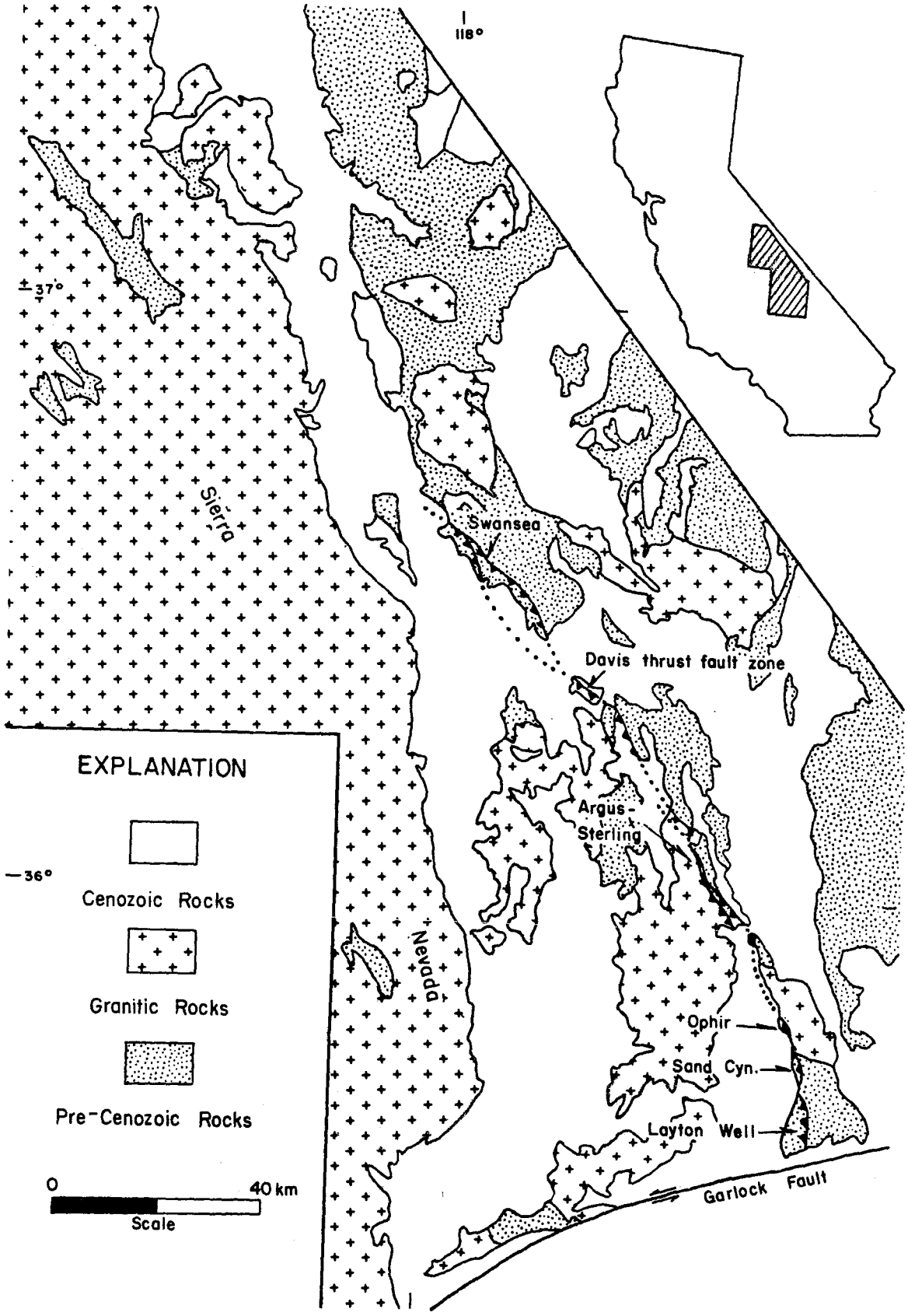
118°
37°
36°
Sierra
Nevada
Swansea
Davis thrust fault zone
Argus-
Sterling
Ophir
Sand Cyn.
Layton Well
Garlock Fault
EXPLANATION
Cenozoic Rocks
Granitic Rocks
Pre-Cenozoic Rocks
0
40 km
Scale

Table 9. Summary of features of the thrust faults belonging to the Swansea-Coso thrust system.

Fault	Location	Age	Direction/Amount of Transport	Allochthonous Rocks	Autochthonous Rocks	Deformational Characteristics of the Thrust Surface	References
Swansea Thrust System	Western side of the southern Inyo Mountains	Post-Early Triassic to pre-Early Jurassic	Eastward movement with slip amounts ranging from 312-625 m per imbricate slice. Amounts up to 1.5 km have been determined.	Devonian (Lost Burro) to Pennsylvanian (Keeler Canyon)	Mississippian (Perdido) to post-Early Triassic volcanic rocks	Series of westward dipping imbricate slices. Trend approximately N.30°W. Dip angle decreases with higher structural position. Intense drag folding, shearing, fragmentation occurs adjacent to thrust surface.	Kelley, J.S. (1973); Kelley, J.S. and Stevens, C.H. (1975)
Davis Thrust Fault System	Darwin Hills, Darwin, California	Post-Early Jurassic pluton, pre-Darwin Tear Fault	East-northeast direction of transport; minimum slip of 1 km.	Devonian through Permian strata; lower Jurassic quartz monzonite	Pennsylvanian and Permian strata, lower Jurassic quartz monzonite	Main north striking thrust which dips 23° to 60° to the west. Numerous drag folds and lineations developed within the hanging wall. Five closely spaced imbricate slices.	Hall, W.E. and MacKevett, E.M. (1962); Gulliver, R.M. (1976); Dunne, G.C. (pers. comm, 1982)
Argus-Sterling Thrust System	Argus and northern Slate Range	Late Jurassic (165 to 140 m.y.)	Northeast direction of transport with a net slip of several km.	Porphyritic quartz monzonite and altered Paleozoic and Mesozoic strata	Silurian through Triassic strata; early Jurassic quartz monzonite (180 m.y. - Hunter Mountain)	Northwest trending thrust zone dipping from 30 to 40° southwest. Shearing, mineral lineations, flow folds and mylonitization of granular rocks. Several imbricate slices along trace.	Moore, S.C. (1974); Holden, K.D. (1975); Moore, S.C. (1976); Moore, S.C. and Harakal, J.E. (1976); Magorien, D.S. (pers. comm., 1979)
Ophir Mine Thrust	Ophir Mine Area, central Slate Range	Late Jurassic	East-southeast direction of transport with a minimum 0.8 km offset.	Metacarbonate, metavolcanic and metaplutonic rocks	Metashales of unknown age	Series of imbricate slices trending roughly N.35°W., and dipping to the southwest. Brecciation, flow folding and mylonitization. Large and small scale folding of autochthonous and allochthonous rocks.	Moore, S.C. (1976); Fowler, J.A. (1979); Fowler, J.A. (this report)
Sand Canyon Thrust	Sand Canyon, southern Slate Range	Post-early Mesozoic	Eastward displacement(?). Amount of slip unknown.	Precambrian(?) metaplutonic and undifferentiated metamorphics	Mesozoic plutonic rocks	Imbricate thrust fault trending about N.20°W. and dipping 25° to southwest. Fault surface is characterized by chlorite gouge zone.	Smith, G.I. and others,
Layton Well Thrust	Layton Canyon, southern Slate Range	Post-early Mesozoic	Eastward displacement(?). Amount of slip unknown.	Cataclasized Mesozoic granitic rock and gneisses of Precambrian age	Mesozoic metavolcanic and granitic rock	North-northwest trending thrust. Small scale folding of allochthonous and autochthonous rocks near the fault zone.	Smith, G.I. and others, (1968); Davis and Burchfiel (1973)
Thrust at Drinkwater Lake	Granite Mountains, northern Mojave Desert	Post-early Mesozoic	Eastward displacement(?). Slip amount unknown.	Sheared phyllonitic crystalline rock	Mesozoic metavolcanic rock	North-northwest trending thrust.	Davis and Burchfiel (1973); Burchfiel and Davis (1981)

in plate motion which resulted in a tensional regime of limited duration (Chen, 1977; Chen and Moore, 1979). Intrusion of these dikes appears to post-date, in part, the development of the Swansea-Coso system (Moore, 1976; Dunne and others, 1978; Dunne, G.C., pers. comm., 1982).

Renewed subduction and magmatism related to the Sierra Nevada batholith began after the emplacement of the Independence dike swarm (Chen, 1977; Dunne and others, 1978; Chen and Moore, 1979). Magmatism associated with Sierran rocks became progressively more silicic until it ended during Late Cretaceous time (about 74 m.y.B.P.; Dunne and others, 1978). Again, overlapping the intrusive activity associated with the Sierra Nevada batholith, are the peraluminous granites emplaced from Cretaceous to mid-Tertiary (94 to 50 m.y.B.P.; Miller and Bradfish, 1980). A final change in plate motion resulted in a change in subduction and a shift in magmatism to the east (Burchfiel and Davis, 1981).

Structures created during deformation pulses in Mesozoic time are contiguous to the south, through the central Slate Range pendant and into the Mojave Desert (Fig. 38). Early phases of folding and faulting within the central Slate Range show characteristics noted in structures exposed to the north. These characteristics include northeast-trending folds with southeast vergence, a well-developed axial plane cleavage, and similar orientation and amount of displacement for the oblique-slip faults seen. These characteristics and their involvement of rocks as young as Permian may be correlated with structures observed in the White Mountains, southern Inyo Mountains, Darwin Hills and Argus Range (Hall and MacKevett, 1962; Dunne and others,

Figure 38. Chronology of Mesozoic deformation and intrusion in the central Slate Range and its relationship to deformation in the White, Inyo, Argus Ranges and the Mojave Desert. Heavy solid lines indicate age of deformation preferred whereas dashed lines indicate possible age range of deformation from cross-cutting relations with other structures or dated rocks. Diagram modified from Dunne and others (1978). Mojave Desert data is from Burchfiel and Davis (1981).

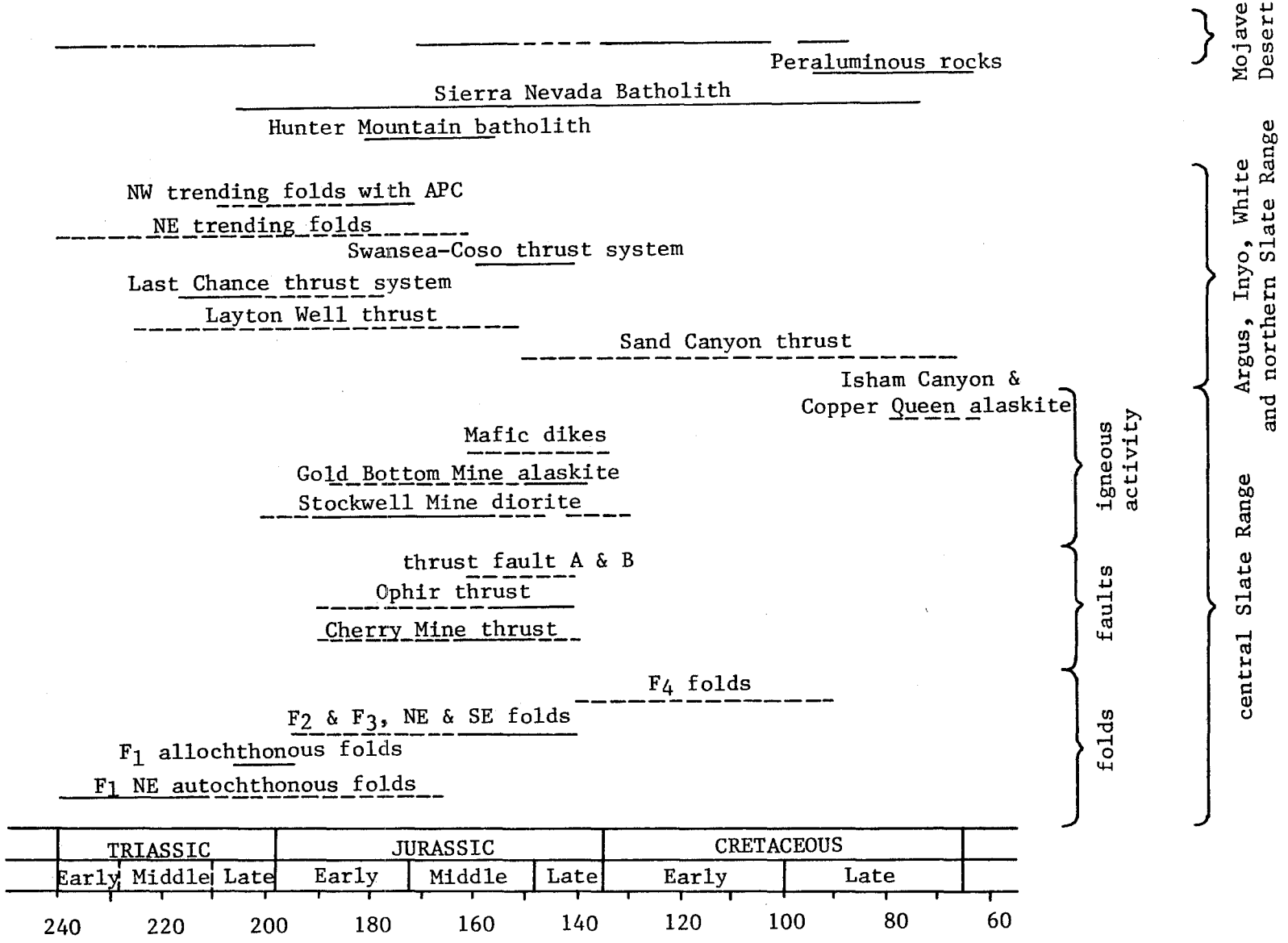
Peraluminous rocks
Sierra Nevada Batholith
Hunter Mountain batholith
NW trending folds with APC
NE trending folds
Swansea-Coso thrust system
Last Chance thrust system
Layton Well thrust
Sand Canyon thrust
Isham Canyon &
Copper Queen alaskite
Mafic dikes
Gold Bottom Mine alaskite
Stockwell Mine diorite
thrust fault A & B
Ophir thrust
Cherry Mine thrust
F4 folds
F2 & F3, NE & SE folds
F1 allochthonous folds
F1 NE autochthonous folds
igneous activity
faults
folds
Mojave Desert
Argus, Inyo, White and northern Slate Range
central Slate Range
TRIASSIC
JURASSIC
CRETACEOUS
Early
Middle
Late
Early
Middle
Late
Early
Late
240
220
200
180
160
140
120
100
80
60

1978; Welch, 1979; Werner, 1980).

Intrusive rocks exposed in the central Slate Range demonstrate the large volumes of magma being generated and emplaced during activity of the Mesozoic arc. Plutonic rocks correlative with the alkalic suite are exposed within the study area. Also present are calc-alkaline "Sierran" rocks similar to those exposed to the north. In the Mojave Desert, plutonic rocks related to the same period of time are exposed and possibly correlative.

Magmatic activity coupled with compressive forces resulted in crustal shortening within the study area. Major structures associated with this phase of deformation include the Ophir and Cherry Mine thrust faults, northwest-striking thrust faults which involve Permian (?) - Triassic (?) rock and crystalline basement. Faults with similar characterisitics are exposed in a linear trend (Fig. 37) from the southern Inyo Mountains southeastward to the Garlock fault, passing through the study area. A continuation of this thrust system has been described by Davis and Burchfiel (1978) in the northern Mojave Desert near Drinkwater Lake.

Folds formed after thrusting have a northwesterly orientation and a poorly-developed axial plane cleavage. Although not as widespread or as strong as earlier structures, they also appear to correlate to regional features. Folds present in the Darwin area show similar characteristics.

Mafic dikes exposed in the study area also appear to correlate with a prominent dike swarm exposed regionally based on chemistry, petrography and structural orientation and position. The Independence

dike swarm can be traced southeastward from the central Sierra Nevada to the Garlock fault. Again, allowing for movement along the Garlock fault, the dikes are present in the northern Mojave Desert.

The youngest suite of plutonism to affect the area is a post-tectonic alaskite possibly related to the peraluminous suite of rocks which intruded the region from 94 to 50 m.y. ago. Rocks related to this younger intrusive suite are present in the Mojave Desert and areas to the north.

CONCLUSIONS

The central Slate Range appear to have experienced a history similar to the surrounding regions to the north (Basin and Range province) and south (Mojave Desert). Arc-influenced sedimentation characteristic of the ranges to the immediate north and east, western Nevada, and areas in the Mojave Desert are also represented in the metamorphic rock units in the study area. Evidence of Mesozoic arc activity as expressed in the plutonic rocks is also abundant in the study area. The presence of three distinctive suites of igneous rocks in the region and in the study area reflects changes in source magma and possibly a changing tectonic regime. Another intrusive rock type represented in the study area, and also present from the Sierra Nevada south into the Mojave Desert, are the Independence dike swarm. Sedimentary and igneous rocks correspond well with rocks exposed regionally.

Major structures and their age relationships in the central Slate Range tend to correlated well with features seen to the north and the south. Folds and faults present in the central Slate Range that are not present on a regional basis, such as F_2, F_3 and F_5 folds, are local features resulting from a local stress regime. Two major structural features of the study area, the Ophir and Cherry Mine thrust faults, correlate well with the Argus-Sterling thrust system to the north and with deformation in the northern Mojave Desert.

In summary, major structural features and intrusives present in the central Slate Range correspond well with features present to the north in the Basin and Range province and to the south in the northern

Mojave Desert, thus providing an important link between the two regions.

REFERENCES CITED

Abbott, E.W., 1972, Stratigraphy and petrology of the Mesozoic volcanic rocks of southeastern California: Ph.D. dissertation, Rice University, Houston, Texas, 196p.

Armstrong, R.L., and Dick, H.J.B., 1974, A model for the development of thin overthrust sheets of crystalline rock: Geology, v. 2, p. 35-39.

Bateman, P.C., 1965, Geology and tungsten mineralization of the Bishop mining district, California: U.S. Geological Survey Professional Paper 470, 208p.

_____Clark, L.C., Huber, D.K., Moore, J.G., and Rhinehart, D.C., 1963, The Sierra Nevada batholith: a synthesis of recent work across the central part: U.S. Geological Survey Professional Paper 414-D, 46p.

_____and Dodge, F.C.W., 1970, Variations of major chemical constituents across the central Sierra Nevada batholith: Geological Society of America Bulletin, v. 81, p. 409-420.

Bingler, E.C., Trexler, D.T., Kemp, W.R., and Bonham, H.F., 1976, PETCAL: a BASIC language computer program for petrologic calculations: Nevada Bureau of Mines and Geology Report 28, 27p.

Burchfiel, B.C., and Davis, G.A., 1975, Nature and controls of Cordilleran orogensis, western United States: extensions of an earlier synthesis: American Journal of Science, v. 275-A, p. 363-396.

_____1981, Mojave Desert and environs: in Ernst, W.G., ed., The geotectonic development of California, Prentice-Hall, New Jersey, p. 217-252.

Chen, J.H-Y., 1977, Uranium-lead isotopic ages from the southern Sierra Nevada batholith and adjacent areas, California: Ph.D. dissertation, University of California, Santa Barbara, 183p.

_____and Moore, J.G., 1979, Late Jurassic Independence dike swarm in eastern California: Geology, v. 7, p. 129-133.

Clarke, D.B., 1981, The mineralogy of peraluminous granites: a review: Canadian Mineralogist, v. 19, p. 3-17.

Davis, G.A., and Burchfiel, B.C., 1973, Garlock Fault: an intercontinental transform structure, southern California: Geological Society of America Bulletin, v. 84, p. 1407-1422.

Donath, F.A., and Parker, R.B., 1964, Folds and folding: Geological Society of America Bulletin, v. 75, p. 45-62.

Duffield, W.A., Bacon, C.R., and Dalrymple, G.B., 1980, Late Cenozoic volcanism, geochronology, and structure of the Coso Range, Inyo County, California: Journal of Geophysical Research, v. 85, p. 2381-2404.

Dunne, G.C., 1979, Hunter Mountain batholith: a large composite alkalic intrusion of Jurassic age in eastern California: Geological Society of America Abstracts with Programs, v. 11, no. 3, p. 76.

_____Gulliver, R.M., Sylvester, A., 1978, Mesozoic evolution of rocks of the White, Inyo, Argus, and Slate Ranges, eastern California: in Howell, D.G., and McDougall, K., eds., Mesozoic paleogeography of the western United States: Society of Economic Paleontologists and Mineralogists, Pacific Coast Paleogeography Symposium 2, p. 189-208.

Fleuty, M.J., 1964, The description of folds: Proceedings of the Geological Association, v. 75, p. 461-489.

Fowler, J.A., 1979, Structural analysis of Mesozoic deformations in the central Slate Range, eastern California: Geological Society of America Abstracts with Programs, v. 11, no. 3, p. 78.

Gulliver, R.M., 1976, Structural analysis of Paleozoic rocks in the Talc City Hills, Inyo County, California: M.S. thesis, University of California, Santa Barbara, 105p.

Hall, W.E., 1971, Geology of the Panamint Butte Quadrangle, Inyo County California: U.S. Geological Survey Bulletin 1299, 67p.

_____and MacKevett, E.M., Jr., 1962, Geology and ore deposits of the Darwin Quadrangle, Inyo County, California: U.S. Geological Survey Professional Paper 368, 83p.

_____and Stephens, H.C., 1963, Economic geology of the Panamint Butte Quadrangle and Modoc District, Inyo County, California: California Division of Mines and Geology Special Report 73, 39p.

Hanson, E., 1971, Strain facies: Springer-Verlag, New York, 207p.

Holden, K.D., 1976, Geology of the central Argus Range: M.S. thesis California State University, San Jose, 64p.

Jennings, C.W., 1977, Geologic map of California: California Division of Mines and Geology, scale 1:750,000.

Johnson, B.K., 1957, Geology of a part of the Manly Peak Quadrangle, southern Panamint Range, California: University of California Publications in the Geological Sciences, v. 50, p. 353-423.

Kelley, J.S., 1973, Structural geology of a portion of the southwest quarter of the New York Butte Quadrangle, Inyo County, California: M.S. thesis, California State University, San Jose, 93p.

_____and Stevens, C.H., 1975, Nature and regional significance of thrust faulting in the southern Inyo Mountains, eastern California: Geology, v. 4, p. 524-526.

Labotka, T.C., Albee, A.L., Lanphere, M.A., and McDowell, S.D., 1980, Stratigraphy, structure, and metamorphism in the central Panamint Mountains (Telescope Peak Quadrangle), Death Valley area, California: Geological Society of America Bulletin, v. 91, p. 843-935.

McAllister, J.F., 1956, Geology of the Ubehebe Peak Quadrangle, California: U.S. Geological Survey Geologic Quadrangle Map GQ-95.

Merriam, C.W., 1963, Geology of the Cerro Gordo mining district, Inyo County, California: U.S. Geological Survey Professional Paper 408, 83p.

Miller, C.F., 1977, Early alkalic plutonism in the calc-alkalic batholithic belt of California: Geology, v. 5, p. 686-688.

_____1978, Early Mesozoic alkaline magmatism in California: in Howell, D.G., and McDougall, K., eds., Mesozoic paleogeography of the western United States: Society of Economic Paleontologists and Mineralogists, Pacific Coast Paleogeography Symposium 2, p. 163-187.

_____and Bradfish, K.J., 1980, An inner Cordilleran belt of muscovite-bearing plutons: Geology, v. 8, p. 412-417.

Moore, J.G., 1963, Geology of the Mount Pinchot Quadrangle, southern Sierra Nevada, California: U.S. Geological Survey Bulletin 1130, 152 p.

_____and Hopson, C.A., 1961, The Independence dike swarm in eastern California: American Journal of Science, v. 250, p. 241-259.

Moore, S.C., 1974, Syn-batholithic thrusting of Jurassic? age in the Argus Range, Inyo County, California: Geological Society of America Abstracts with Programs, v. 6, no. 3, p. 233.

_____1976, Geology and thrust fault tectonics of parts of the Argus and Slate Ranges, Inyo County, California: Ph.D. dissertation, University of Washington, 127p.

_____and Harakal, J.E., 1976, K-Ar age bracket on a Late Jurassic thrust fault, southeastern California: Isochron/West, no. 16, p. 7-10.

Oborne, M.S., and Dunne, G.C., 1982, Stratigraphy of Early to Middle(?) Triassic marine to terrestrial rocks, southern Inyo Mountains, California: Geological Society of America Abstracts with Programs, v. 14, no. 4, p. 221.

Oldow, J.S., 1978, Triassic Pamlico Formation: an allochthonous sequence of volcanogenic-carbonate rocks in west-central Nevada: in Howell, D.G., and McDougall, K., eds., Mesozoic paleogeography of the western United States: Society of Economic Paleontologists and Mineralogists, Pacific Coast Paleogeography Symposium 2, p. 223-237.

Ramsay, J.G., 1967, Folding and fracturing of rocks: McGraw-Hill, New York, 568p.

_____1974, Development of chevron folds: Geological Society of America Bulletin, v. 85, p. 1741-1754.

Ross, D.C., 1965, Geology of the Independence Quadrangle, Inyo County, California: U.S. Geological Survey Bulletin 1181-O, 64p.

_____1969, Descriptive petrography of three large granitic bodies in the Inyo Mountains, California: U.S. Geological Survey Professional Paper 601, 47p.

Smith, G.I., and Church, J.P., 1980, Twentieth-century crustal deformation in the Garlock fault-Slate Range area, southeastern California: Geological Society of America Bulletin, v. 91, p. 524-534.

_____Troxel, B.W., Gray, C.H., Jr., and von Huene, R., 1968, Geologic reconnaissance of the Slate Range, San Bernardino and Inyo Counties, California: California Division of Mines and Geology Special Report 96, 33p.

Speed, R.C., 1977, Excelsior Formation, west central Nevada: stratigraphic appraisal, new divisions and paleogeographic interpretations: in Stewart, J.H., Stevens, C.H., and Fritsche, A.E., eds., Paleozoic paleogeography of the western United States: Society of Economic Paleontologists and Mineralogists, Pacific Coast Paleogeography Symposium 1, p. 325-336.

_____1978, Paleogeography and plate tectonic evolution of the early Mesozoic marine province of the western Great Basin: in Howell, D.G., and McDougall, K., eds., Mesozoic paleogeography of the western United States: Society of Economic Paleontologists and Mineralogists, Pacific Coast Paleogeography Symposium 2, p. 253-270.

Streickeisen, A., 1976, To each plutonic rock its proper name: Earth Science Reviews, v. 12, p. 1-33.

Sylvester, A.G., Miller, C.F., and Nelson, C.A., 1978, Monzonites of the White-Inyo Range, California and their relation to the calc-alkaline Sierra Nevada batholith: Geological Society of America Bulletin, v. 89, p. 1677-1687.

Werner, M.R., 1979, Superposed Mesozoic deformations, southeastern Inyo Mountains, California: M.S. thesis, California State University, Northridge, 69p.

Wright, L.A., 1976, Late Cenozoic fault patterns and stress fields in the Great Basin and westward displacement of the Sierra Nevada block: Geology, v. 4, p. 489-494.

_____Troxel, B.W., Burchfiel, B.C., Chapman, R.H., and Labotka, T.C., 1981, Geologic cross section from the Sierra Nevada to the Las Vegas valley, eastern California to southern Nevada: Geological Society of America Map and Chart Series, MC-28M, 15p.

APPENDIX I. ANALYTICAL METHODS

Sample Preparation

Rocks analyzed for major element chemistry were trimmed to remove as much of the weathered material as possible. They were then sectioned, slabbed for staining (if applicable) and the remaining portion was crushed.

Slabs were etched with hydrofluoric acid and immersed in sodium colbaltinitrite stain (potassium feldspar stains yellow). One wt % rock solutions for chemical analysis were made from the finely crushed rock by the method described in Appendix II.

Analytic Procedures

Nine major elements were analyzed by a combination of X-ray fluorescence and atomic absorption. A Norelco Universal Vacuum Path X-Ray Fluorescence Spectrometer with a chromium target tube was used for the analysis of SiO_2, CaO, K_2O and TiO_2. A PET (pentaerytritol) or lithium fluoride analyzing crystal was used in conjunction with the parameters presented in Appendix III.

Concentrations of Al_2O_3, FeO-total, MgO, Na_2O and MnO were determined using a Instrumentation Laboratory Model 151/251 atomic absorption spectrometer. Parameters used are presented in Appendix IV.

A Bausch and Lomb Spectronic 20 Spectrophotometer was used in the determination of the P_2O_5 concentration. No determinations were made for H_2O, FeO and Fe_2O_3 (FeO and Fe_2O_3 concentrations are represented as FeO-total).

Precision and Accuracy

Accuracy was maintained by using International Rock Standards (Appendix V) for calibration curves. Elemental concentrations for the various rock samples were then determined by applying the method of least squares.

Two pellets and two solutions were analyzed for each sample. Blanks were run with each set of solutions to check for possible contamination. Each oxide was run on two separate occasions. Error expressed as the coefficient of variation was determined to be 0.5% of the measurement, generally < 0.5 wt % of the oxide.

The chemical analyses determined were then run through the computer using a petrologic program, PETCAL (Bingler and others, 1976; modified by R.D. LeFever, 1978), which calculates normative minerals and petrologic indices.

APPENDIX II. DISSOLVING PROCEEDURE FOR ATOMIC ABSORPTION ANALYSIS.

1. Prepare the following solutions:
   A. 1:3 HCL:HF (50 ml/sample)
   B. 1:1:8 HCL:HNO_3:H_2O (50 ml/sample)

2. Weigh 0.500 gm powdered rock sample into Teflon beaker.

3. Measure 50 ml solution A into plastic graduated cylinder. Add about 10 ml to sample, swirl to insure wetting, then add the rest.

4. Cover with Teflon watchglass and heat for about 12 hours.

5. Remove watchglass, increase heat to just below boiling point and remove beaker from heat after sample has evaporated to dryness. Do not burn or sample will be difficult to redissolve.

6. Measure 50 ml of solution B into graduated cylinder. Add about 10 ml to dried sample, wetting well, and break up sample with Teflon rod. Add remaining solution while rinsing rod.

7. Replace beaker on hot plate and evaporate to 35 ml (about 1 hour).

8. Let cool, then transfer to 50 ml volumetric flask. Rinse beaker twice with deionized water, adding rinse to flask.

9. Dilute to 50 ml with deionized water, mix well, and store solutions in labelled plastic bottles.

10. Run a blank (add all reagents but no sample) with each set of samples.

11. Full strength, 1% by weight, rock solutions are used for trace-element analyses. Solutions diluted to 200 ppm are used for major-element analyses. All determinations must be corrected for weight by dividing intensity values by the factor (sample wt./0.5000).

APPENDIX III. INSTRUMENT PARAMETERS FOR X-RAY FLUORESCENCE

Element	Si	Ca	Ti	K
Tube Anode	Cr	Cr	Cr	Cr
Crystal	PET	PET	PET	PET
Detector Voltage	1450	1475	1450	1450
Volts (Kv)	40	20	30	40
Current (mA)	35	12	15	20
Gain	128	128	128	128
Window	150	250	170	150
Baseline	10	30	30	10
Counting Interval (sec)	30	30	30	30
Path	vac.	vac.	vac.	vac.
Counter	gas-flow	gas-flow	gas-flow	gas-flow

APPENDIX IV. INSTRUMENT PARAMETERS FOR ATOMIC ABSORPTION SPECTROMETRIC ANALYSIS

Element	Al	Fe_T	Mn	Mg	Na
Slit Width	320	80	160	320	160
Wavelength	309.2	248.2	279.5	285.2	589.0
Current (H.C.)	10	10	10	5	--
Volts (H.V.)	530	620	530	620	530
Integration (sec)	4	4	4	4	4
Burner Height	6.5	4.5	4.8	5.6	5.2
Oxidizer	Na_2O	air	air	air	air

APPENDIX V. INTERNATIONAL ROCK STANDARDS

Calibration curves were drawn for each element using selected standards from this list.

U.S. Geological Survey	AGV1, BCR1, GSP1, and W1
Japanese Geological Survey Basalt Standard	JB1
Centre de Recherches Petrographiques Basalt Standard	BR
Queen Mary College Basalt Standard	QMC-I3
University of North Carolina Dolerite Standard	BD1

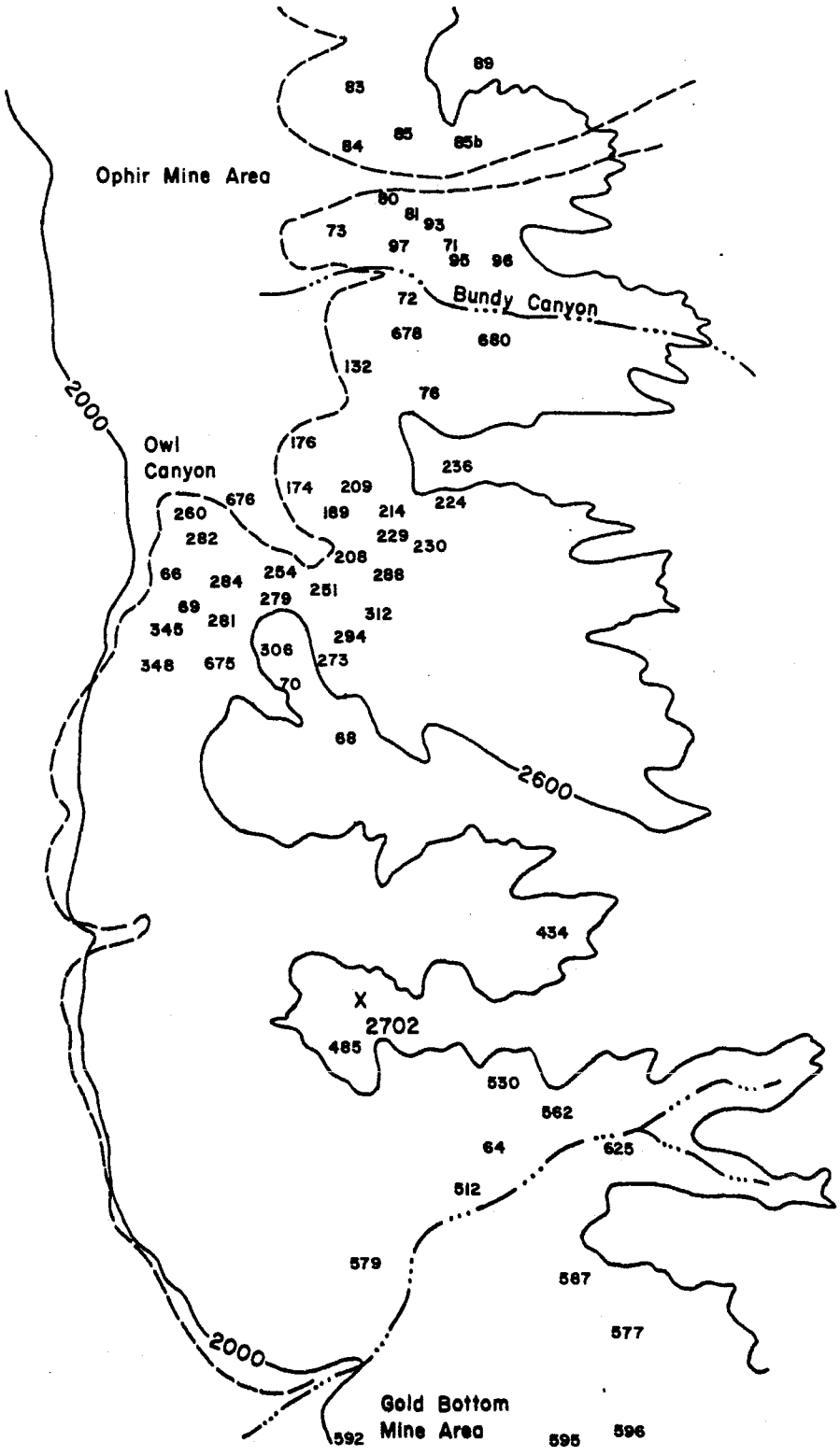

APPENDIX VI. SAMPLE LOCATION MAP